Supporting Information

Photo-Medicated Synthesis of 1,2-Dideoxy-2-phosphinylated Carbohydrates from Glycals: The Reduction of Glycosyl Radicals to Glycosyl Anions

Hai Li[a], Kai-Cheng Yu[a], Jia-Kun Su[c],Wei Ouyang[a], Nai-Li Fan[a*] and Xiang-Guo Hu[ab*]

[a.] *National Engineering Research Center for Carbohydrate Synthesis, Jiangxi Normal University, Nanchang, 330022, China. E-mail: Xiangguo.hu@jxnu.edu.cn*

Contents

1. General Information

All purchased reagents were used without further purification unless otherwise noted. All solvents were dried over 4Å molecular sieves before used unless stated. Reactions were stirred using Teflon-coated magnetic stirrers. Analytical TLC was performed with 0.20 mm silica gel 60F plates with a 254 nm fluorescent indicator. TLC plates were visualized by ultraviolet light or by treatment with a spray of Pancaldi reagent {$(NH_4)_6MoO_4$, $Ce(SO_4)_2$, H_2SO_4, H_2O} or a solution 10% H_2SO_4 in ethanol. Chromatographic purification of products was carried out by flash column chromatography on silica gel (200-300 mesh). Melting points were determined using a WRX-4 visual melting point apparatus. Both melting points and boiling points are uncorrected. Infrared spectra were recorded on an IR Affinity-1. spectra were measured in $CDCl_3$ (TMS, ^1H δ = 0; $CDCl_3$, ^1H δ = 7.26, ^{13}C δ = 77.16) or DMSO-d_6 (TMS, ^1H δ = 0; DMSO-d_6, ^1H δ = 2.50, ^{13}C δ = 39.52) or Methanol-d_4 (TMS, ^1H δ = 0; Methanol-d_4, ^1H δ = 3.31, ^{13}C δ = 49.00)on a Bruker AV 400 (^1H at 400 MHz, ^{13}C at 100 MHz, ^{31}P at 162 MHz, ^{19}F at 376 MHz) magnetic resonance spectrometer. Chemical shifts (δ) are reported in ppm, and coupling constants (J) are in Hz. The following abbreviations were used to explain the multiplicities: s = singlet, d = doublet, t = triplet, q = quartet, m = multiplet. ESI mass spectra were recorded on an AB sciex Triple-TOF 5600+ mass instrument. Photochemical reactions were performed by cylindrical LED strips kit (360-420 nm, 45 W), or simply by placing LED lamps (45 W 360-420 nm blue, purchased from Shenzhen Hongye Optoelectronics Technology Corporation) approximately 6 cm away from reaction tube; the temperature of the reaction was maintained at approximately 25 ºC by fans.

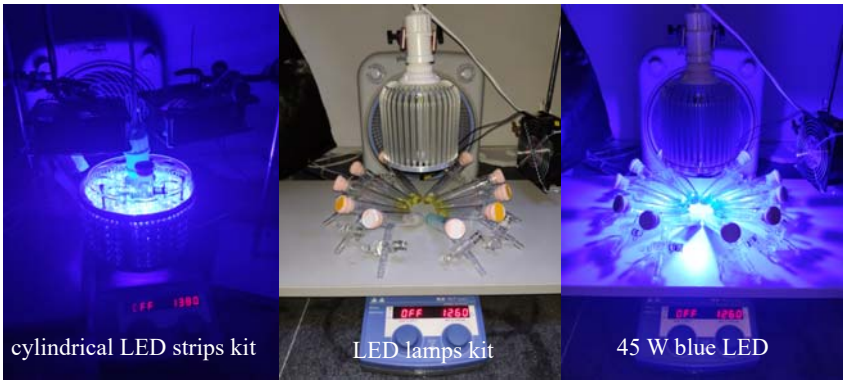

2. Experimental Section

2.1 General procedure for the synthesis of phosphinylated carbohydrates from protected glycals

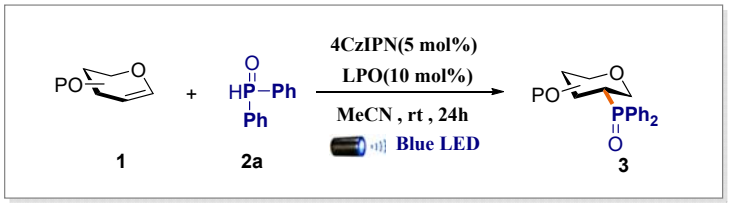

To a dried Schlenk tube equipped with a stir bar, glycal **1**(0.2 mmol, 1.0 equiv), 4CzIPN (8 mg, 0.01 mmol, 5 mol%), phosphine oxide **2a** (81 mg, 0.4 mmol, 2.0 equiv), dilauroyl peroxide (LPO) (8 mg, 0.02 mmol, 0.1 equiv) was added. The Schlenk tube was capped with a rubber septum. After evacuated and backfilled with N_2 three times via branch, degassed acetonitrile (2 mL) was added via a syringe. The reaction was irradiated with Blue LED lamps (45 W) for 24 hours and monitored by TLC. The temperature was kept under 25 °C by fans. After the reaction was completed, organic layers were concentrated under reduced pressure and the residue was purified with chromatography column on silica gel (200-300 mesh) or preparative TLC to afford products **3**.

2.2 General procedure for the synthesis of phosphinylated carbohydrates from various diaryl phosphines oxides

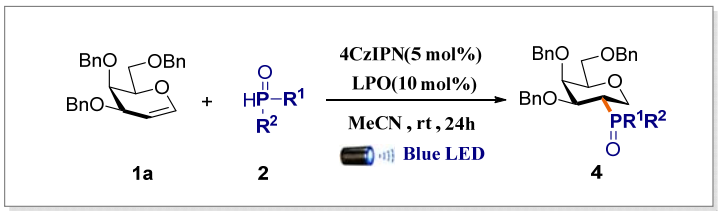

To a dried Schlenk tube equipped with a stir bar, glycal **1a** (0.2 mmol, 1.0 equiv) , 4CzIPN (8 mg, 0.01 mmol, 5 mol%), phosphine oxide **2** (0.4 mmol, 2.0 equiv), LPO (8 mg, 0.02 mmol, 0.1 equiv) was added. The Schlenk tube was capped with a rubber septum. After evacuated and backfilled with N_2 three times via branch, degassed acetonitrile (2 mL) was added via a syringe.

The reaction was irradiated with Blue LED lamps (45 W) for 24 hours and monitored by TLC. The temperature was kept under 25 °C by fans. After the reaction was completed, organic layers were concentrated under reduced pressure and the residue was purified with chromatography column on silica gel (200-300 mesh) or preparative TLC to afford products **4**.

2.3 Procedure for the gram scale reaction

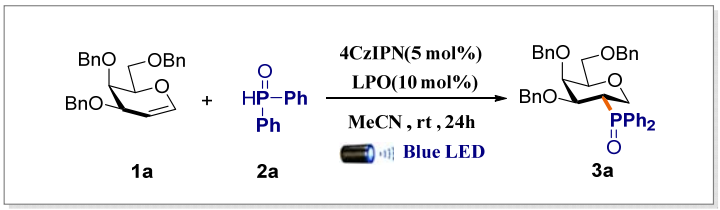

To a dried 50 mL Schlenk tube equipped with a stir bar, glycal **1a** (1.249 g, 3.0 mmol, 1.0 equiv) , 4CzIPN (118 mg, 0.15mmol, 5 mol%), phosphine oxide **2a** (1.213 g, 6.0 mmol, 2.0 equiv), LPO (120 mg , 0.3 mmol, 0.1 equiv) was added. The Schlenk tube was capped with a rubber septum. After evacuated and backfilled with N_2 three times via branch, degassed acetonitrile (30 mL) was added via a syringe. The reaction was irradiated with Blue LED lamps (45 W) for 24 hours and monitored by TLC. The temperature was maintained under 25 °C by fans. After the reaction was completed, organic layers were concentrated under reduced pressure and the residue was purified with chromatography column (Hexane /EtOAc = 1:1) on 200-300 mesh silica gel to afford product **3a** (1.24 g, 67% yield).

2.4 Procedure for the late-stage modification

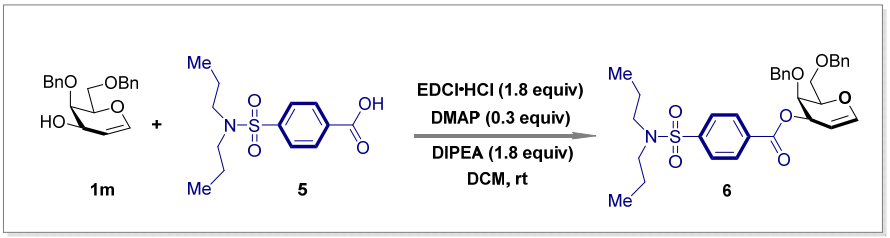

To a solution of compound **1m** (261 mg, 0.800 mmol, 1.00 equiv) in dry DCM (4.00 mL, 0.20 M) were added Probenecid **5** (274 mg, 0.960 mmol, 1.20 equiv), DMAP (29.3 mg, 0.240 mmol, 0.300 equiv), EDCI·HCl (276 mg, 1.44 mmol, 1.80 equiv) and DIPEA (0.25 mL, 1.44 mmol, 1.80 equiv). After stirring at room temperature for 12 h, the reaction mixture was diluted with DCM and washed with saturated $NaHCO_3$ and brine successively. The organic phase was dried over Na_2SO_4, filtered, and concentrated in vacuo. The residue was purified by silica gel column chromatograph Hexanes: EtOAc [3:1 (v/v)] to give **6** (475 mg, 88% yield) as a colorless oil.

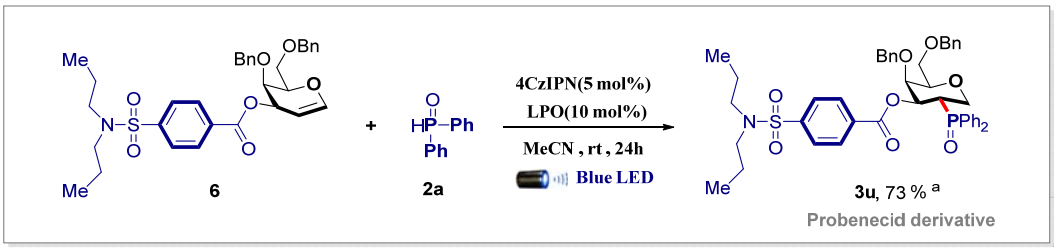

To a dried Schlenk tube equipped with a stir bar, glycal **6** (119 mg, 0.2 mmol, 1.0 equiv) , 4CzIPN (8 mg, 0.01 mmol, 5 mol%), phosphine oxide **2a** (81 mg, 0.4 mmol, 2.0 equiv), LPO (8 mg, 0.02 mmol, 0.1 equiv)was added. The Schlenk tube was capped with a rubber septum. After evacuated and backfilled with N_2 three times via branch, degassed acetonitrile (2 mL) was added via a syringe. The reaction was irradiated with Blue LED lamps (45 W) for 24 hours and monitored by TLC. The temperature was kept under 25 °C by fans. After the reaction was completed, organic layers were concentrated under reduced pressure and the residue was purified with chromatography column on silica gel (200-300 mesh) or preparative TLC to afford products **3u**(116 mg, 73% yield).

2.5 Mechanistic studies

2.5.1 Radical trapping experiments

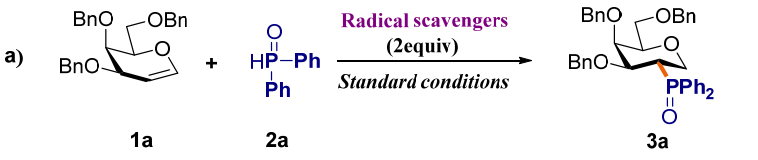

Radical scavengers	Yield of 3a (%)
TEMPO	0
BHT	0

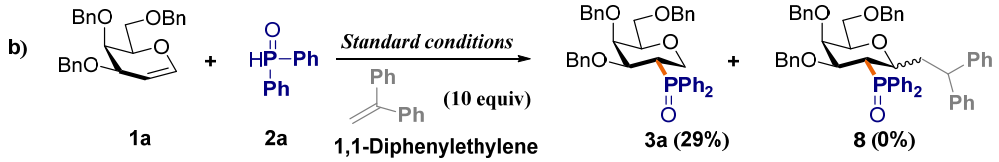

(I) With TEMPO: To a dried Schlenk tube equipped with a stir bar, glycal **1a** (83 mg, 0.2 mmol, 1.0 equiv) , 4CzIPN (8 mg, 0.01 mmol, 5 mol%), phosphine oxide **2a** (81 mg, 0.4 mmol, 2.0 equiv), LPO (8 mg, 0.02 mmol, 0.1 equiv) was added, followed by the addition of TEMPO (2.0 equiv). The Schlenk tube was capped with a rubber septum. After evacuated and backfilled with N_2 three times via branch, degassed acetonitrile (2 mL) was added via a syringe. The reaction was irradiated with Blue LED lamps (45W) for 24 hours and monitored by TLC. The temperature was kept under 25 °C by fans. After the reaction was completed, organic layers were concentrated under reduced pressure and the residue was purified with chromatography column on silica gel (200-300 mesh) failed to obtain **3a**.

(II): The control experiment with 2.0 equiv BHT failed to obtain **3a**.

(III): With 1,1-Diphenylethylene: To a dried Schlenk tube equipped with a stir bar, glycal **1a** (83 mg, 0.2 mmol, 1.0 equiv) , 4CzIPN (8 mg, 0.01 mmol, 5 mol%), phosphine oxide **2a** (81 mg, 0.4 mmol, 2.0 equiv), LPO (8 mg, 0.02 mmol, 0.1 equiv) was added, followed by the addition of 1,1-Diphenylethylene (360mg, 2equiv, 10.0 equiv). The Schlenk tube was capped with a rubber septum. After evacuated and backfilled with N_2 three times via branch, degassed acetonitrile (2 mL) was added via a syringe. The reaction was irradiated with Blue LED lamps (45W) for 24 hours under 25 °C and monitored by TLC. After the reaction was completed, concentrated organic layers under reduced pressure and the residue was purified with chromatography column on silica gel (200-300 mesh, petroleum ether/AcOEt = 1:2) to afford

3a(36 mg, 29% yield).

2.5.2 Experiments that indicate the presence of the anion intermediate

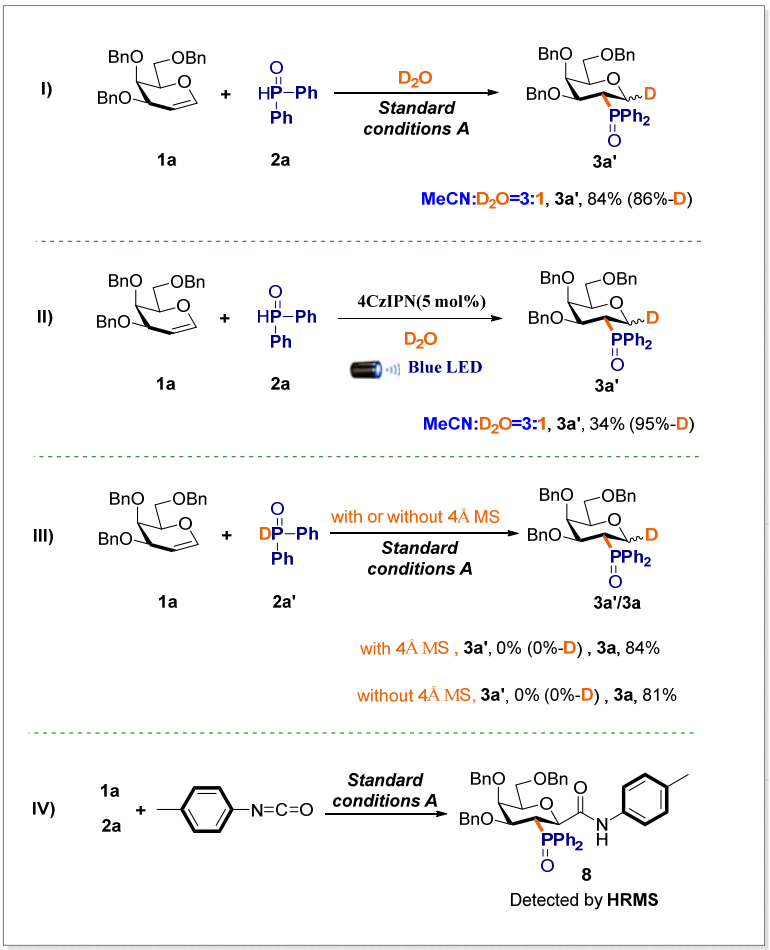

(I) To a dried Schlenk tube equipped with a stir bar, glycal **1a** (83 mg, 0.2 mmol, 1.0 equiv) , phosphine oxide **2a** (81 mg, 0.4 mmol, 2.0 equiv), 4CzIPN (8 mg, 0.01 mmol, 5 mol%), LPO (8 mg, 0.02 mmol, 0.1 equiv) was added. The Schlenk tube was capped with a rubber septum. After evacuated and backfilled with N_2 three times via branch, degassed acetonitrile (1.5 mL) and D_2O (0.5 mL) were added via a syringe. The reaction was irradiated with Blue LED lamps (45W) for 24 hours under 25 °C and monitored by TLC. After the reaction was completed, organic layers were concentrated under reduced pressure and the residue was purified with chromatography column on silica gel (200-300 mesh, Hexane /EtOAc = 1:1) to afford **3a'** (104 mg, 84% yield, 86% [D], light yellow syrup).

(II) To a dried Schlenk tube equipped with a stir bar, glycal **1a** (83 mg, 0.2 mmol, 1.0 equiv) , phosphine oxide **2a** (81 mg, 0.4 mmol, 2.0 equiv), 4CzIPN (8 mg, 0.01 mmol, 5 mol%),

was added. The Schlenk tube was capped with a rubber septum. After evacuated and backfilled with N_2 three times via branch, degassed acetonitrile (1.5 mL) and D_2O (0.5 mL) were added via a syringe. The reaction was irradiated with Blue LED lamps (45W) for 24 hours under 25 ^oC and monitored by TLC. After the reaction was completed, organic layers were concentrated under reduced pressure and the residue was purified with chromatography column on silica gel (200-300 mesh, Hexane /EtOAc = 1:1) to afford **3a'** (42 mg, 34% yield, 95% [D], light yellow syrup).

(III) To a dried Schlenk tube equipped with a stir bar, glycal **1a** (83 mg, 0.2 mmol, 1.0 equiv) , 4CzIPN (8 mg, 0.01 mmol, 5 mol%), phosphine oxide **2a** (81 mg, 0.4 mmol, 2.0 equiv), LPO (8 mg, 0.02 mmol, 0.1 equiv) was added, followed by the addition of 4 Å MS (100 mg). The Schlenk tube was capped with a rubber septum. After evacuated and backfilled with N_2 three times via branch, degassed acetonitrile (1.5 mL) and D_2O (0.5 mL) was added via a syringe. The reaction was irradiated with Blue LED lamps (45 W) for 24 hours under 25 ^oC and monitored by TLC. After the reaction was completed, concentrated organic layers under reduced pressure and the residue was purified with chromatography column on silica gel (200-300 mesh, Hexane /EtOAc = 1:1) to afford **3a** (104 mg, 84% yield).

(IV) To a dried Schlenk tube equipped with a stir bar, glycal **1a** (83 mg, 0.2 mmol, 1.0 equiv) , 4CzIPN (8 mg, 0.01 mmol, 5 mol%), phosphine oxide **2a** (81 mg, 0.4 mmol, 2.0 equiv), LPO (8 mg, 0.02 mmol, 0.1 equiv) was added. The Schlenk tube was capped with a rubber septum. After evacuated and backfilled with N_2 three times via branch, degassed acetonitrile (1.5 mL) and p-Tolyl isocyanate (76 μl, 0.6 mmol, 3.0 equiv) were added via a syringe. The reaction was irradiated with Blue LED lamps (45W) for 24 hours under 25 ^oC and monitored by TLC. After the reaction was completed, organic layers were concentrated under reduced pressure. Product **8** was detected by HRMS {calcd for $C_{47}H_{46}NO_6PH^+$ $[M+H]^+$ 752.3136, found 752.3126.}.

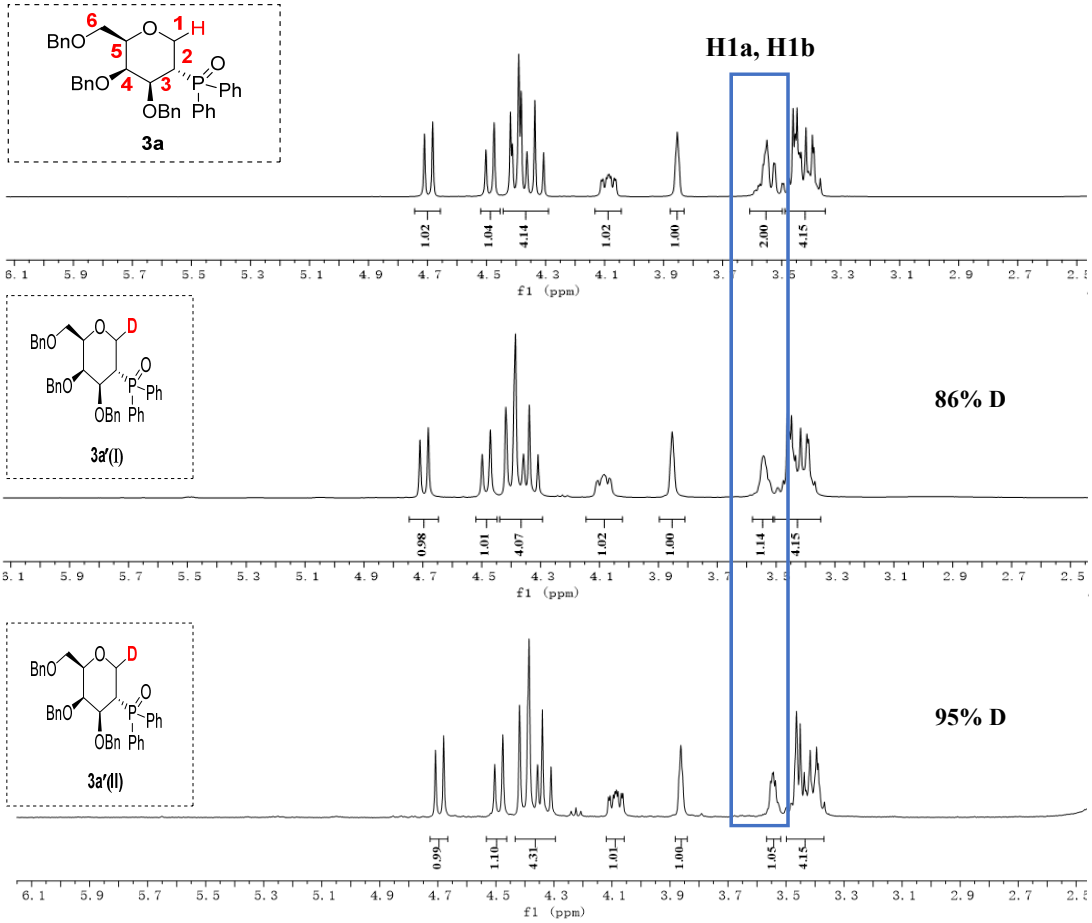

Compound **7**: HRMS (ESI) m/z calcd for $C_{47}H_{46}NO_6P$ H^+ $[M+H]^+$752.3136, found 752.3126.

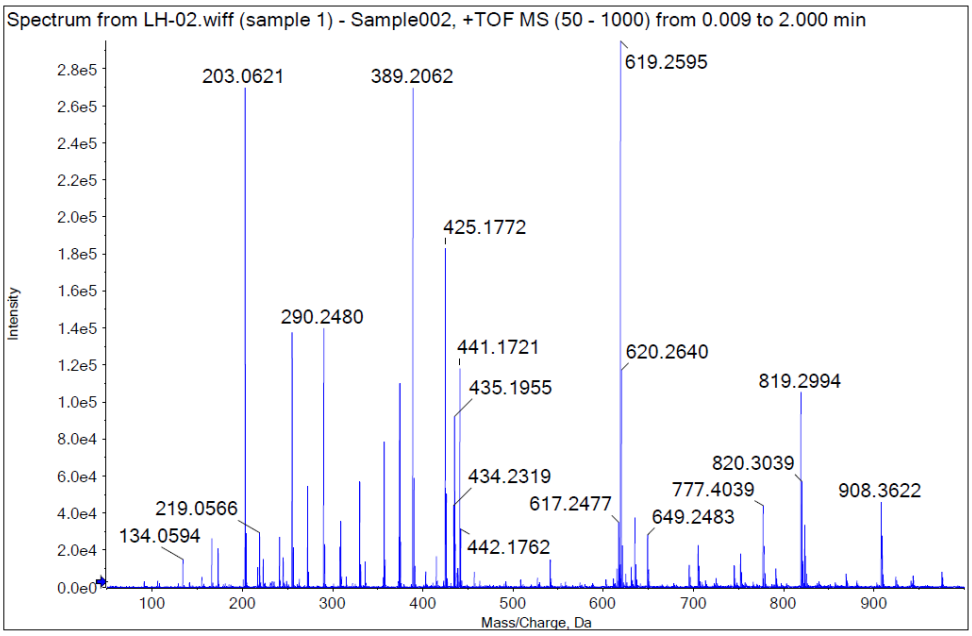

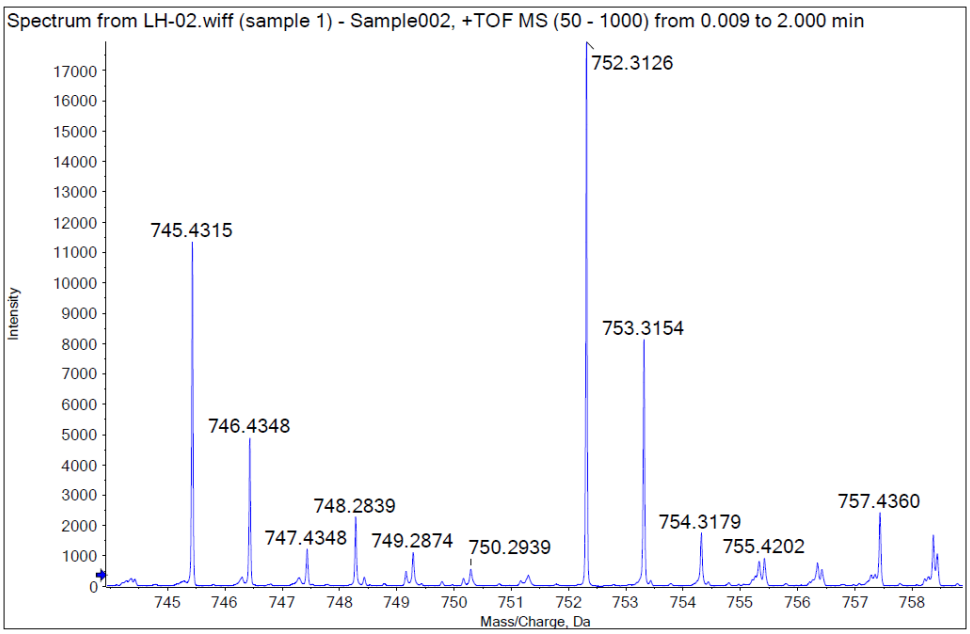

2.6 Reaction optimization using green solvents

Thirteen green solvents[1] were selected for the reaction optimization and *iso*-propanol was found to be a good alternative to CH_3CN.

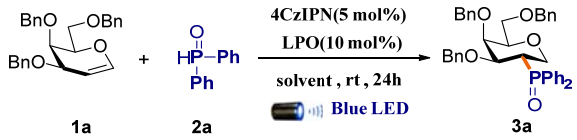

Entry	Solvent	Yields (%)	Entry	Solvent	Yields (%)
1	n-BuOH	32%	8	EA	77%
2	BnOH	Trac	9	Ethyl Lactate	No reaction
3	EtOH	52%	10	Ethyl Propionate	71%
4	**i-PrOH**	**82%**	11	Isobutyl acetate	69%
5	t-BuOH	53%	12	Isobutyl butyrate	62%
6	Acetone	Trac	13	Ethylene glycol	No reaction
7	Cyclohexanone	56%			

Conditions: **1a** (0.2mmol, 1 equiv), **2a** (0.4mmol, 2 equiv), photosensitizer (5 mol%), LPO (10 mol%), Blue LED, solvent (2 mL, degassed), N_2, RT; [a] Yields determined by ^1H NMR analysis using 4-(trifluoromethyl)benzyl alcohol as an internal standard;

[1] D. Prat, A. Wells, J. Hayler, H. Sneddon, C. R. McElroy, S. Abou-Shehada and P. J. Dunn, *Green Chem.*, 2016, **18**, 288-296.

3.Computational Details

Calculations were performed using the Gaussian 09[1] software package. All of the geometries and energetics were fully optimized at the B3LYP[2]/6-311+G(d,p)[3] level of theory. Single-point energy calculations on the optimized geometries were then evaluated using Truhlar and co-workers' B3LYP and 6-311+G(d,p) basis set within the SMD model (acetonitrile)[4]. The thermal corrections evaluated from the unscaled vibrational frequencies at the B3LYP /6-311+G(d,p) level on the optimized geometries were then added to the B3LYP /6-311+G(d,p) electronic energies to obtain the free energies. The structural representations were generated with Gaussian View.

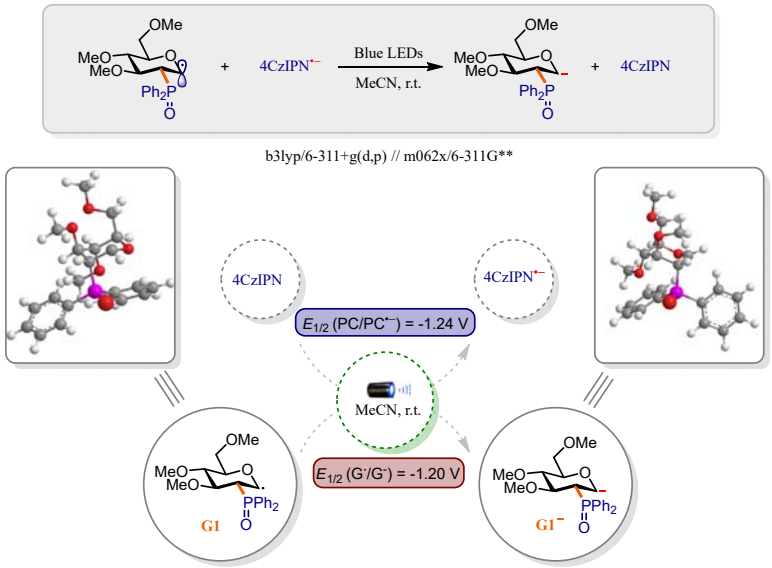

Under solvation conditions, the first electron transfer is described by the half-reaction where $G^{\cdot-}$ is the sugar ring radical anion.

$$G^{\cdot}_{(sol)} + e^{-}_{(g)} \longrightarrow G^{\cdot-}_{(sol)} \qquad (1)$$

By electrochemical convention, the reaction is defined using a gas-phase electron[5]. The electrochemical half-cell potential for this reaction is the one electron reduction potential, E^0, which quantifies the tendency for the reaction to occur. E^0 is related to the standard state free energy change for reaction 1, $\Delta_{red}G^0$, by the Nernst equation

$$E^0[V] = -\Delta_{red}G^0[eV]/F, \qquad (2)$$

where F = 1 eV/V is the Faraday constant. The ^{0} superscript indicates that the species are in their standard states, which in this work is a temperature of 298.15 K. All reduction potentials

in this work are reported for reduction in acetonitrile at 298.15 K. The reduction potential is measured and reported relative to a reference potential such as the normal hydrogen electrode (NHE), which is described by the oxidation half-reaction.

$$1/2\ H_{2(g)} \rightarrow H^{+}_{(sol)} + e^{-}_{(g)} \qquad (3)$$

The oxidation potential for the NHE is $E^{0}_{NHE} = -\Delta_{NHE}G^{0}/F$ [using eq. (2)], where $\Delta_{NHE}G^{0}$ is the free energy change for reaction 3. The value of E^{0}_{NHE} is often quoted as -(4.6±0.10) V, as recommended by the S. Trasatti in 1986[6]. So the one-electron reduction potential of an G relative to the NHE is

$$E^{0}_{H} = E^{0} + E^{0}_{NHE} = E^{0} - (4.60\pm0.10)\ V \qquad (4)$$

That is, E^{0}_{H} is the electrochemical potential associated with the net reaction formed by summing reactions (1) and (3),

$$G^{\cdot}_{(sol)} + 1/2\ H_{2(g)} \longrightarrow G^{\cdot-}_{(sol)} + H^{+}_{(sol)}$$

Equations (2) and (4), show that $\Delta_{red}G^{0}$ is the only unknown required to calculate E^{0}_{H}.

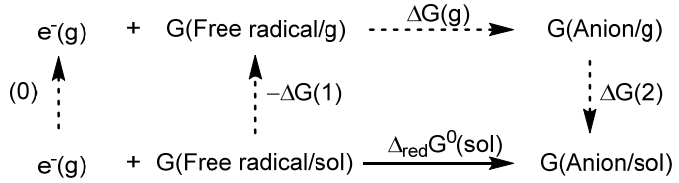

Figure 1. Thermodynamic cycle used to calculate $\Delta_{red}G^{0}$(aq). The solid arrow indicates the direct calculation path, whereas the dashed arrows indicate the indirect calculation path. The two paths are thermodynamically equivalent; that is, the net free energy change along both paths is equal to $\Delta_{red}G^{0}$(aq).

According to the Figure 1, we can get the following relationship, then E^{0}_{H} and $\Delta_{red}G^{0}$ can also be predicted accurately.

$$\Delta_{red}G^{0}(sol) = -\Delta G(1) + \Delta G(g) + \Delta G(2) \qquad (a)$$

$$-\Delta G(1) = G(Free\ radical/sol) - G(Free\ radical/g) \qquad (b)$$

$$\Delta G(2) = G(Anion/sol) - G(Anion/g) \qquad (c)$$

	G(0)/a.u.			
G(Free radical/g)	-1533.25		ΔG(1)/a.u.	0.31917
G(Free radical/aq)	-1532.93		ΔG(2)/a.u.	0.397449
G(Anion/g)	-1533.29		ΔG(g)/a.u.	-0.03425
G(Anion/aq)	-1532.89		Δ_{red}G(aq)/a.u.	0.044031
			Δ_{red}E(aq)/V	-1.19795

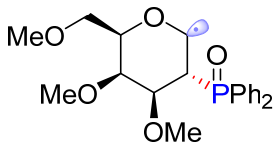

E(UM062X) = -1532.93209553 a.u.

Zero-point correction=	0.433887 (Hartree/Particle)
Thermal correction to Energy=	0.461455
Thermal correction to Enthalpy=	0.462400
Thermal correction to Gibbs Free Energy=	0.371174
Sum of electronic and zero-point Energies=	-1533.188553
Sum of electronic and thermal Energies=	-1533.160984
Sum of electronic and thermal Enthalpies=	-1533.160040
Sum of electronic and thermal Free Energies=	-1533.251266

C	-2.25333877	-5.17935394	2.26888804
C	-0.70825467	-5.22322272	2.20578599
C	-0.15632367	-3.81214472	2.20578599
C	-0.70598667	-3.00760772	3.36644699
C	-2.25439208	-3.09953276	3.36185871
H	-2.62602677	-4.74632494	1.30350304
H	-0.33345167	-3.44245272	4.33105799
H	-0.42494167	-3.30651172	1.24123999
O	-2.71065318	-4.36885046	3.30565923
O	1.27077752	-3.85551021	2.28579610
C	-2.76935589	-6.62770301	2.35613080
H	-2.06571984	-7.22502492	2.89742817
H	-3.71201285	-6.64060492	2.86222505
O	-2.92907547	-7.15706580	1.03735686
C	-1.64253437	-7.38961521	0.45801865
H	-0.94025470	-7.62291746	1.23085325
H	-1.70304295	-8.20851483	-0.22801497
H	-1.32164883	-6.51141883	-0.06227318
O	-0.22951042	-5.92465103	1.05526339
H	-0.35289834	-5.74367639	3.07051130
C	1.20048788	-5.92350363	1.05714542
C	1.83227967	-3.22882905	1.12955821
H	1.55850078	-5.94731887	0.04909800
H	1.55580747	-5.03776505	1.54099990
H	1.55715412	-6.78456843	1.58274660
H	2.77581133	-3.67944460	0.90241589
H	1.16884465	-3.35251413	0.29922335
H	1.97232799	-2.18561315	1.32187836

P	-0.09544591	-1.29602729	3.26578700
O	1.27395970	-1.28883671	2.65367870
C	-1.22540444	-0.30841820	2.23611618
C	-0.88341954	-0.00629977	0.91769204
C	-2.43331157	0.14634743	2.76497978
C	-1.74889988	0.75099045	0.12859316
H	0.06929377	-0.36432544	0.50128267
C	-3.29961620	0.90304568	1.97546478
H	-2.70308734	-0.09182795	3.80402865
C	-2.95756429	1.20553181	0.65749679
H	-1.47912642	0.98969445	-0.91041559
H	-4.25211763	1.26112506	2.39259116
H	-3.63983054	1.80256250	0.03511148
C	-0.01649212	-0.58078053	4.93748924
C	1.16082956	-0.67233918	5.68045770
C	-1.13290712	0.05899726	5.47586647
C	1.22141993	-0.12480715	6.96176922
H	2.04057276	-1.17746600	5.25602799
C	-1.07215272	0.60761374	6.75717000
H	-2.06084452	0.13140601	4.89035968
C	0.10470316	0.51569936	7.50020365
H	2.14916525	-0.19748601	7.54768979
H	-1.95242522	1.11235247	7.18123764
H	0.15273219	0.94738419	8.51046983
H	-2.62822453	-2.63950183	4.25265658

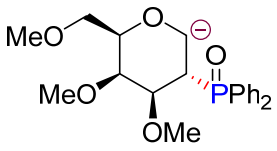

E(RM062X) = -1532.88806500 a.u.

Zero-point correction= 0.431109 (Hartree/Particle)

Thermal correction to Energy= 0.458271

Thermal correction to Enthalpy= 0.459215

Thermal correction to Gibbs Free Energy= 0.371600

Sum of electronic and zero-point Energies= -1533.226005

Sum of electronic and thermal Energies= -1533.198844

Sum of electronic and thermal Enthalpies= -1533.197899

Sum of electronic and thermal Free Energies= -1533.285514

C	-2.25333877	-5.17935394	2.26888804
C	-0.70825467	-5.22322272	2.20578599
C	-0.15632367	-3.81214472	2.20578599
C	-0.70598667	-3.00760772	3.36644699

C	-2.25439208	-3.09953276	3.36185871
H	-2.62602677	-4.74632494	1.30350304
H	-0.33345167	-3.44245272	4.33105799
H	-0.42494167	-3.30651172	1.24123999
O	-2.71065318	-4.36885046	3.30565923
O	1.27077752	-3.85551021	2.28579610
C	-2.76935589	-6.62770301	2.35613080
H	-2.06571984	-7.22502492	2.89742817
H	-3.71201285	-6.64060492	2.86222505
O	-2.92907547	-7.15706580	1.03735686
C	-1.64253437	-7.38961521	0.45801865
H	-0.94025470	-7.62291746	1.23085325
H	-1.70304295	-8.20851483	-0.22801497
H	-1.32164883	-6.51141883	-0.06227318
O	-0.22951042	-5.92465103	1.05526339
H	-0.35289834	-5.74367639	3.07051130
C	1.20048788	-5.92350363	1.05714542
C	1.83227967	-3.22882905	1.12955821
H	1.55850078	-5.94731887	0.04909800
H	1.55580747	-5.03776505	1.54099990
H	1.55715412	-6.78456843	1.58274660
H	2.77581133	-3.67944460	0.90241589
H	1.16884465	-3.35251413	0.29922335
H	1.97232799	-2.18561315	1.32187836
P	-0.09544591	-1.29602729	3.26578700
O	0.67882644	-0.96750326	4.50779114
C	0.98651718	-1.12234067	1.81265630
C	2.37234502	-1.10561206	1.97288352
C	0.43031472	-1.00606474	0.53881688
C	3.20169039	-0.97195546	0.85953546
H	2.81051431	-1.19652964	2.97736521
C	1.25979775	-0.87335074	-0.57507485
H	-0.66190913	-1.01940953	0.41233366
C	2.64529026	-0.85614167	-0.41491447
H	4.29400866	-0.95813096	0.98581368
H	0.82098375	-0.78210456	-1.57936099
H	3.29940143	-0.75082733	-1.29260679
C	-1.50631870	-0.15674266	3.11129267
C	-2.08140521	0.40030370	4.25385396
C	-2.01260434	0.15959398	1.85067611
C	-3.16296067	1.27295254	4.13577128
H	-1.68251782	0.15010835	5.24760087
C	-3.09385667	1.03326239	1.73232585
H	-1.55935312	-0.27921627	0.95004415

C	-3.66915851	1.58984277	2.87459687
H	-3.61670249	1.71157127	5.03634248
H	-3.49256678	1.28281839	0.73823014
H	-4.52189574	2.27796543	2.78173808
H	-2.65494298	-2.13365615	3.13483150

4. References

1. Gaussian 09, Revision E.01, M. J. Frisch, G. W. Trucks, H. B. Schlegel, G. E. Scuseria, M. A. Robb, J. R. Cheeseman, G. Scalmani, V. Barone, B. Mennucci,

G. A. Petersson, H. Nakatsuji, M. Caricato, X. Li, H. P. Hratchian, A. F. Izmaylov, J. Bloino, G. Zheng, J. L. Sonnenberg, M. Hada, M. Ehara, K. Toyota, R. Fukuda, J. Hasegawa, M. Ishida, T. Nakajima, Y. Honda, O. Kitao, H. Nakai, T. Vreven, J. A. Montgomery, Jr., J. E. Peralta, F. Ogliaro, M. Bearpark, J. J. Heyd, E. Brothers, K. N. Kudin, V. N. Staroverov, T. Keith, R. Kobayashi, J. Normand, K. Raghavachari, A. Rendell, J. C. Burant, S. S. Iyengar, J. Tomasi, M. Cossi, N. Rega, J. M. Millam, M. Klene, J. E. Knox, J. B. Cross, V. Bakken, C. Adamo, J. Jaramillo, R. Gomperts, R. E. Stratmann, O. Yazyev, A. J. Austin, R. Cammi, C. Pomelli, J. W. Ochterski, R. L. Martin, K. Morokuma, V. G. Zakrzewski, G. A. Voth, P. Salvador, J. J. Dannenberg, S. Dapprich, A. D. Daniels, O. Farkas, J. B. Foresman, J. V. Ortiz, J. Cioslowski, and D. J. Fox, Gaussian, Inc., Wallingford CT, 2013.

2. (a) Bachman, J. E.; Curtiss, L. A.; Assary, R. S., Investigation of the redox chemistry of anthraquinone derivatives using density functional theory. *J Phys Chem A*, **2014**, *118*, 8852-60. (b) Phillips, K. L.; Sandler, S. I.; Chiu, P. C., A method to calculate the one-electron reduction potentials for nitroaromatic compounds based on gas-phase quantum mechanics. *J Comput Chem*, **2011**, *32*, 226-39.

3. Hehre, W. J.; Radom, L.; Schleyer, P. v. R.; Pople, J. A. Ab Initio Molecular Orbital Theory; John Wiley & Sons: New York, 1986 and references cited therein.

4. Truhlar, D. G., Universal Solvation Model Based on Solute Electron Density and on a Continuum Model of the Solvent Defined by the Bulk Dielectric Constant and Atomic Surface Tensions. *J. Phys. Chem. B*, **2009**, *113*, 6378–6396.

5. Winget, P.; Cramer, C. J.; Truhlar, D. G. *Theor. Chem. Acc.* **2004**, *112*, 217–227.

6. S. Trasatti.; The absolute electrode potential : an explanatory note (Recommendations 1986). Pure & AppL Chem., Vol. 58, No.7, pp. 955—966, 1986.

5. Copies of NMR Spectra

^{1}H NMR ($CDCl_3$, 400 MHz) of **3a**

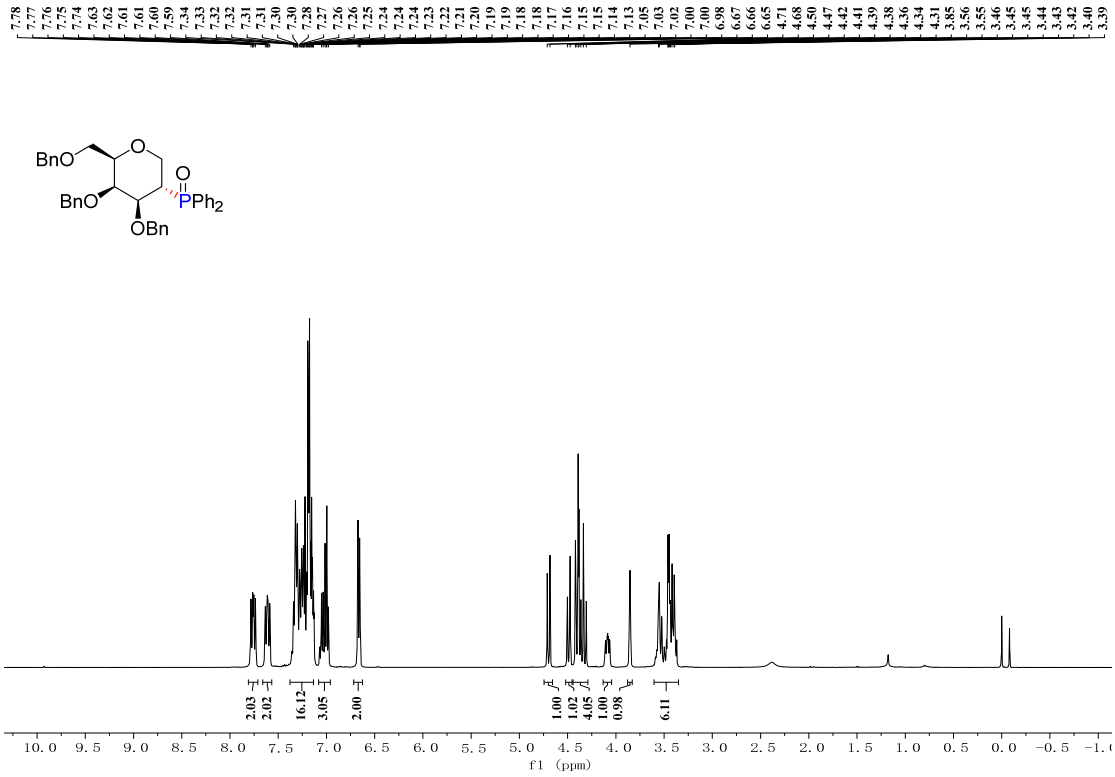

^{13}C NMR ($CDCl_3$, 100 MHz) of **3a**

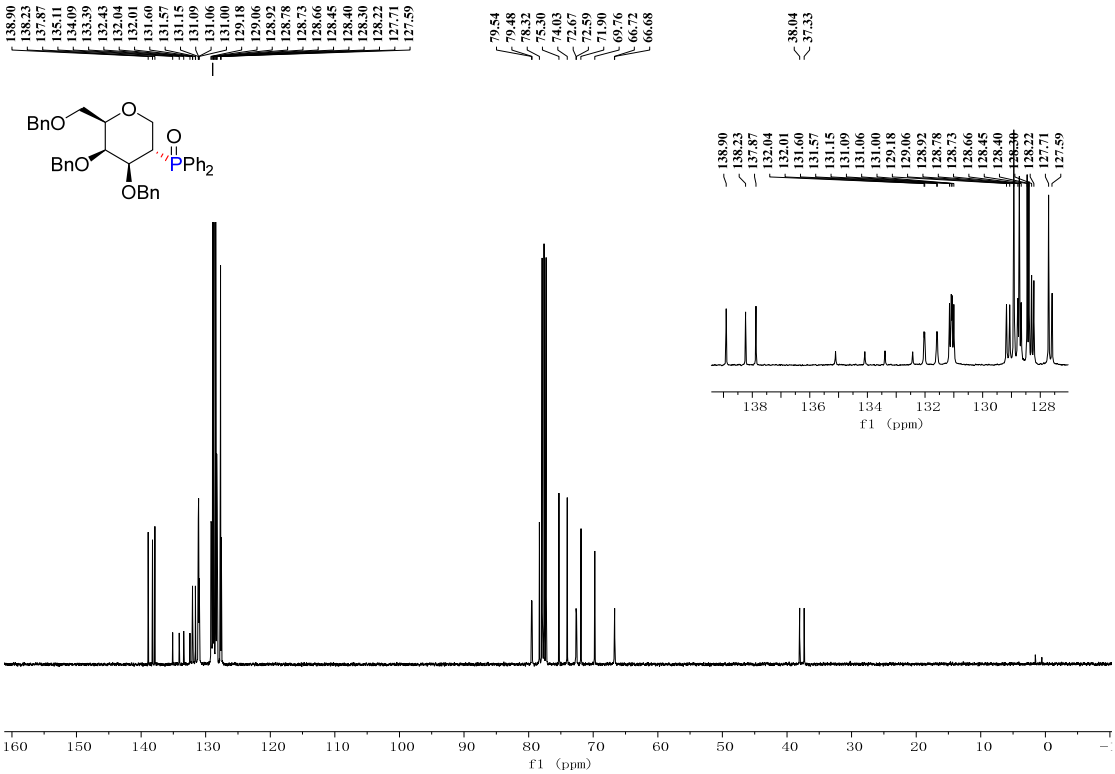

^{31}P NMR ($CDCl_3$, 162 MHz) **of 3a**

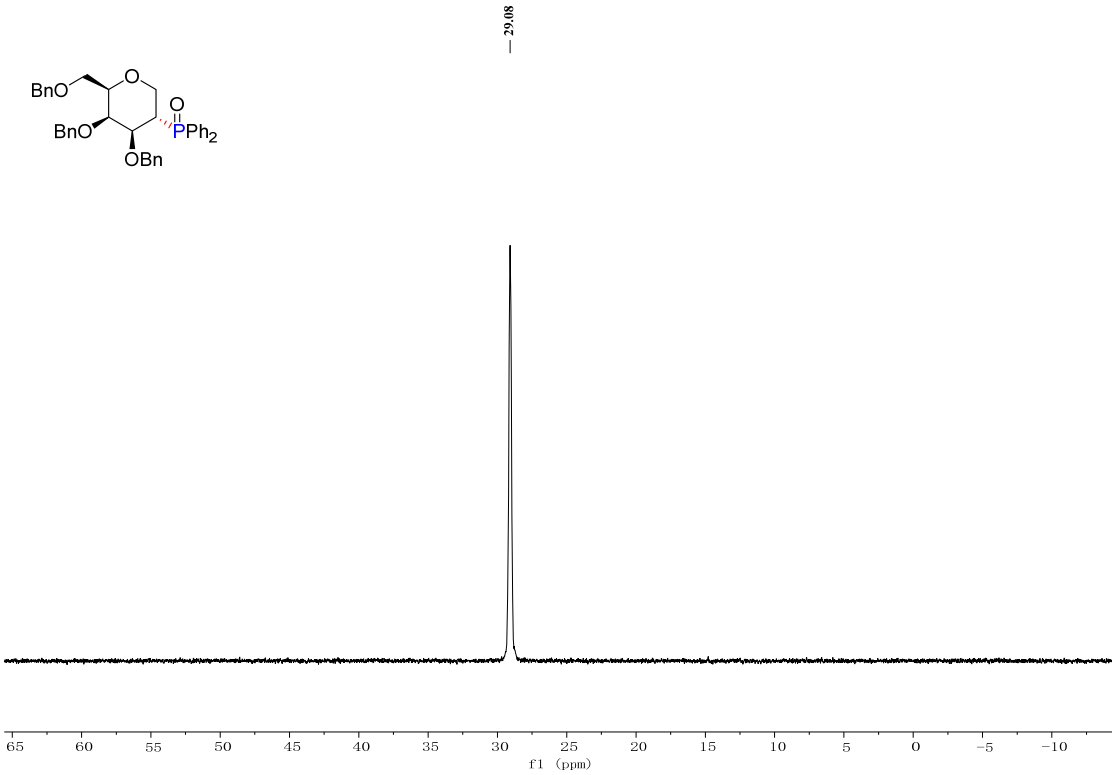

^{1}H NMR ($CDCl_3$, 400 MHz) **of 3b**

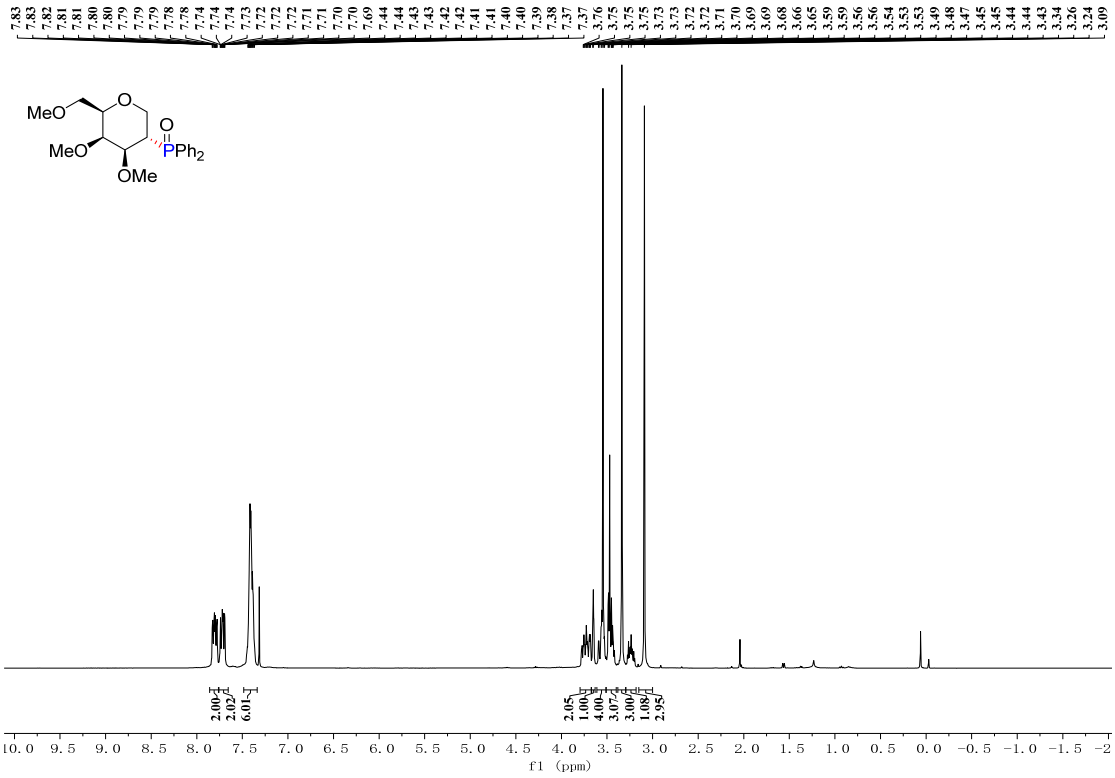

^{13}C NMR ($CDCl_3$, 100 MHz) of 3b

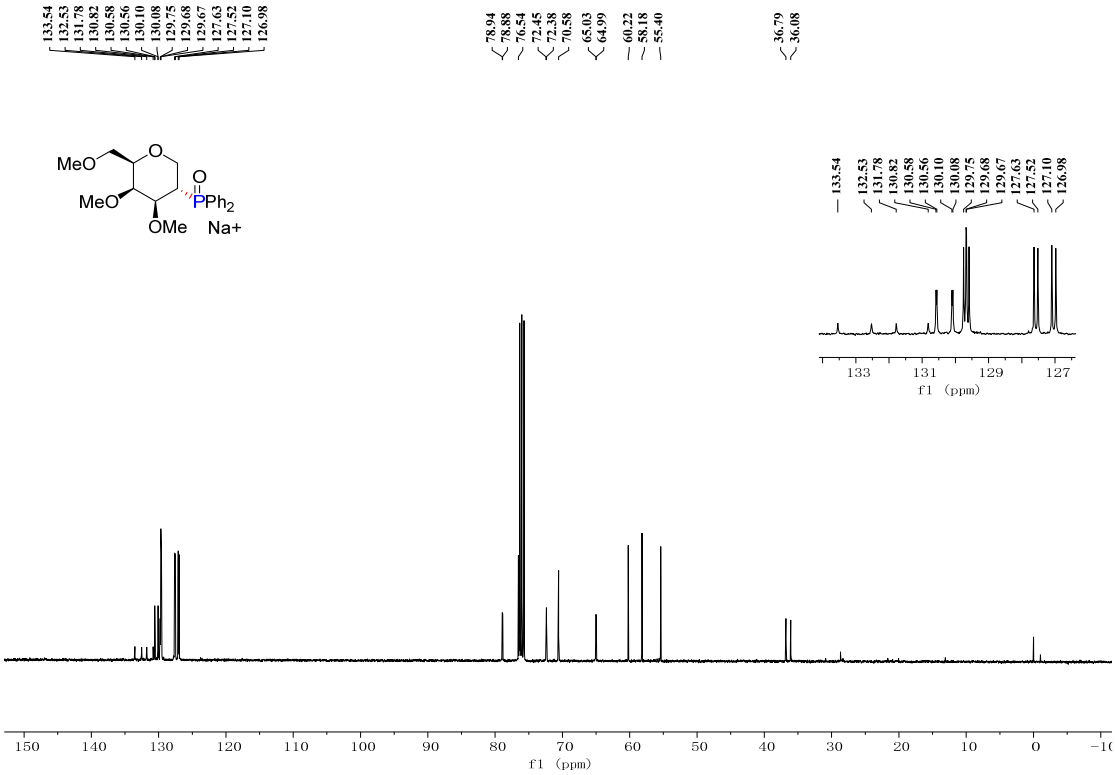

^{31}P NMR ($CDCl_3$, 162 MHz) of 3b

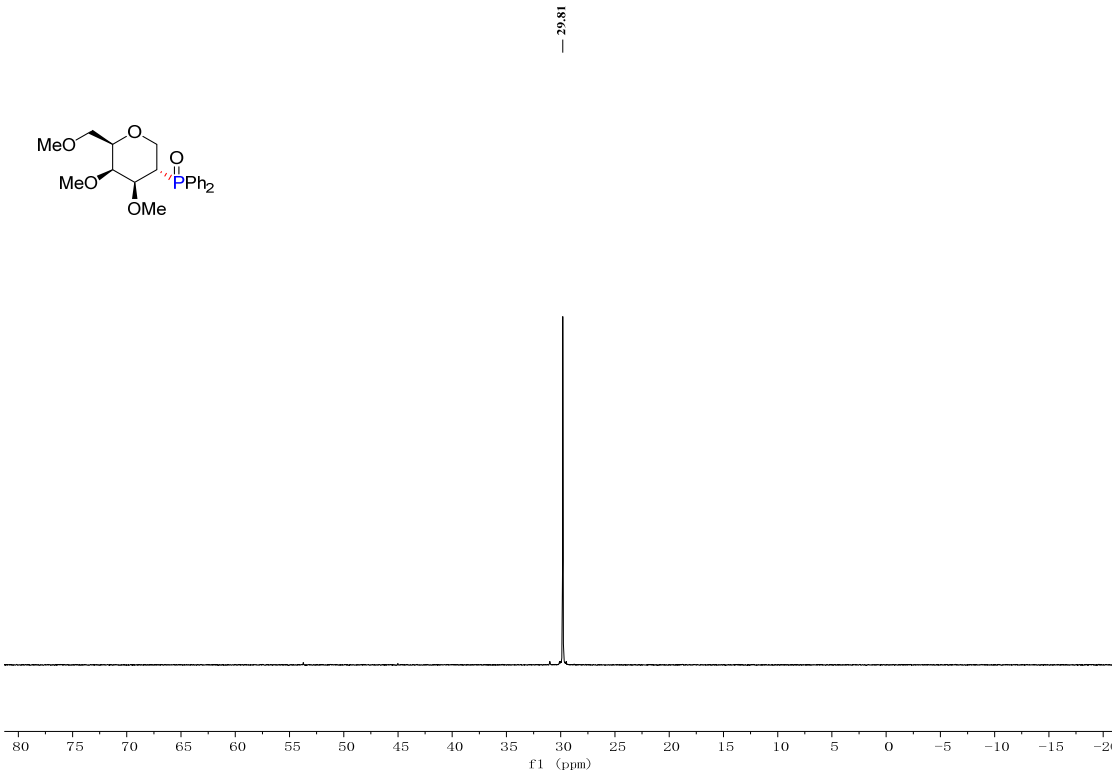

^{1}H NMR ($CDCl_3$, 400 MHz) of 3c

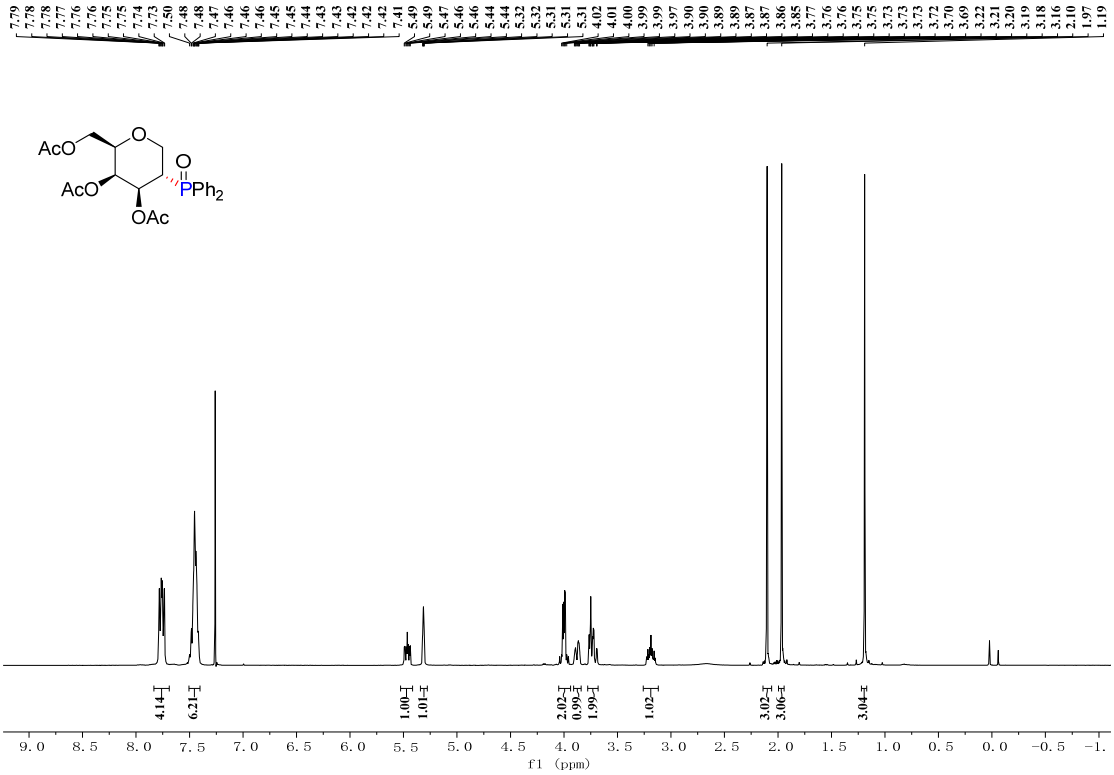

^{13}C NMR ($CDCl_3$, 100 MHz) of **3c**

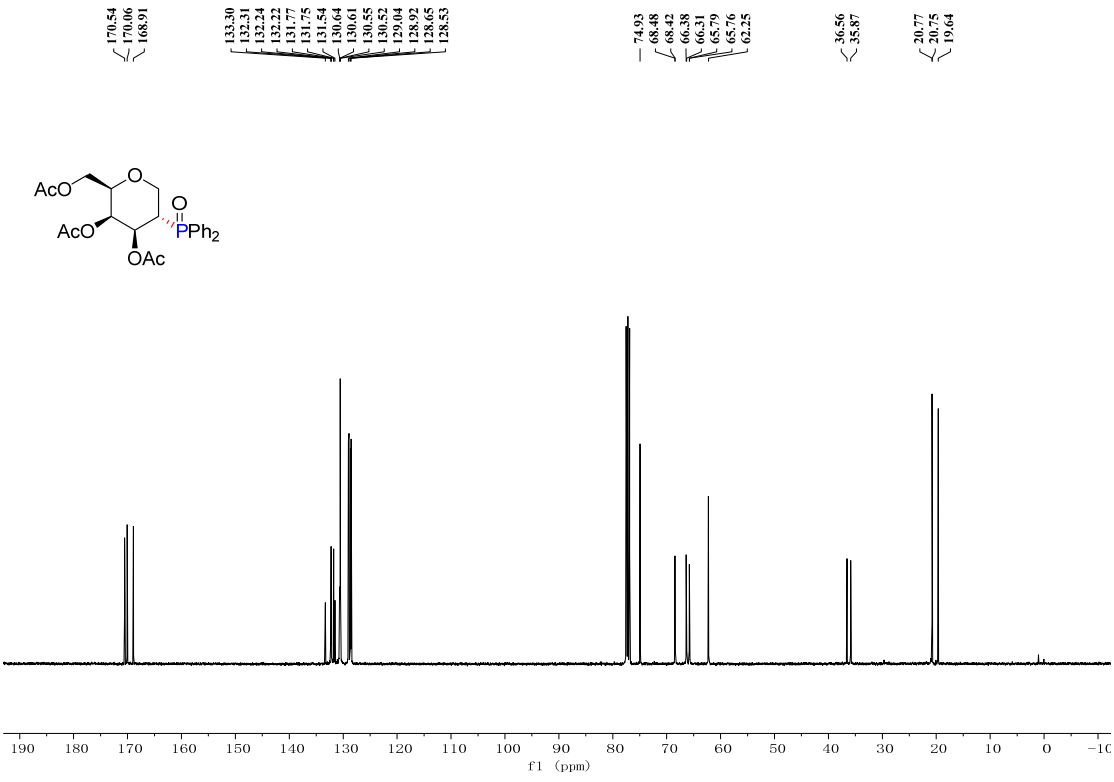

^{31}P NMR ($CDCl_3$, 162 MHz) of **3c**

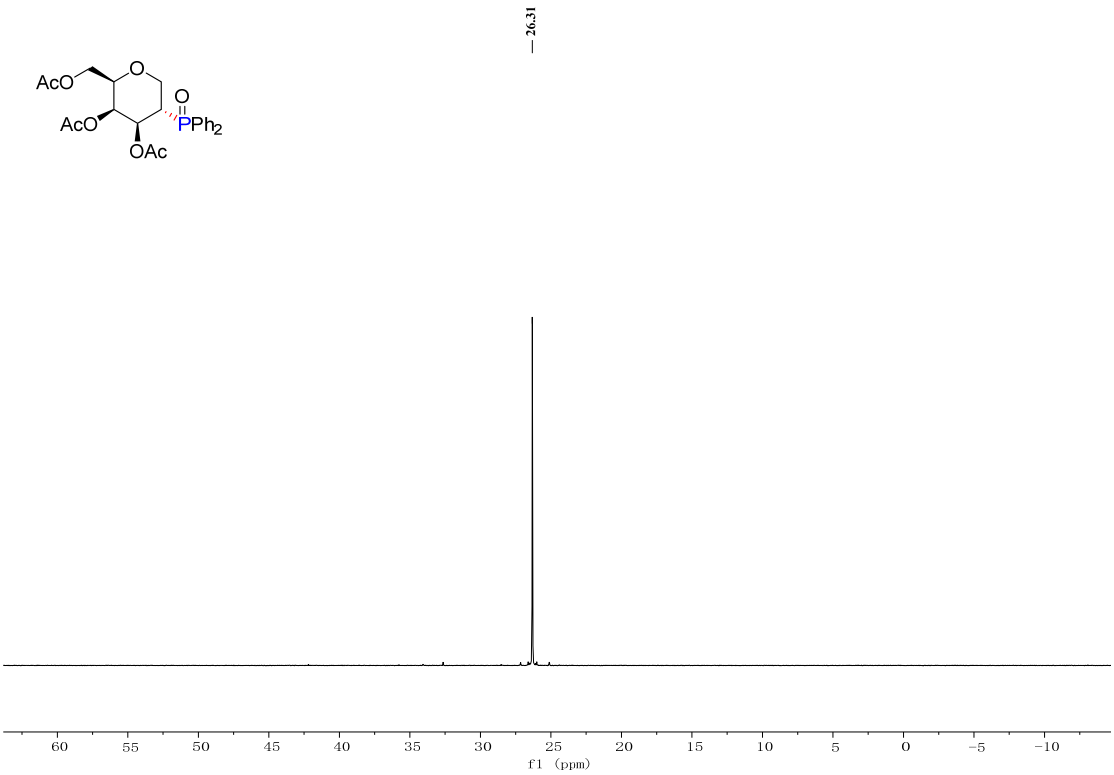

^{1}H NMR ($CDCl_3$, 400 MHz) of **3d**

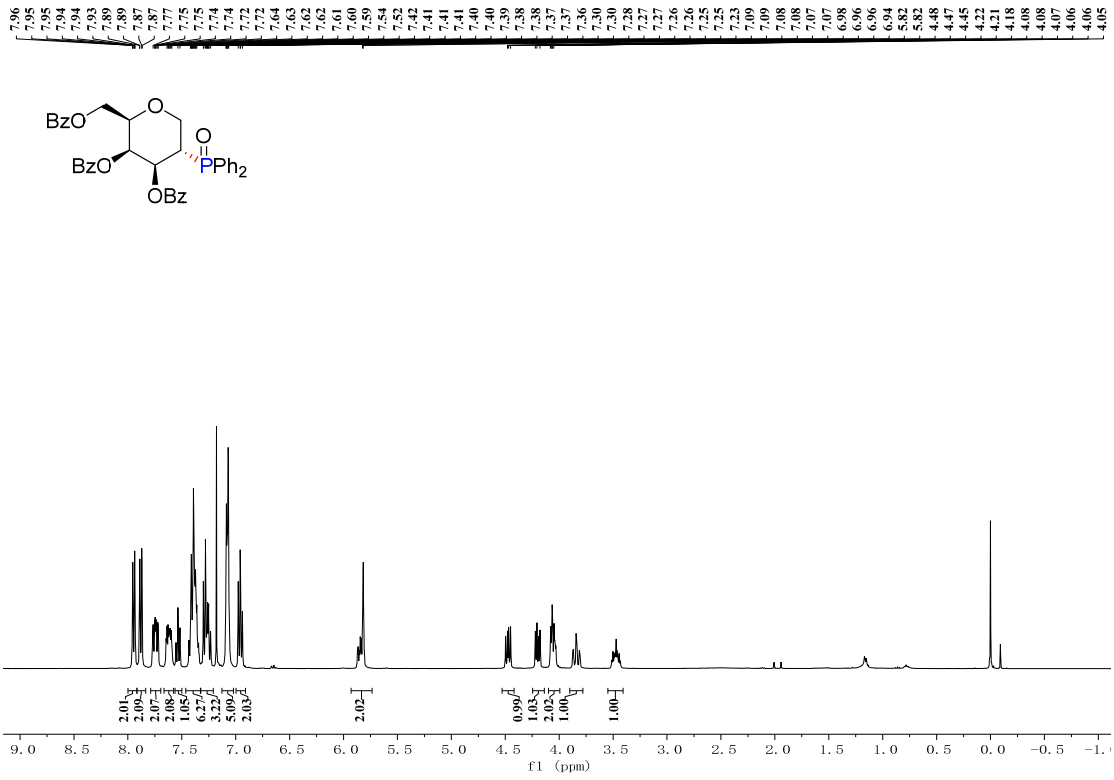

^{13}C NMR ($CDCl_3$, 100 MHz) of **3d**

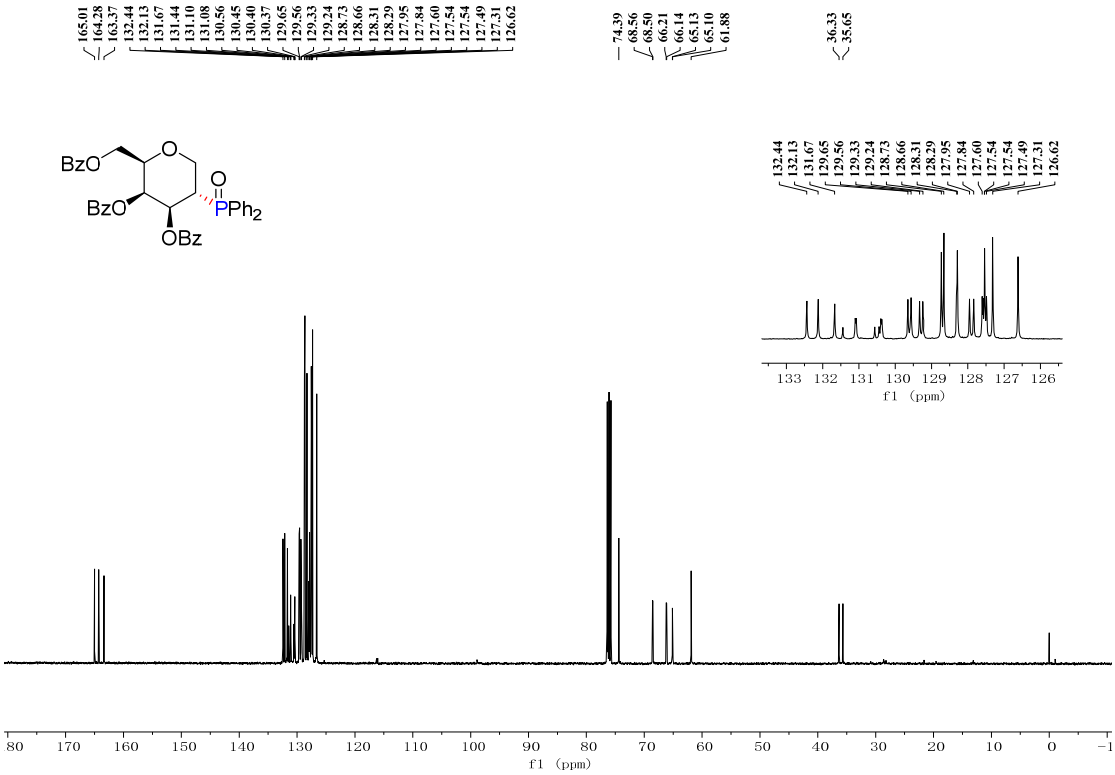

^{31}P NMR ($CDCl_3$, 162 MHz) of **3d**

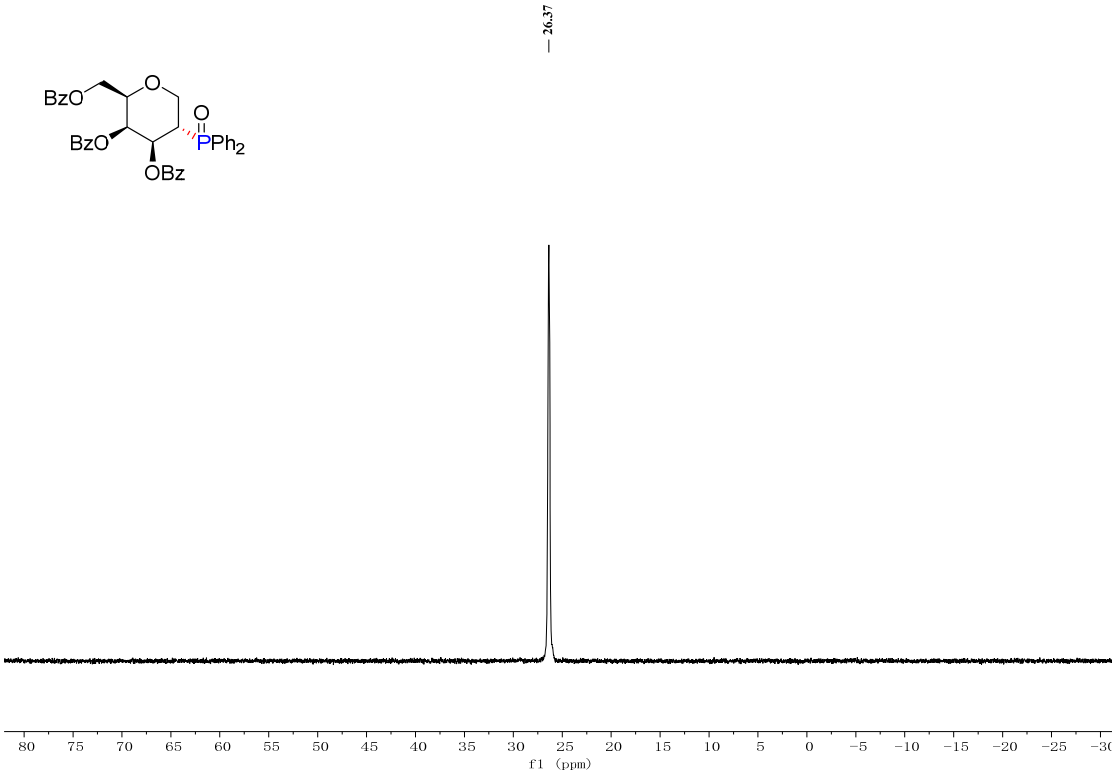

^{1}H NMR ($CDCl_3$, 400 MHz) of **3e**

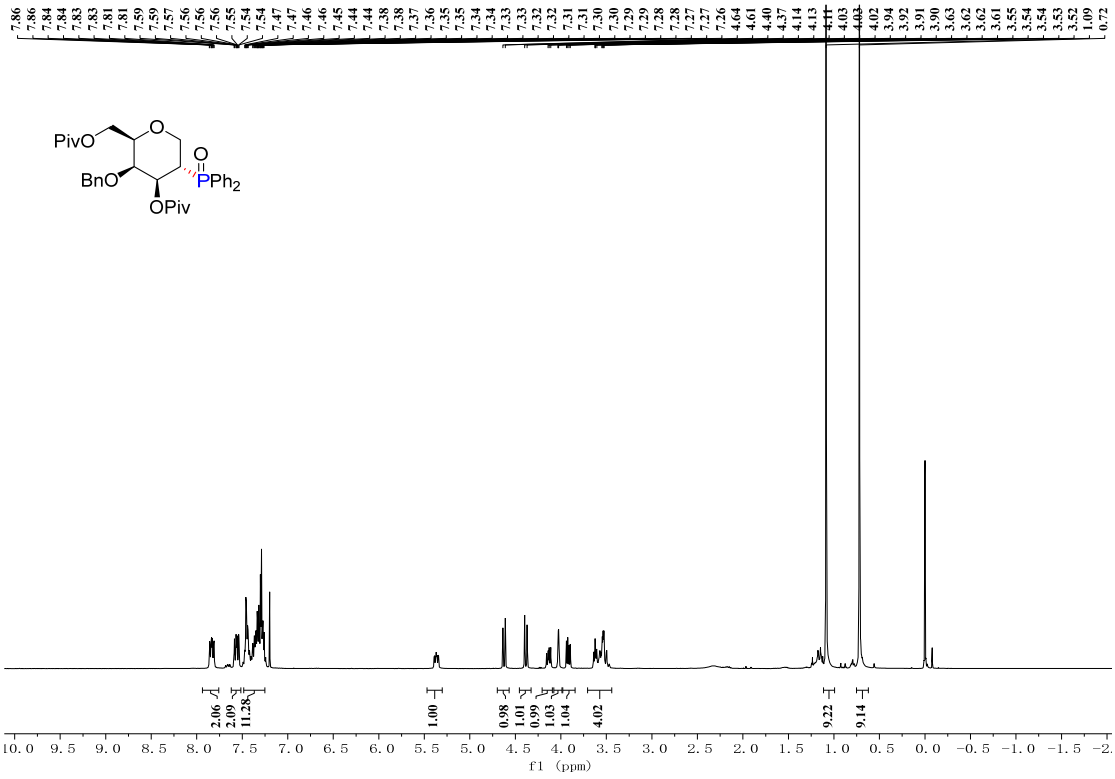

^{13}C NMR ($CDCl_3$, 100 MHz) of **3e**

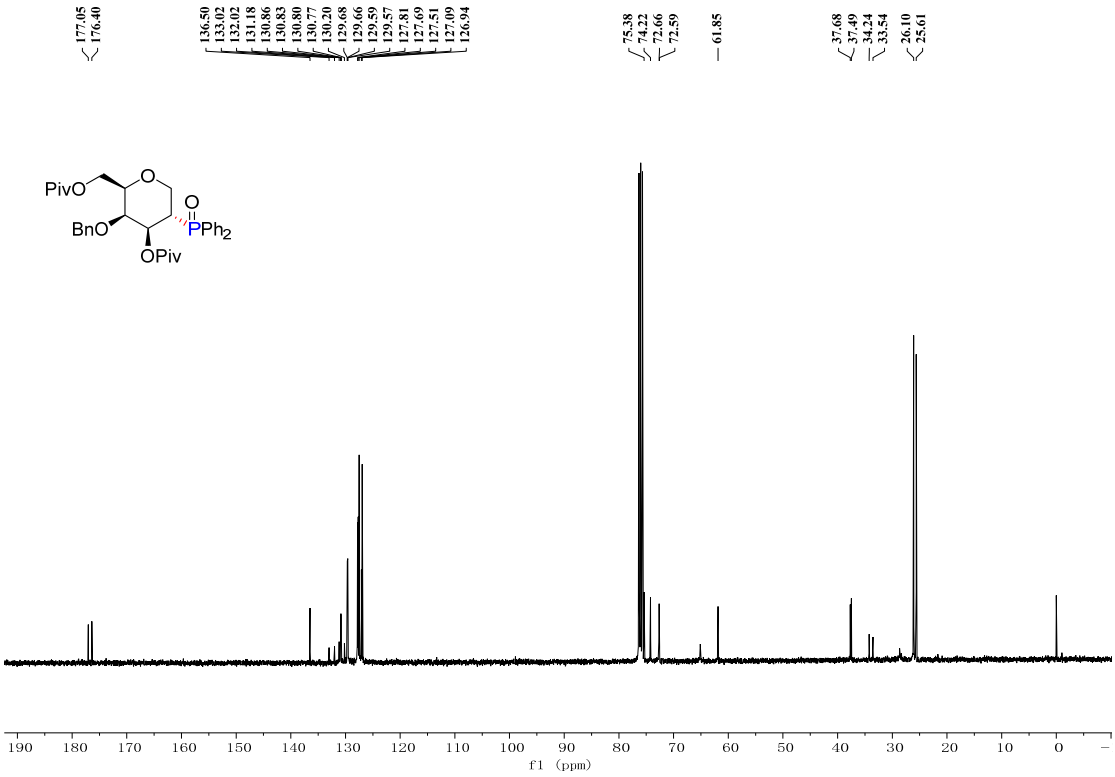

^{31}P NMR ($CDCl_3$, 162 MHz) of **3e**

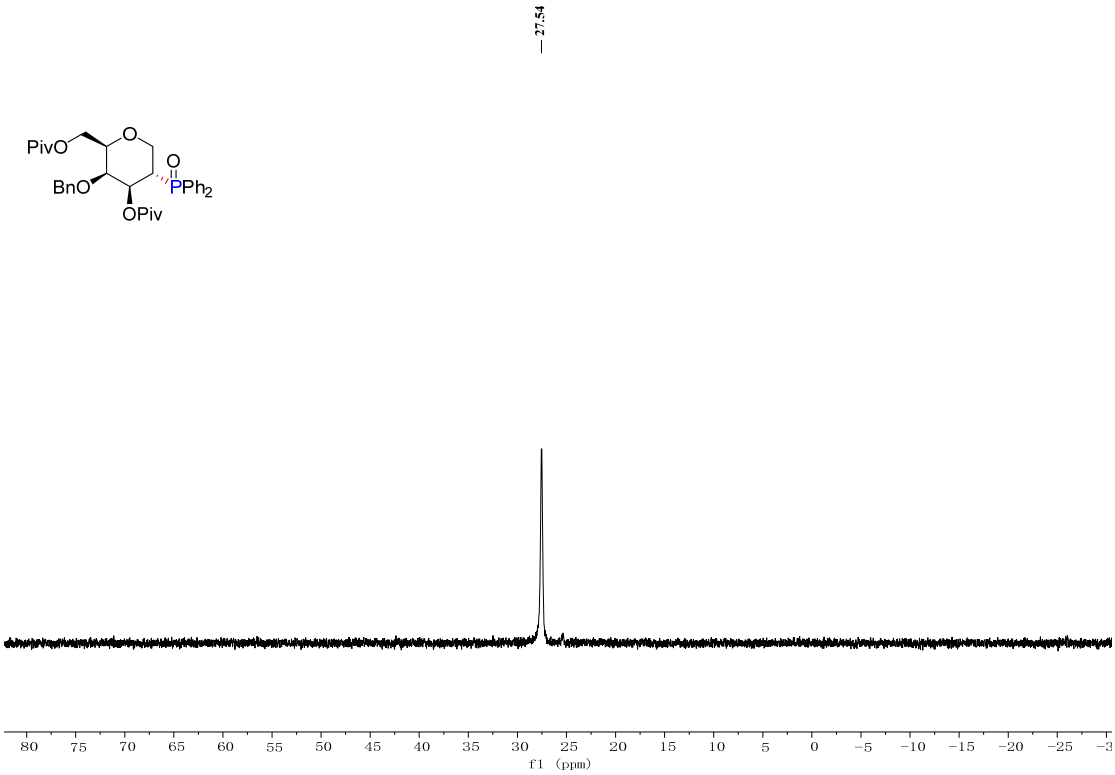

^{1}H NMR ($CDCl_3$, 400 MHz) of **3f**

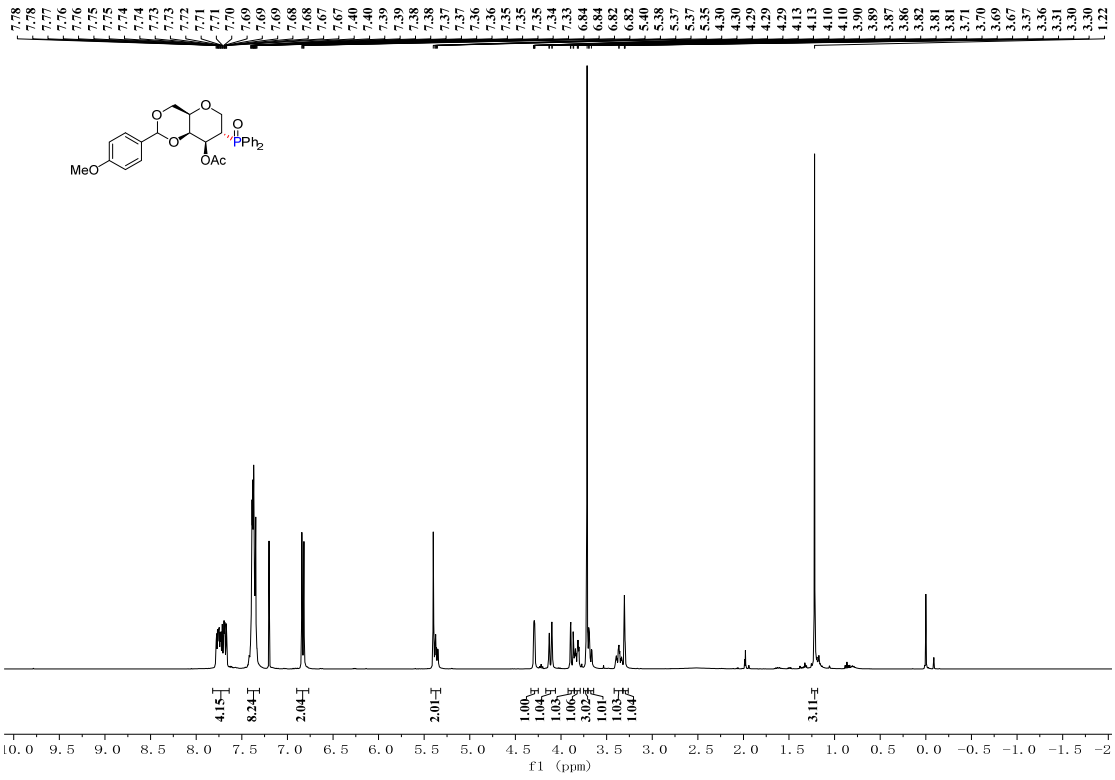

^{13}C NMR ($CDCl_3$, 100 MHz) of **3f**

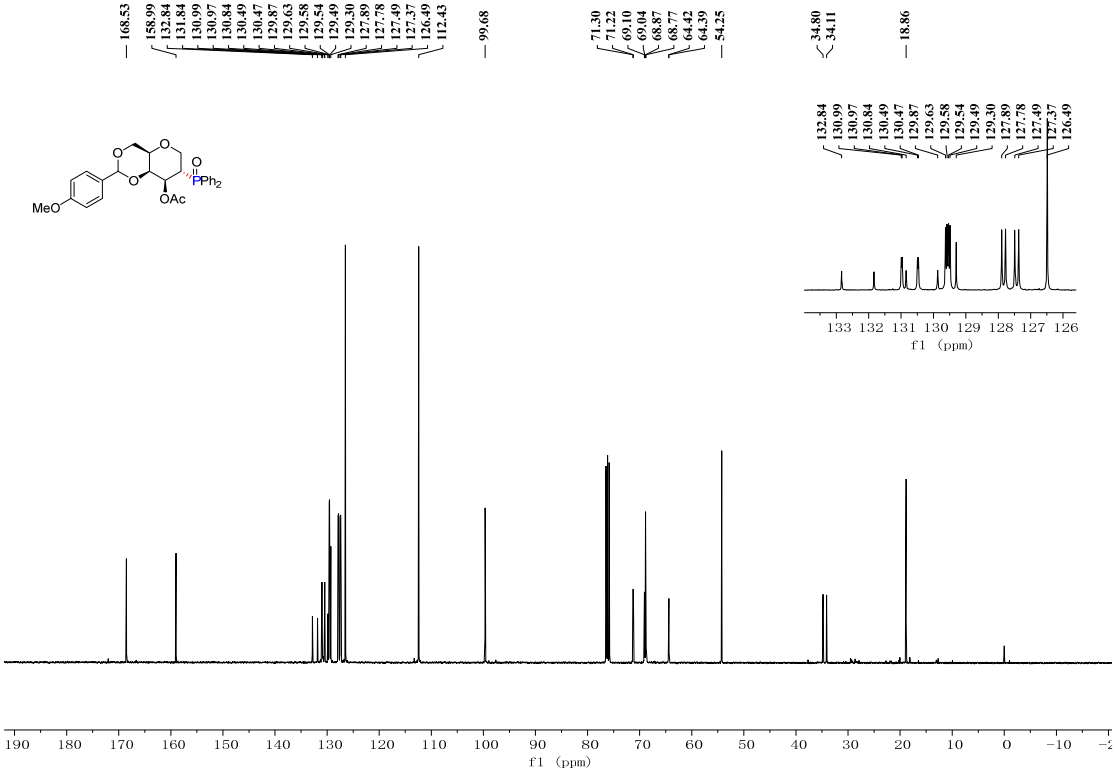

^{31}P NMR ($CDCl_3$, 162 MHz) of **3f**

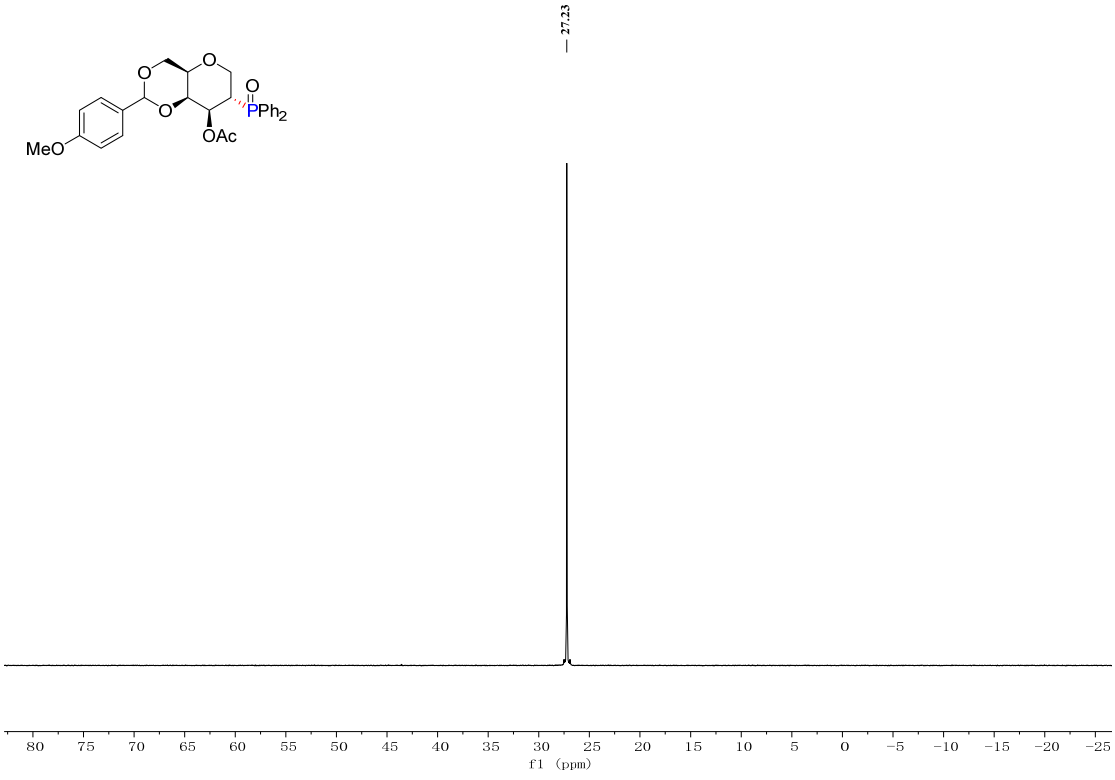

^{1}H NMR ($CDCl_3$, 400 MHz) of **3g**

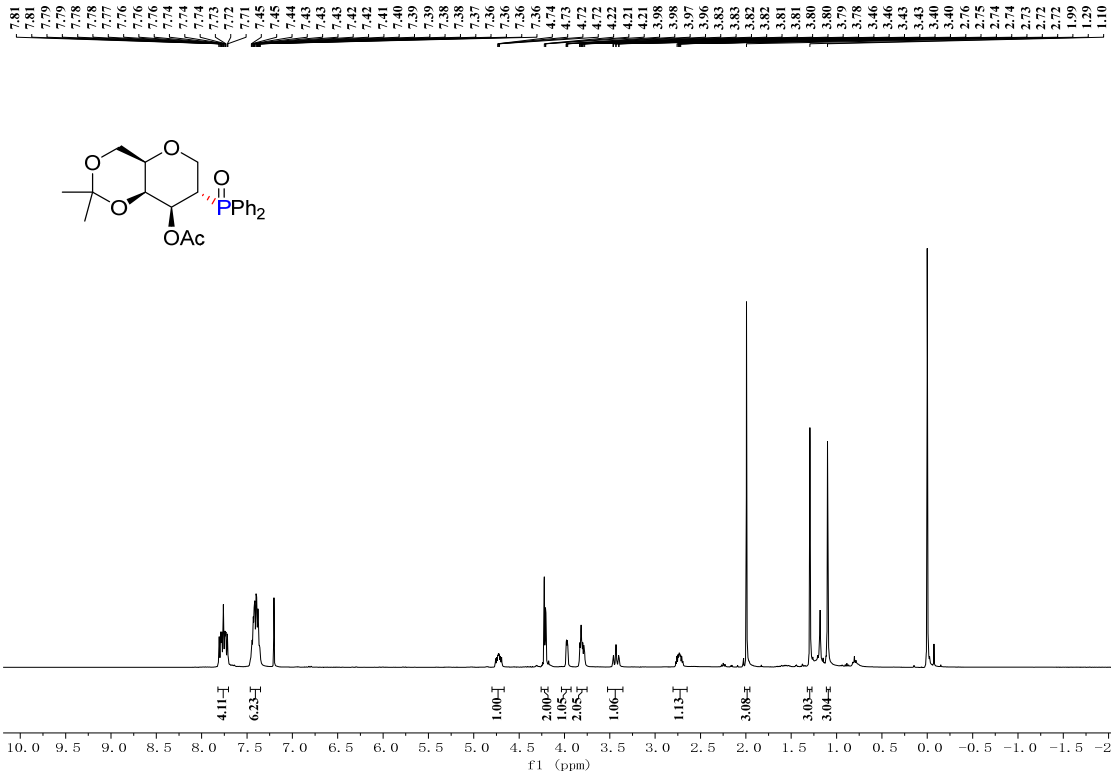

^{13}C NMR ($CDCl_3$, 100 MHz) of **3g**

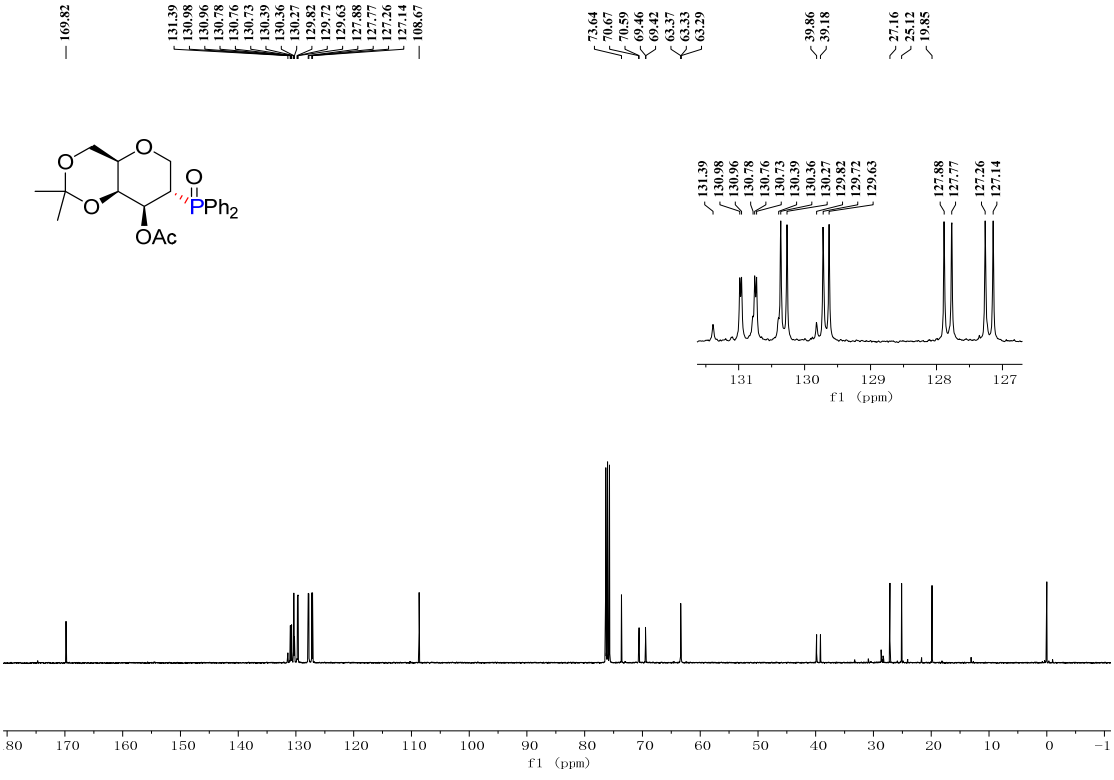

^{31}P NMR ($CDCl_3$, 162 MHz) of **3g**

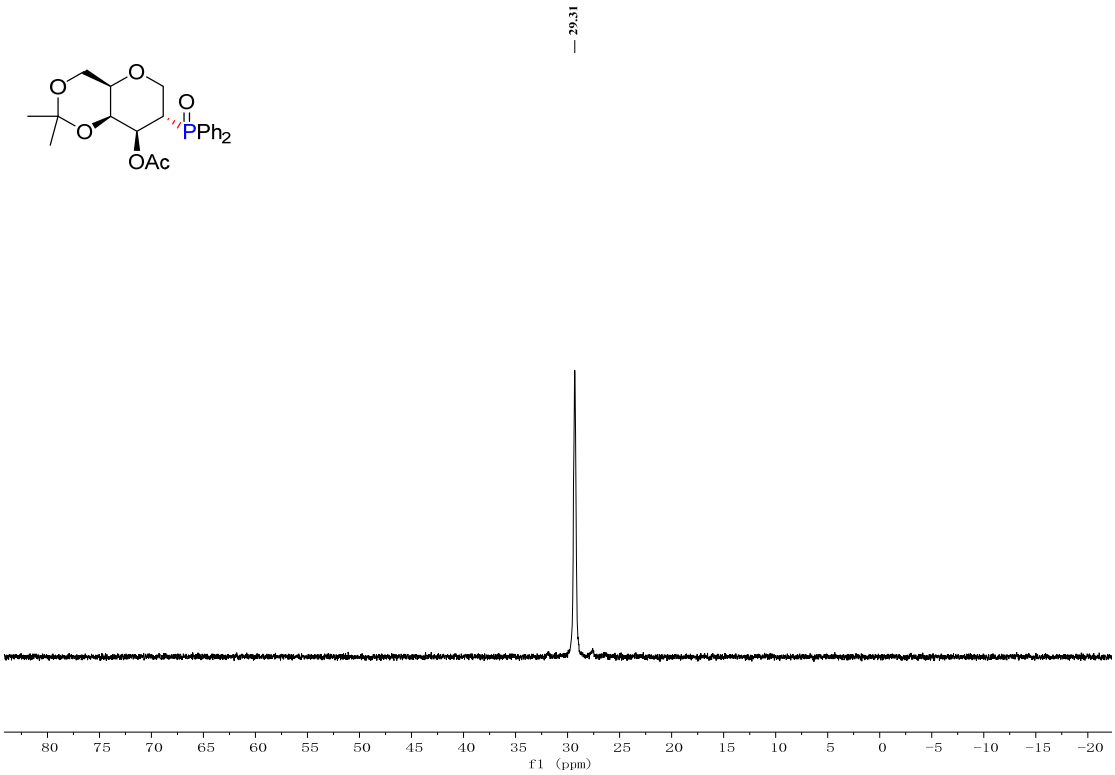

^{1}H NMR ($CDCl_3$, 400 MHz) of **3h**

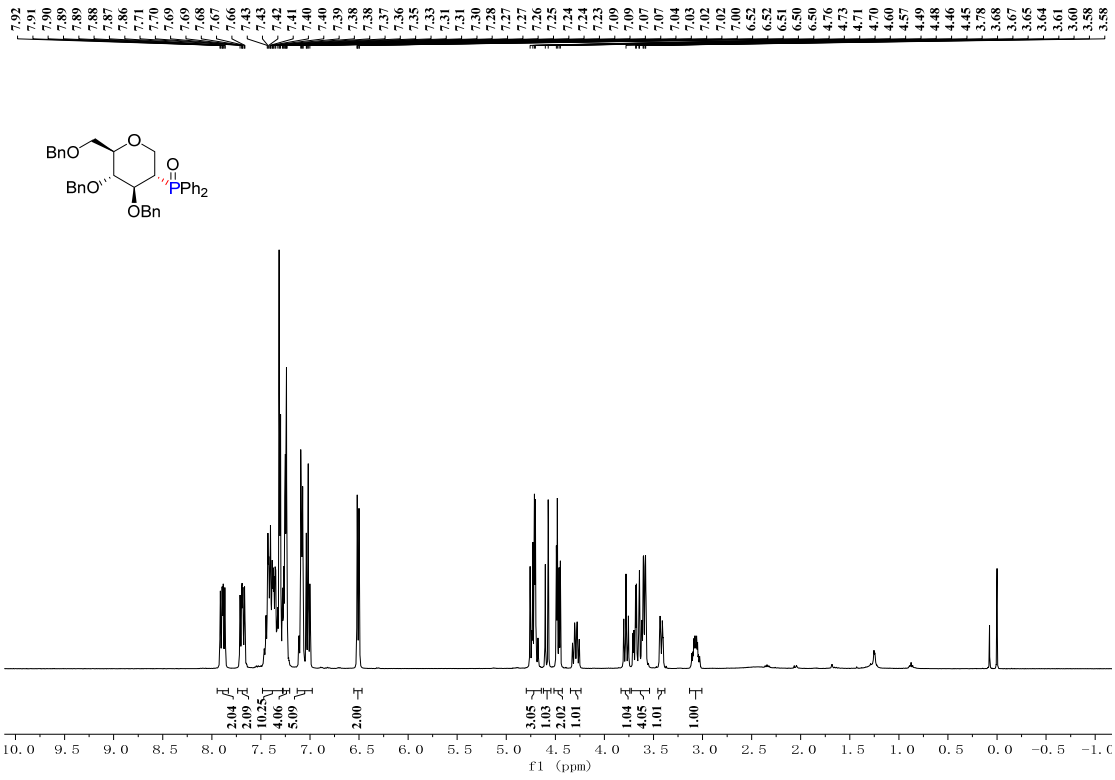

^{13}C NMR ($CDCl_3$, 100 MHz) of **3h**

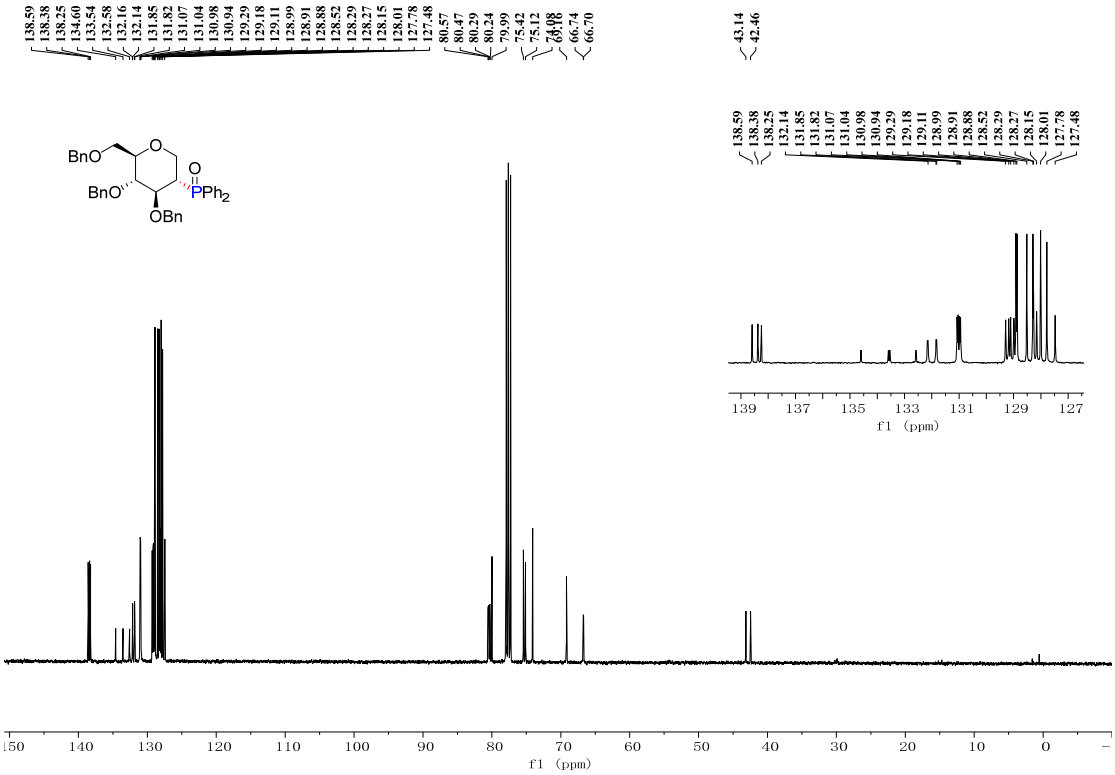

^{31}P NMR ($CDCl_3$, 162 MHz) of **3h**

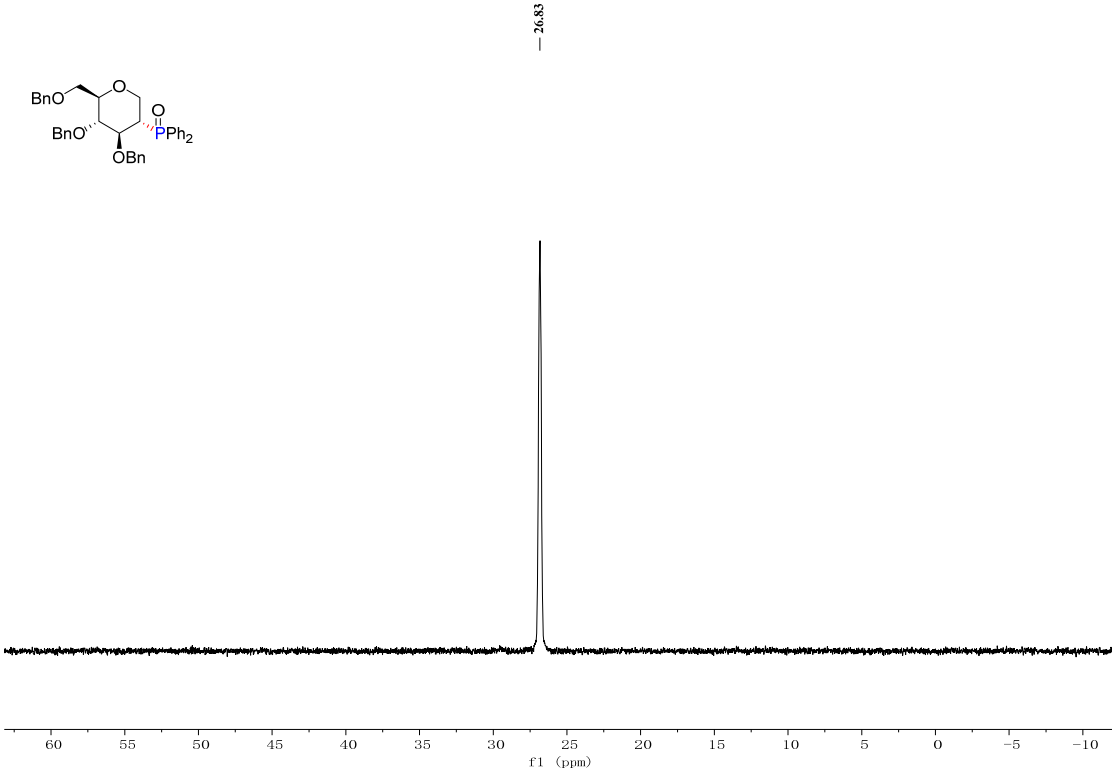

^{1}H NMR ($CDCl_3$, 400 MHz) of **3h'**

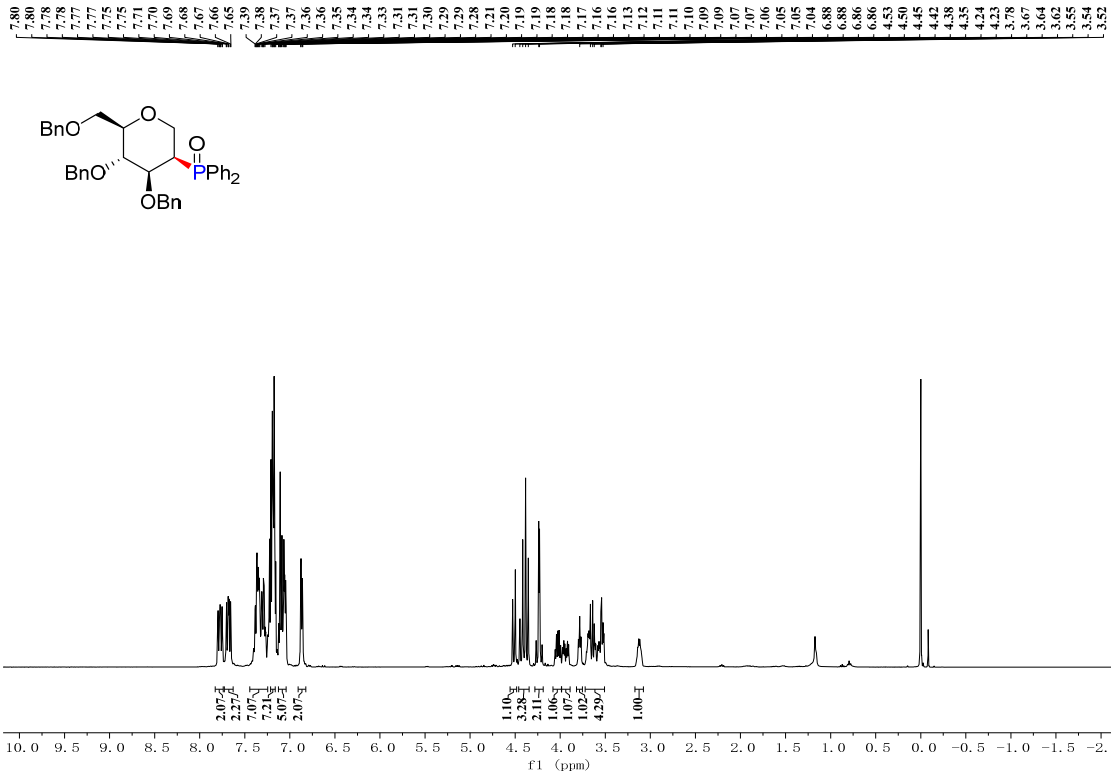

^{13}C NMR ($CDCl_3$, 100 MHz) of **3h'**

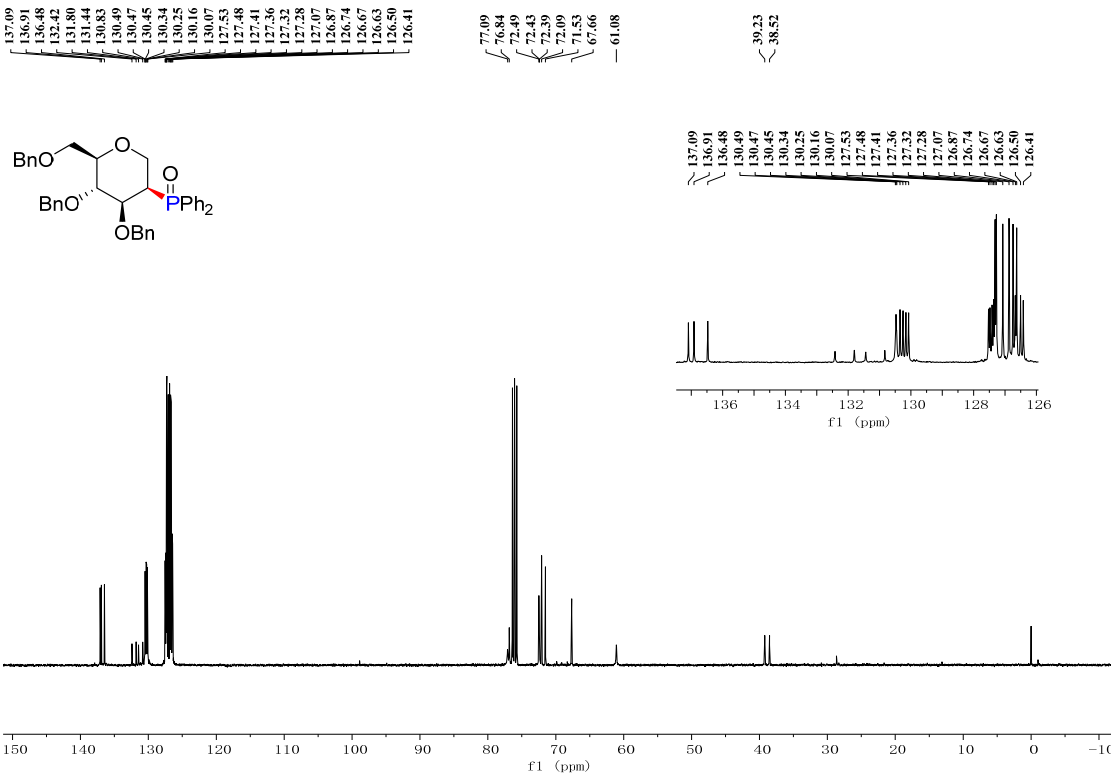

^{31}P NMR ($CDCl_3$, 162 MHz) of **3h'**

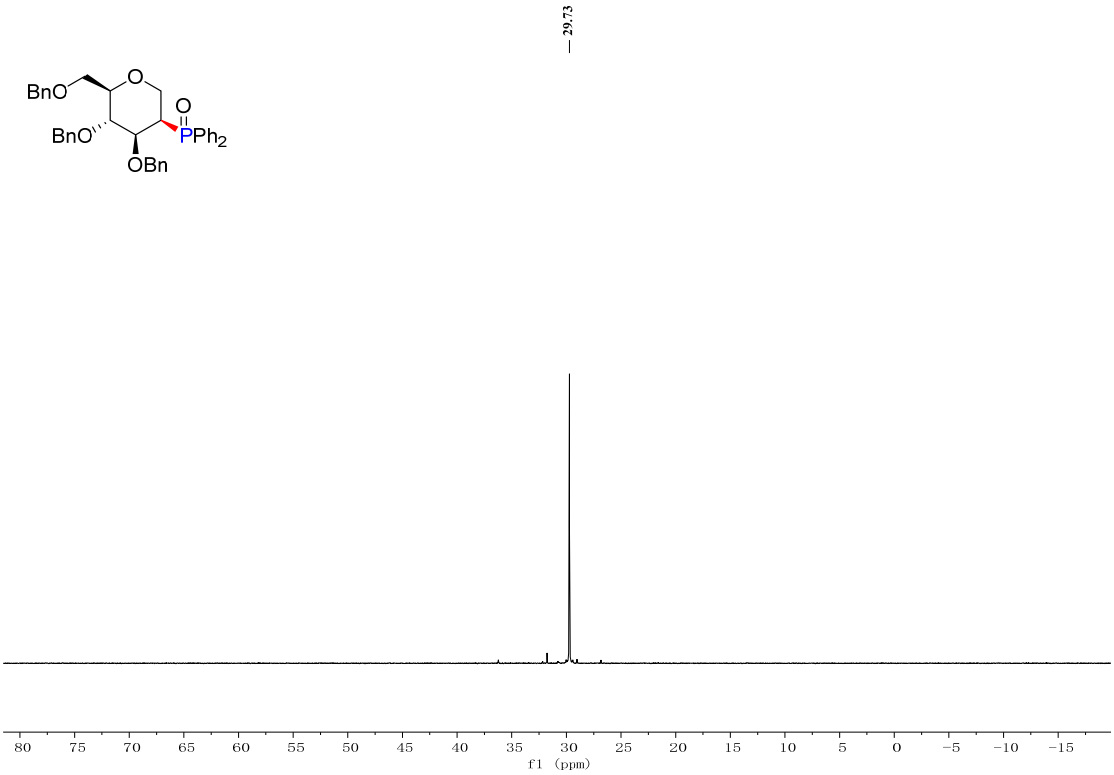

^{1}H NMR ($CDCl_3$, 400 MHz) of **3i**

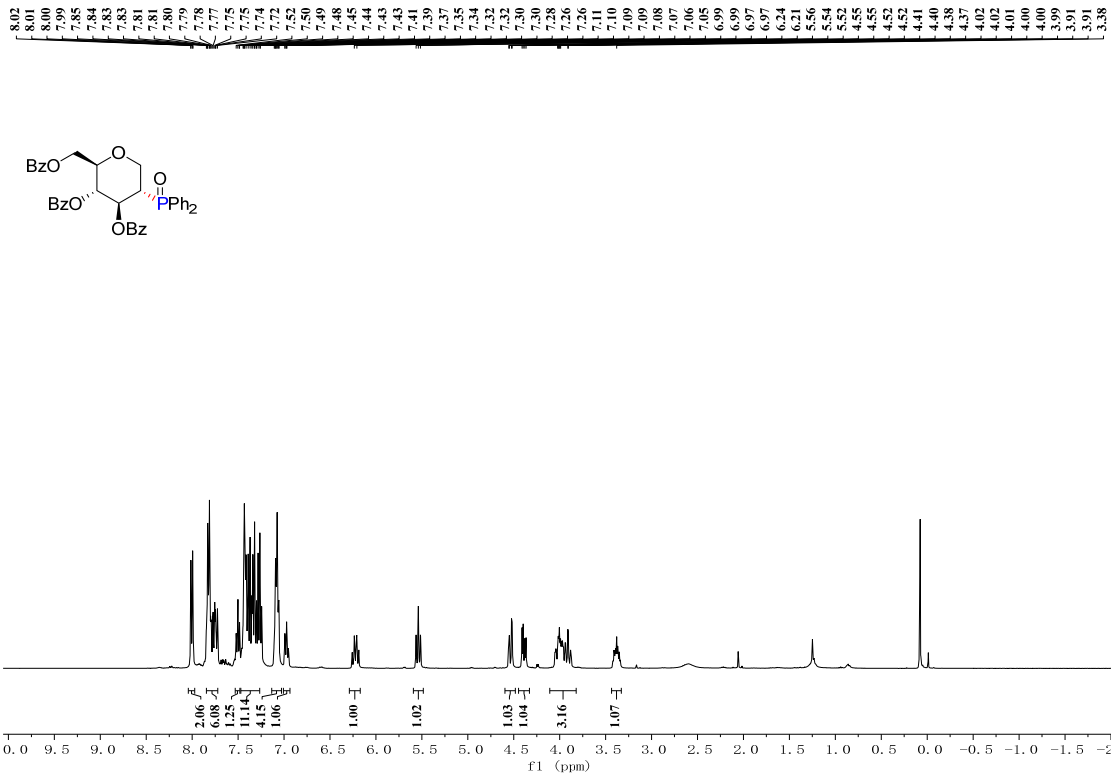

^{13}C NMR ($CDCl_3$, 100 MHz) of **3i**

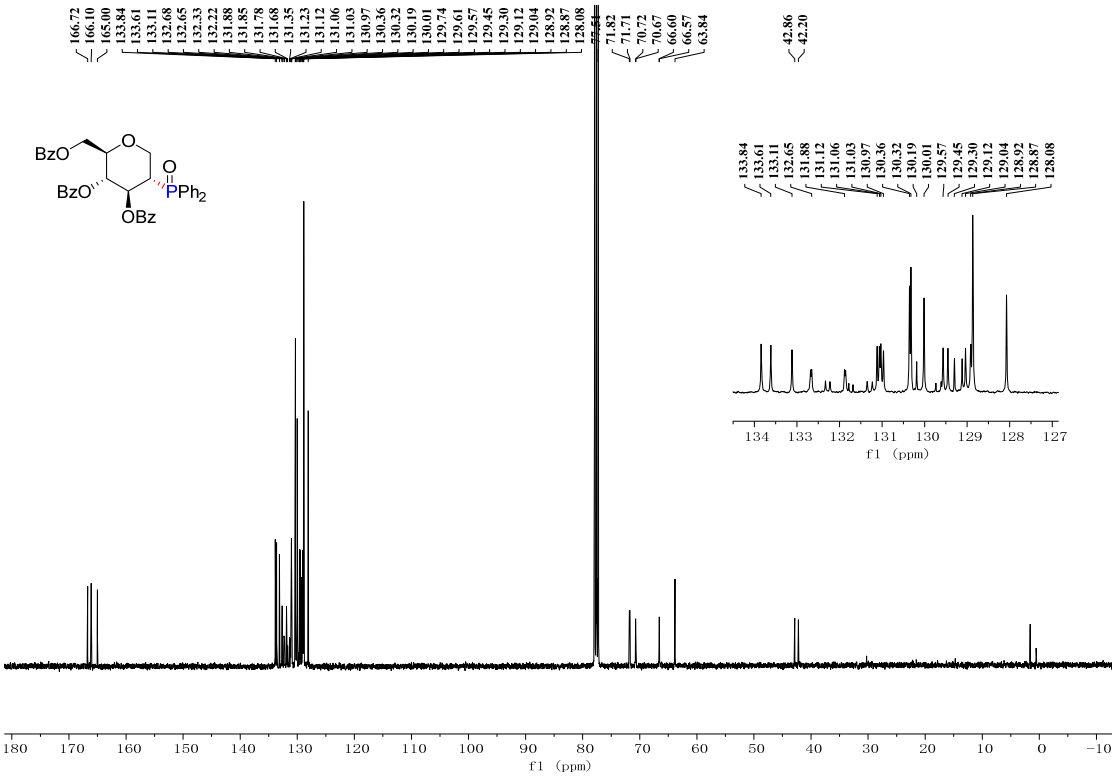

^{31}P NMR ($CDCl_3$, 162 MHz) of **3i**

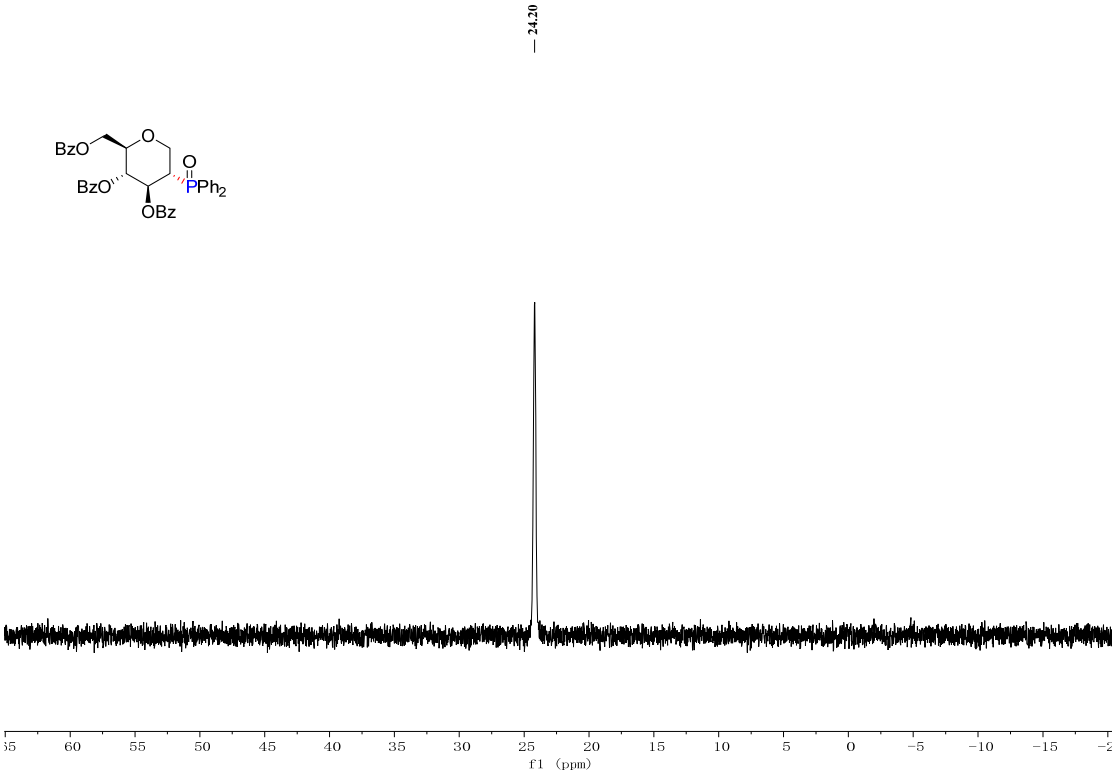

^{1}H NMR ($CDCl_3$, 400 MHz) of **3i'**

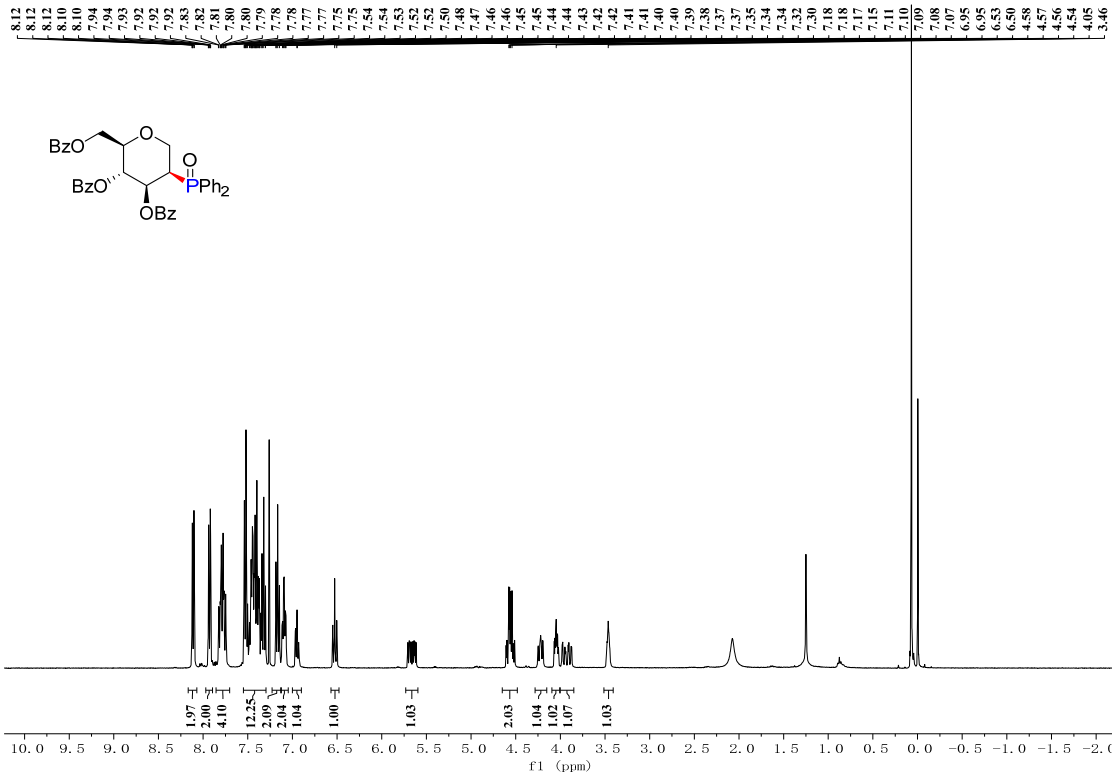

^{13}C NMR ($CDCl_3$, 100 MHz) of **3i'**

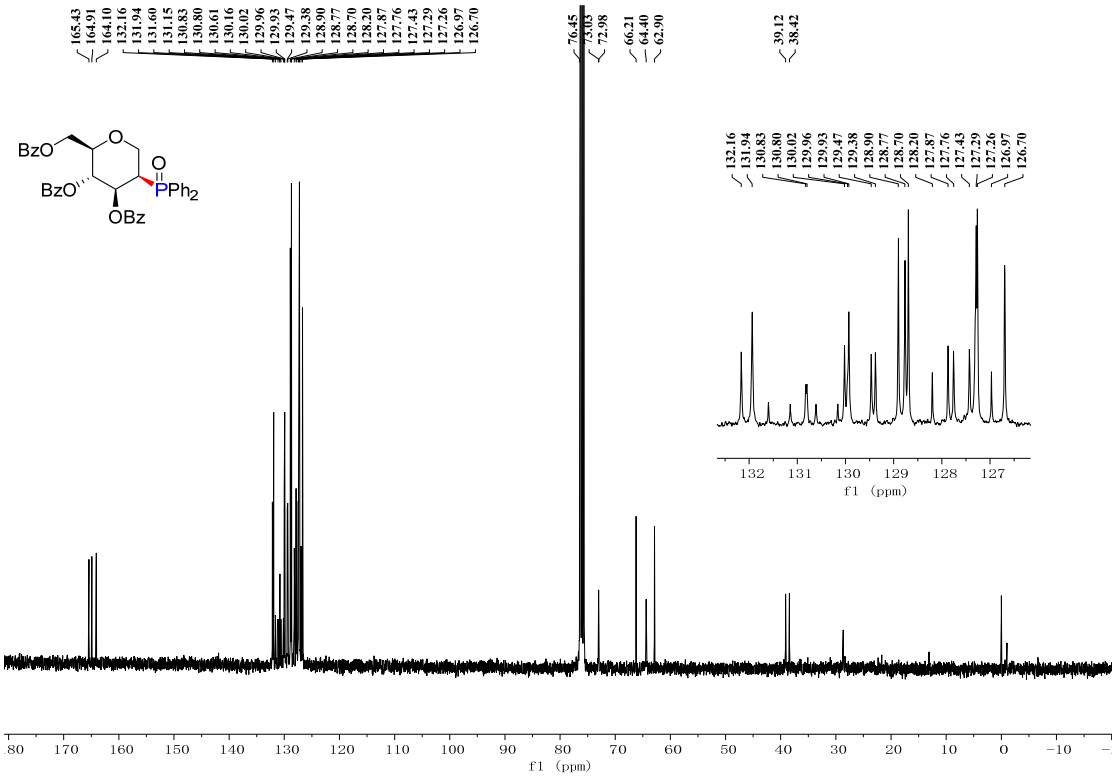

^{31}P NMR ($CDCl_3$, 162 MHz) of **3i'**

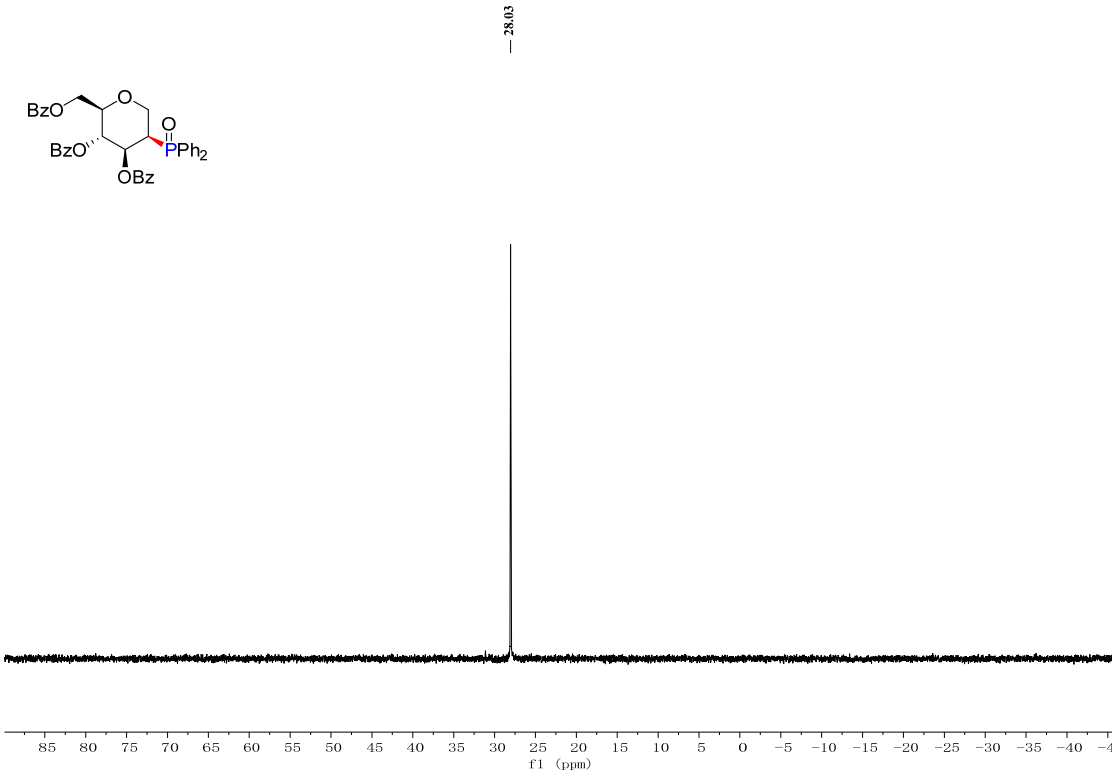

^{1}H NMR ($CDCl_3$, 400 MHz) of **3j**

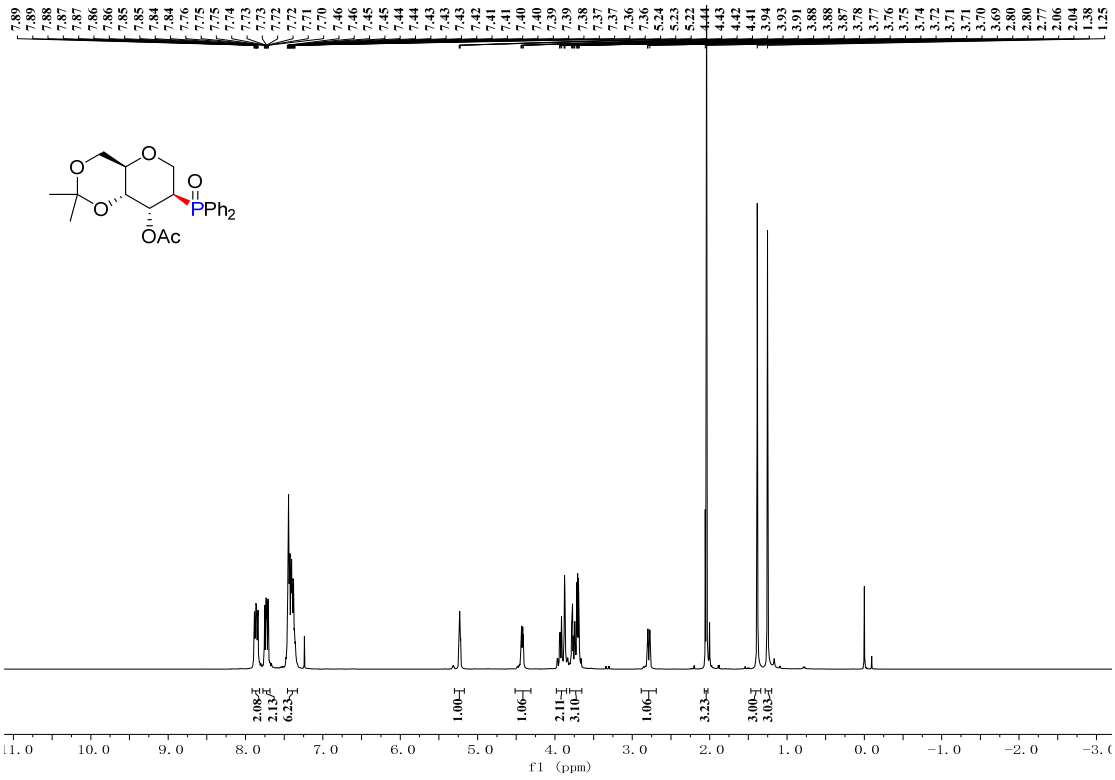

^{13}C NMR ($CDCl_3$, 100 MHz) of **3j**

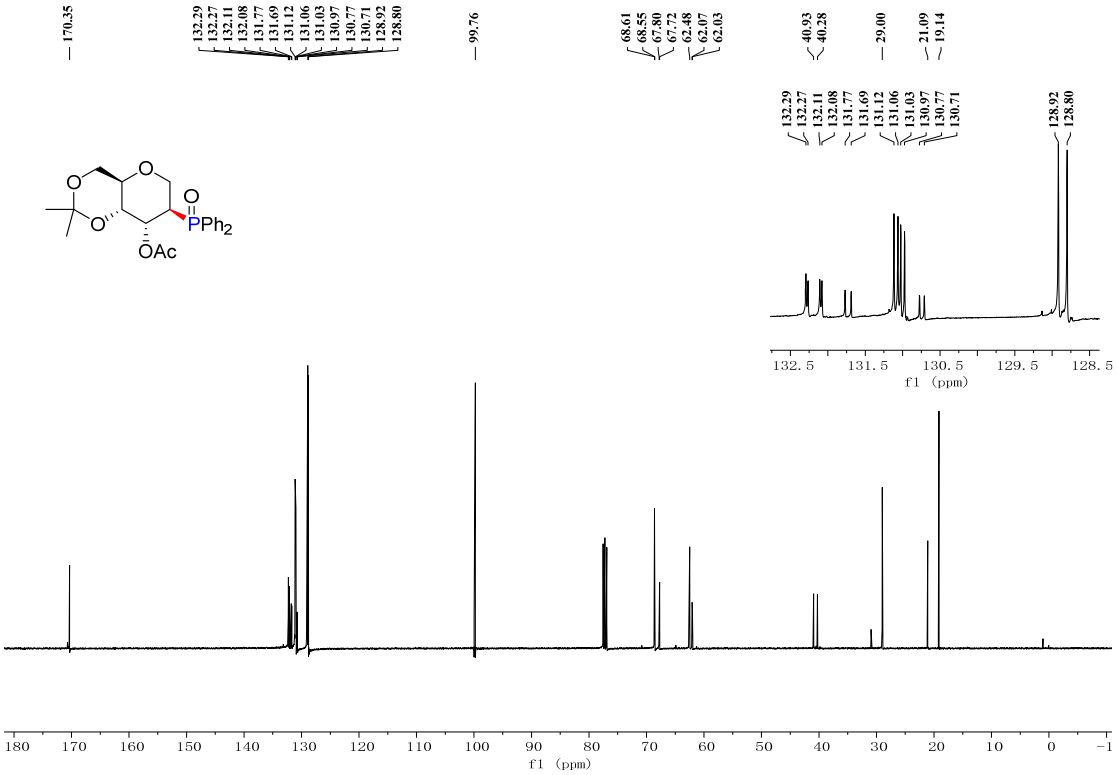

^{31}P NMR ($CDCl_3$, 162 MHz) of **3j**

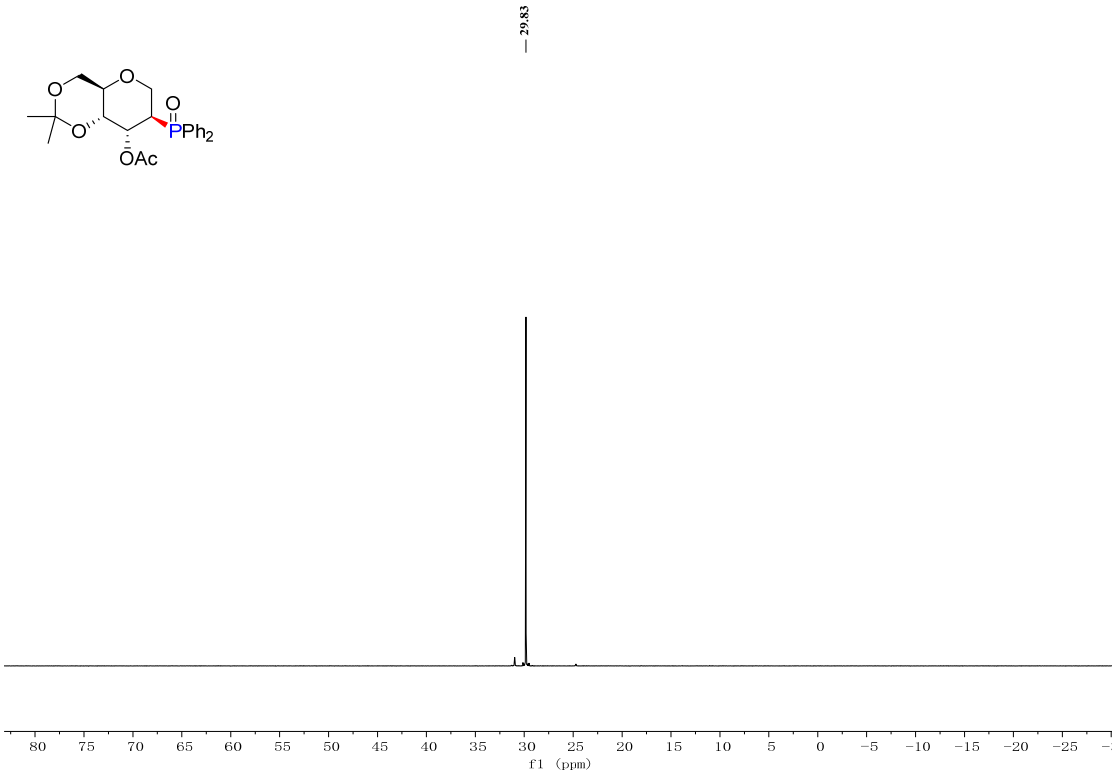

^{1}H NMR ($CDCl_3$, 400 MHz) of **3k**

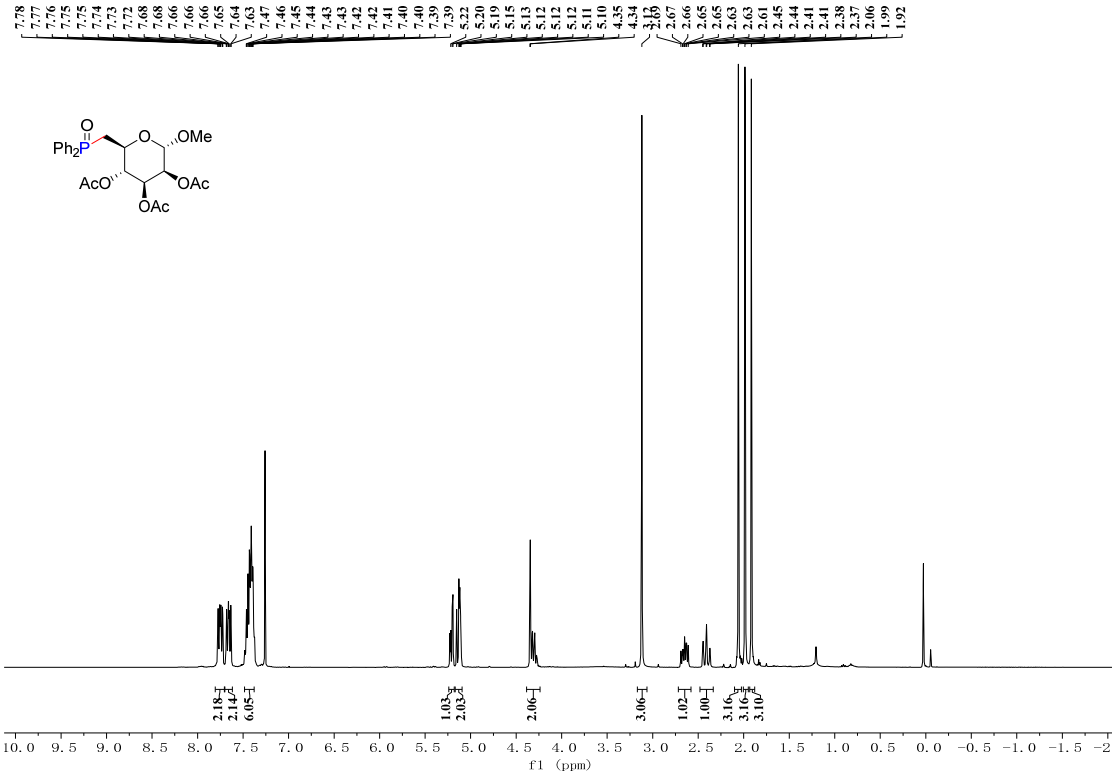

^{13}C NMR ($CDCl_3$, 100 MHz) of **3k**

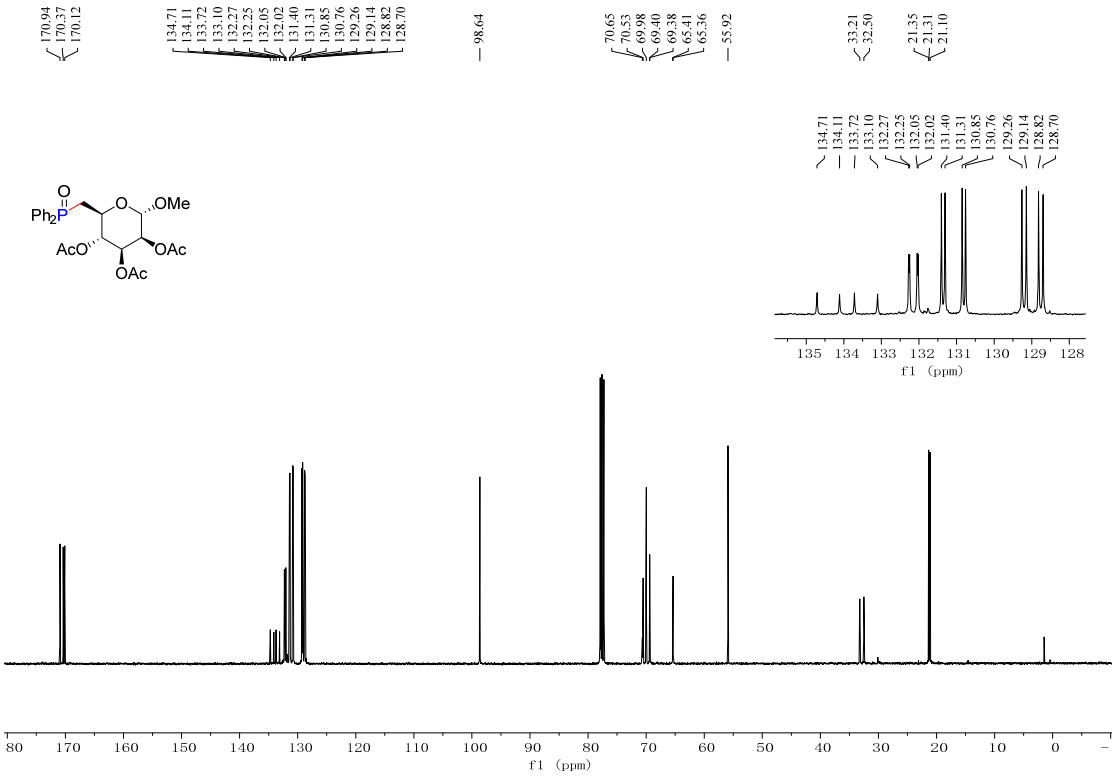

^{31}PNMR ($CDCl_3$, 162 MHz) of **3k**

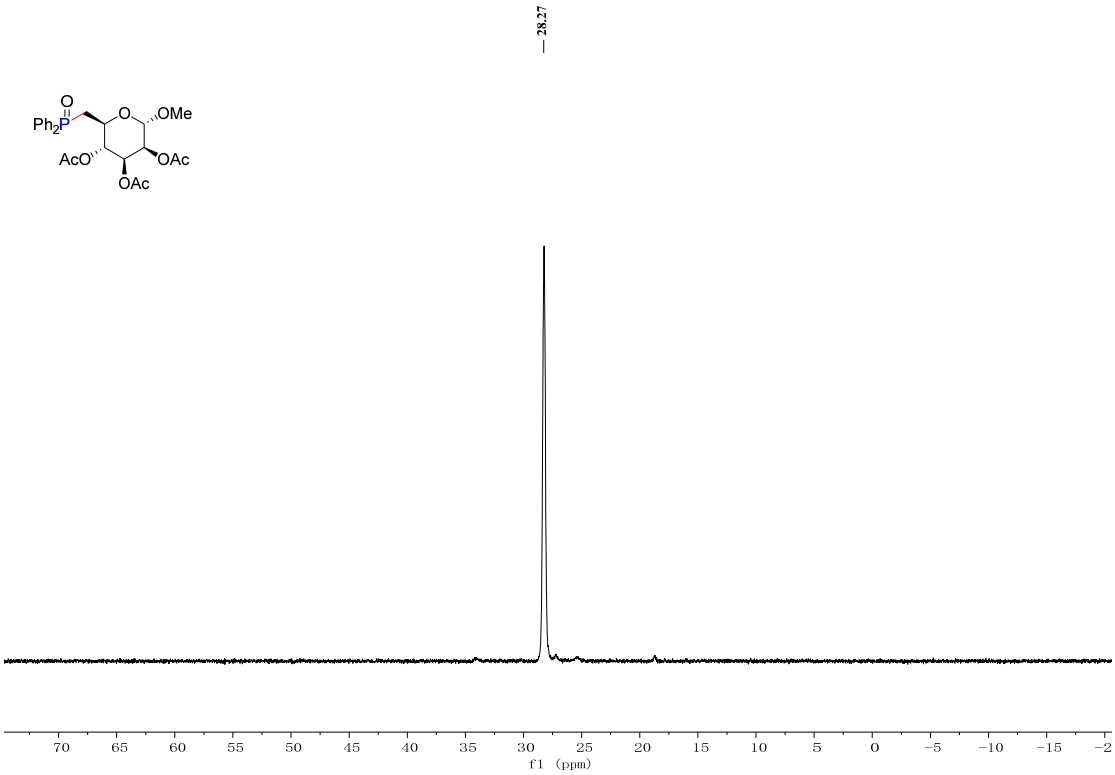

^{1}H NMR ($CDCl_3$, 400 MHz) of **3m**

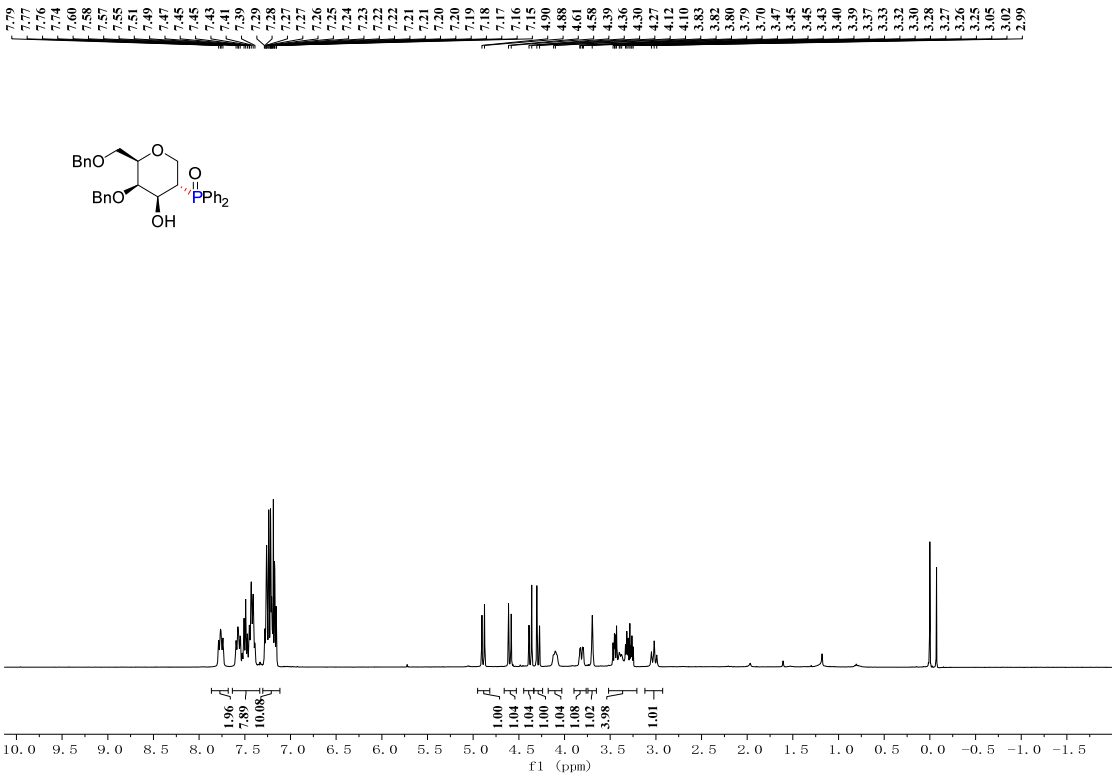

^{13}C NMR ($CDCl_3$, 100 MHz) of **3m**

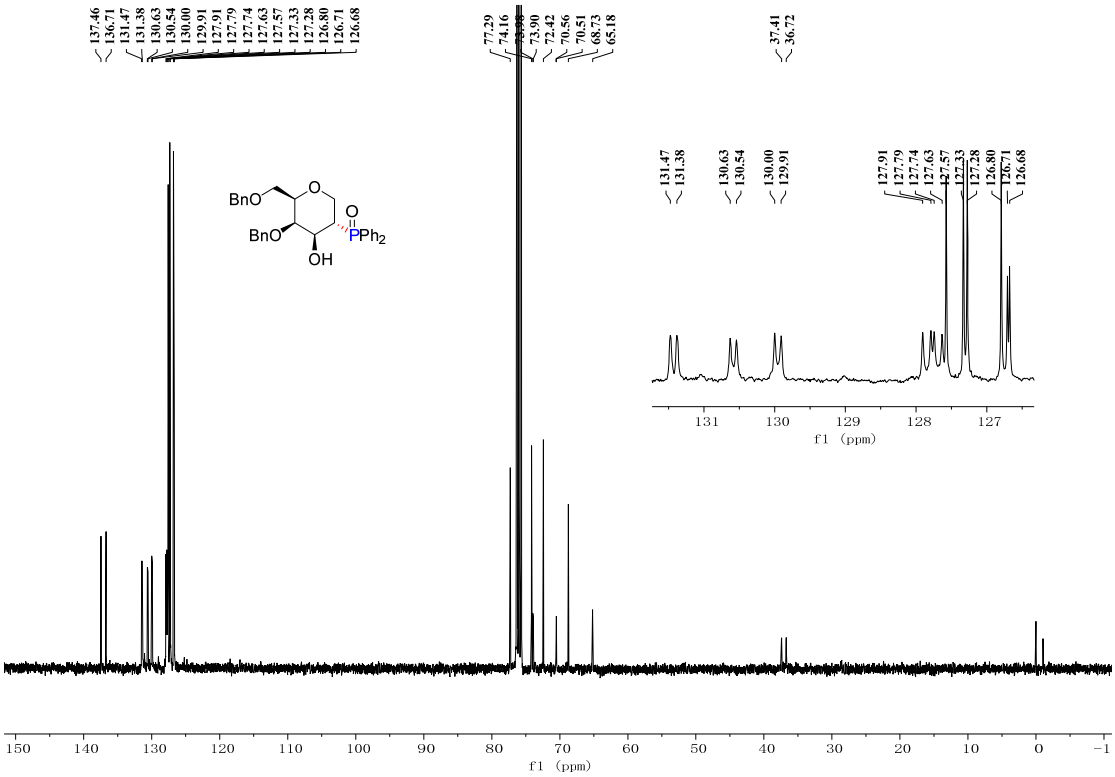

^{31}P NMR ($CDCl_3$, 162 MHz) of **3m**

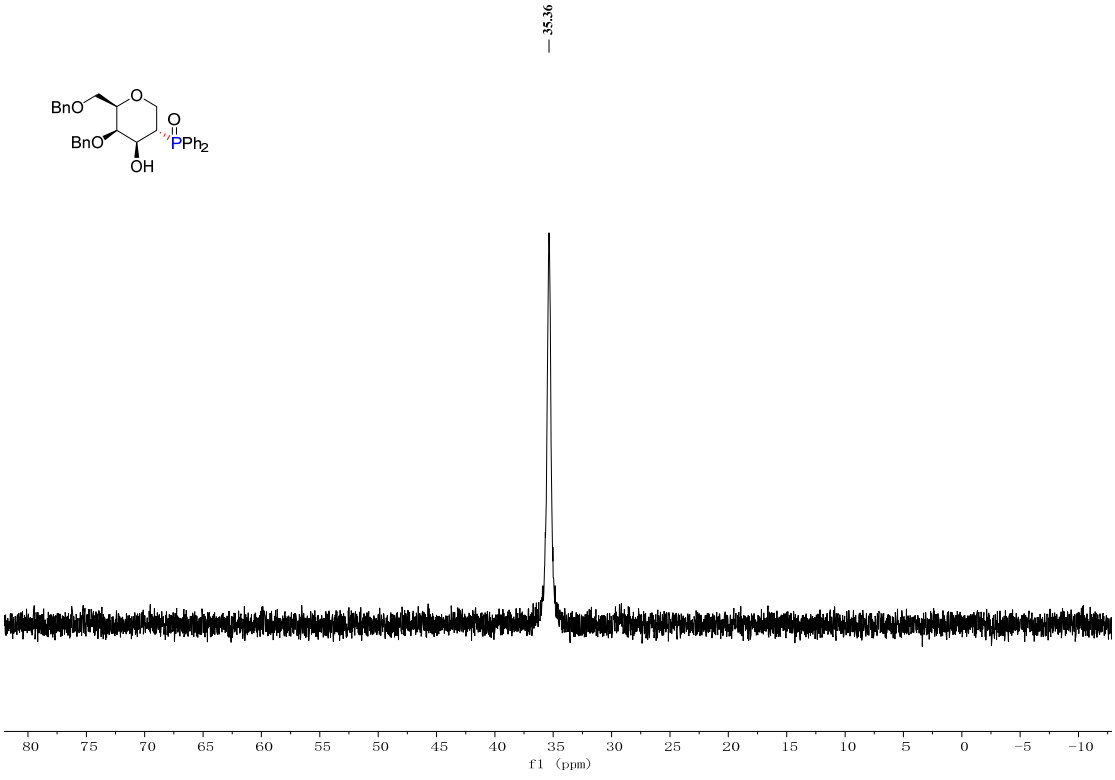

^{1}H NMR ($CDCl_3$, 400 MHz) of **3n**

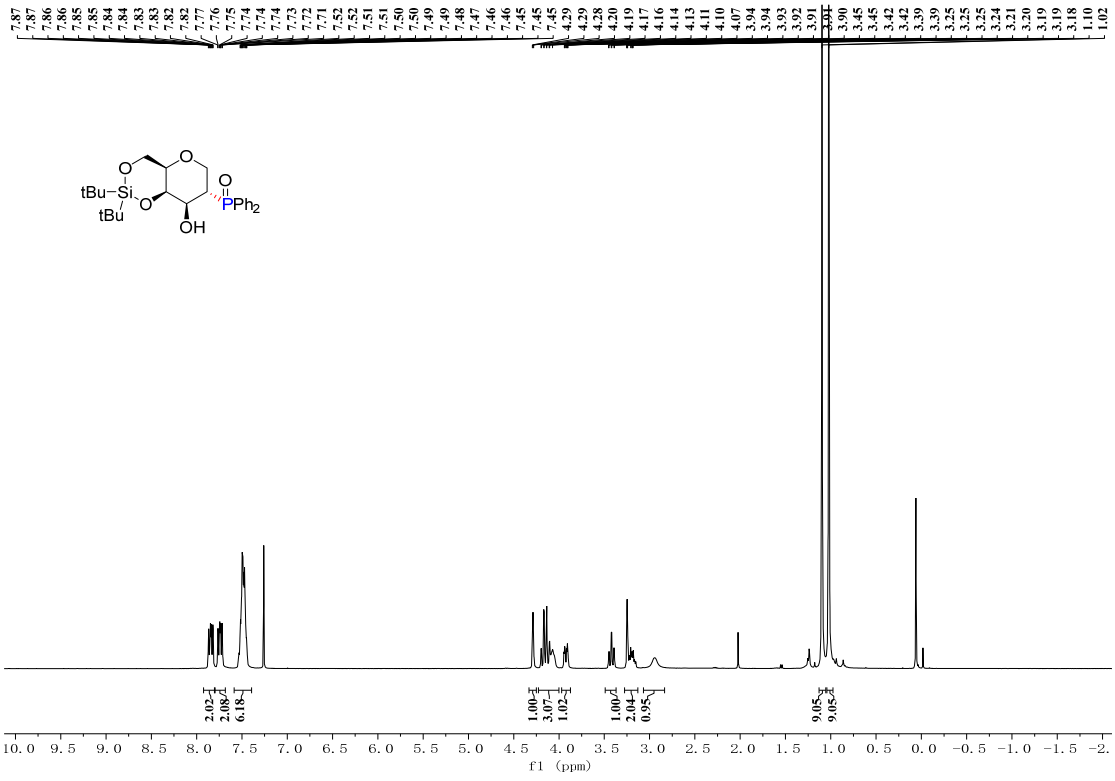

^{13}C NMR ($CDCl_3$, 100 MHz) of **3n**

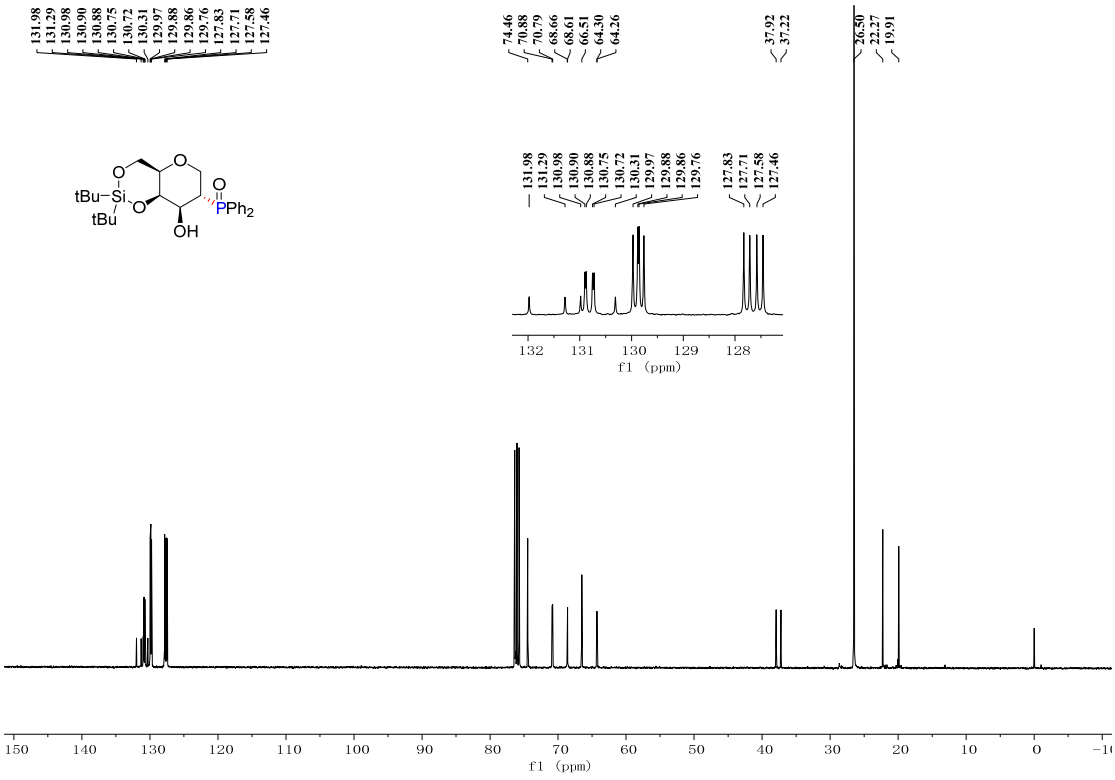

^{31}P NMR ($CDCl_3$, 162 MHz) of **3n**

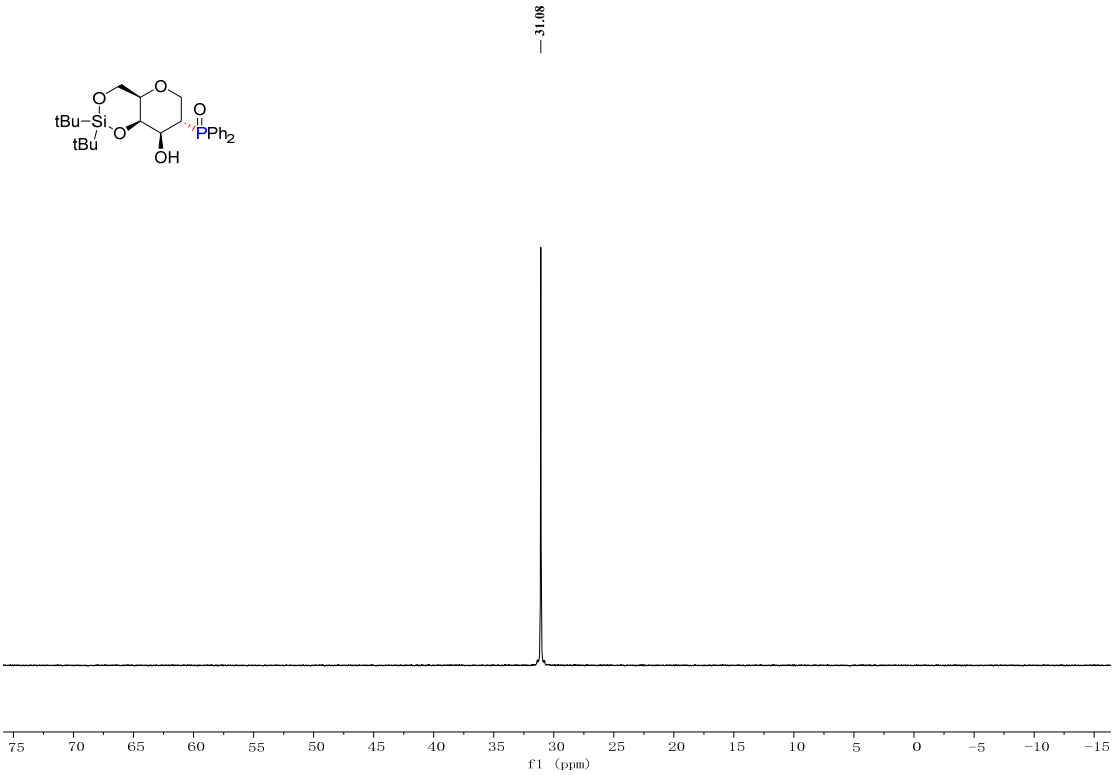

^{1}H NMR ($CDCl_3$, 400 MHz) of **3o**

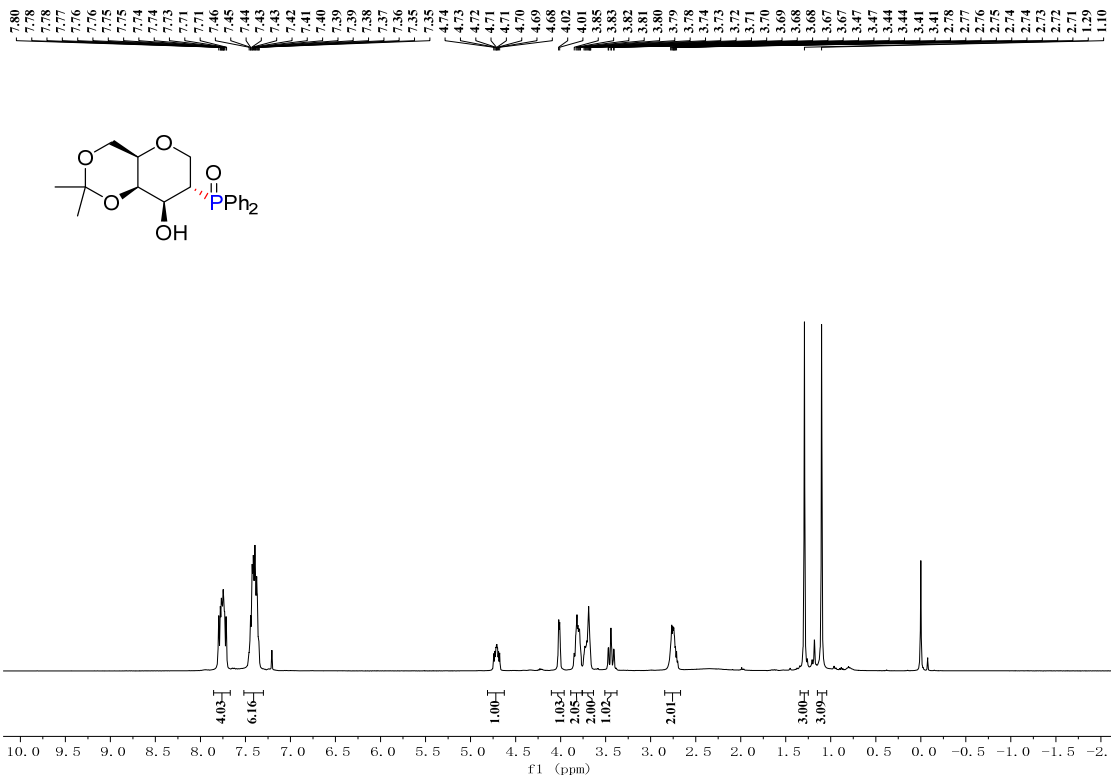

^{13}C NMR ($CDCl_3$, 100 MHz) of **3o**

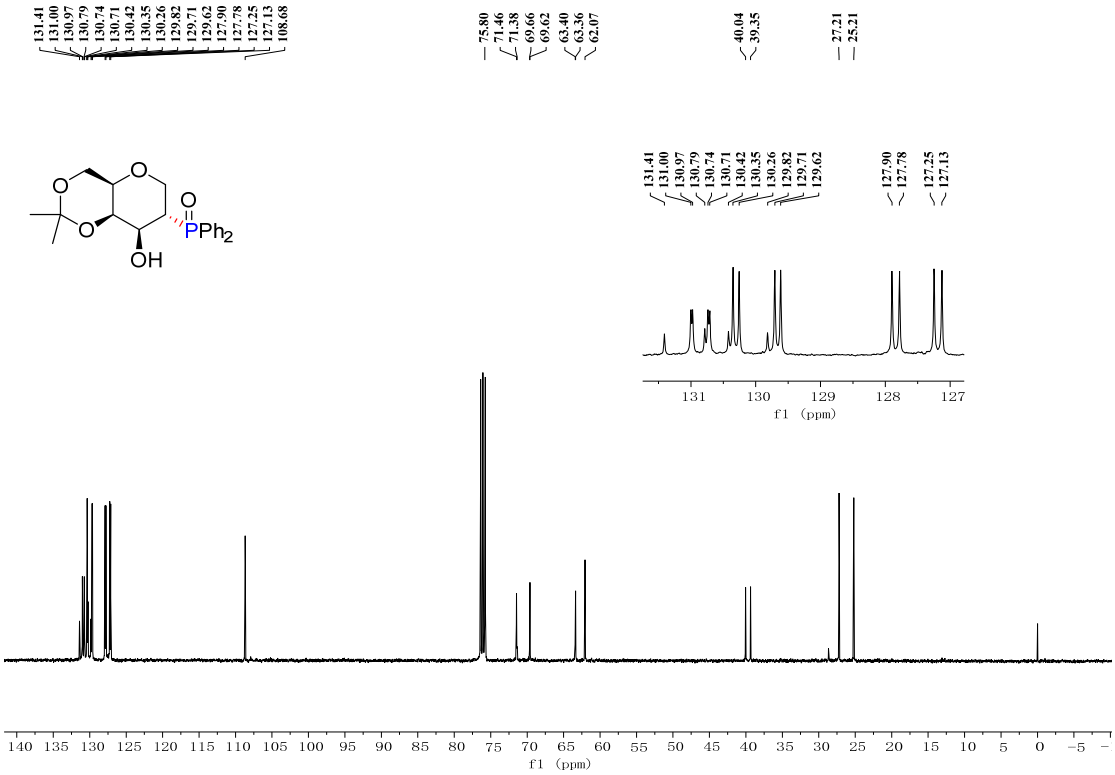

^{31}P NMR ($CDCl_3$, 162 MHz) of **3o**

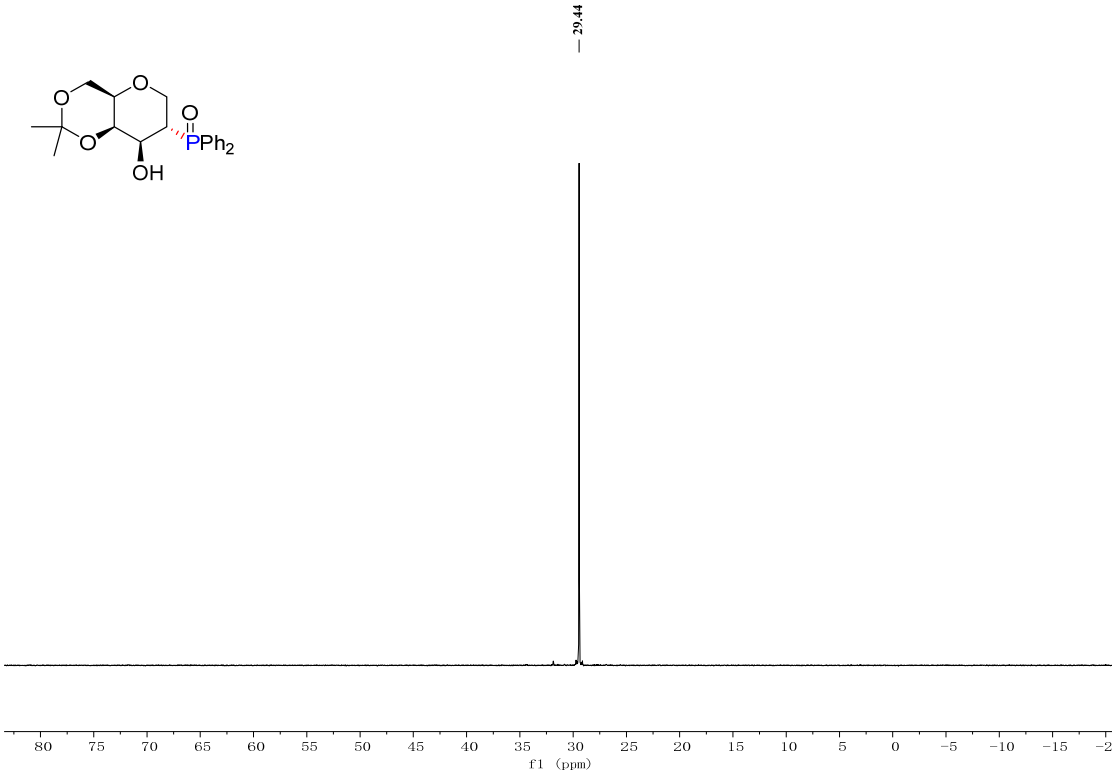

^{1}H NMR ($CDCl_3$, 400 MHz) of **3p**

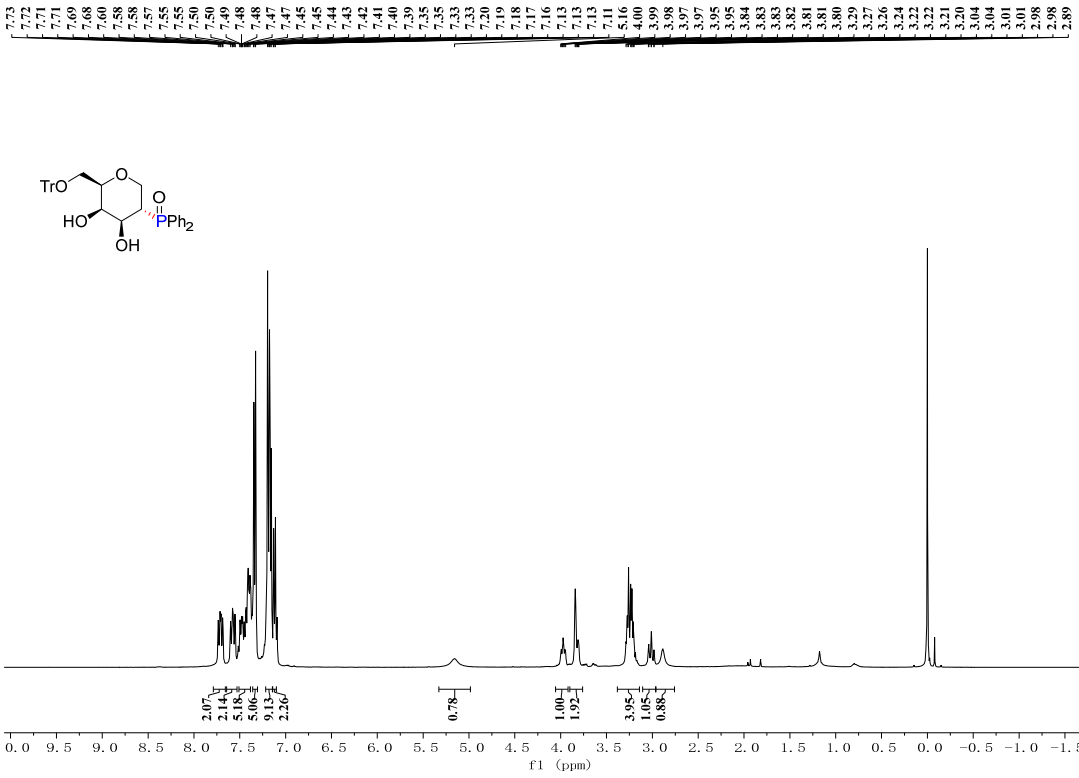

^{13}C NMR ($CDCl_3$, 100 MHz) of **3p**

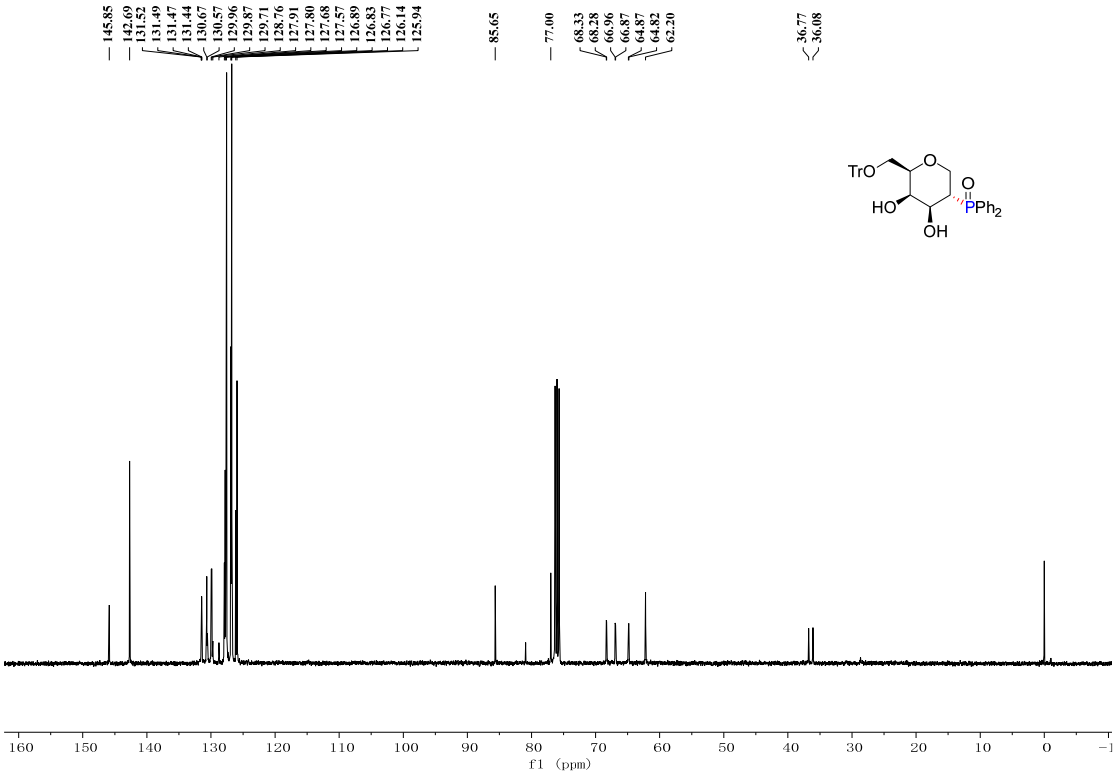

^{31}P NMR ($CDCl_3$, 162 MHz) of **3p**

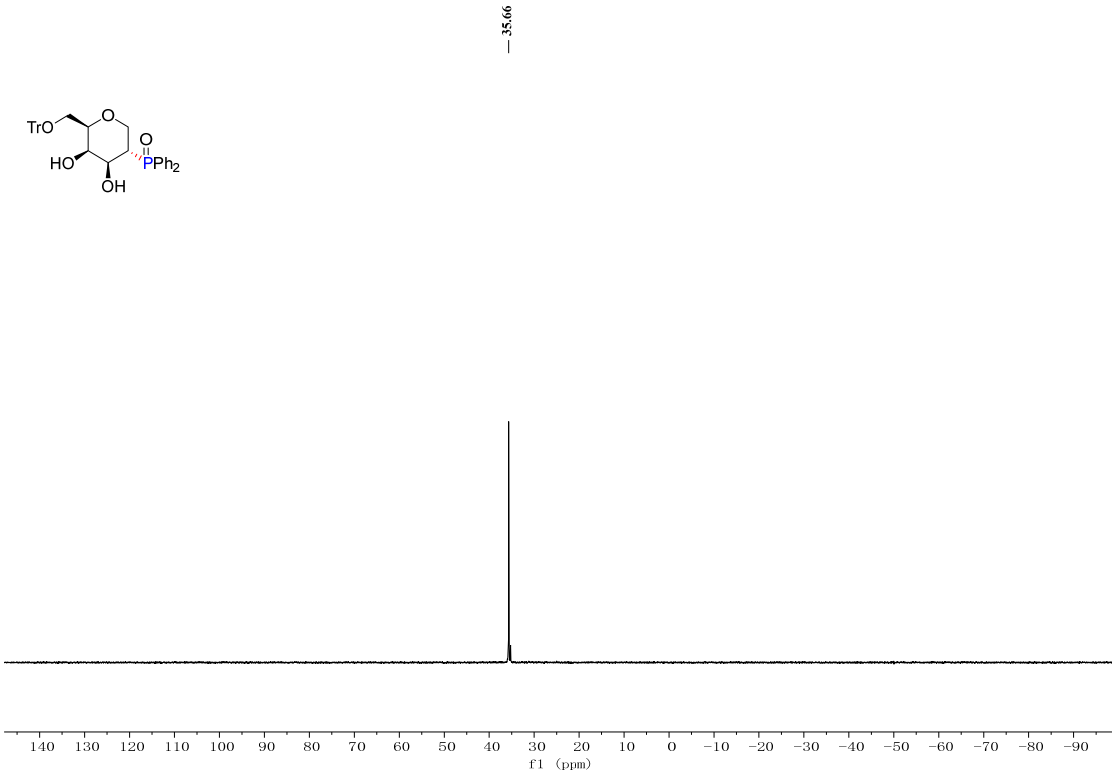

^{1}H NMR ($CDCl_3$, 400 MHz) of **3q**

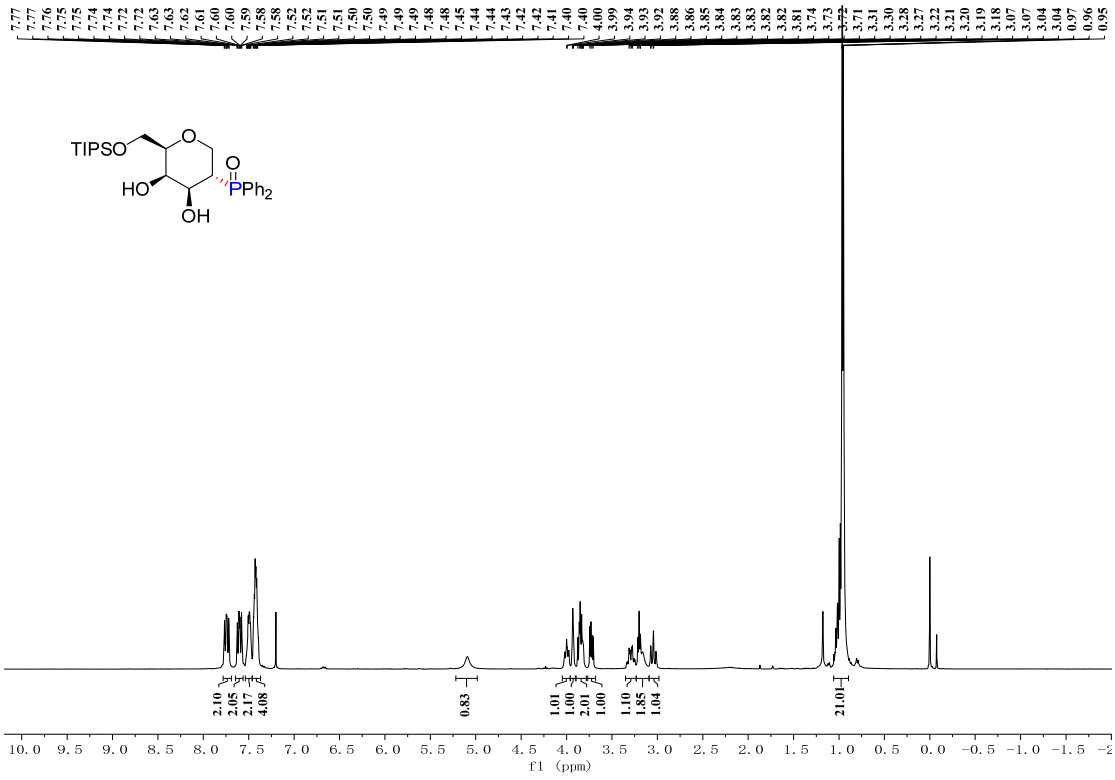

^{13}C NMR ($CDCl_3$, 100 MHz) of **3q**

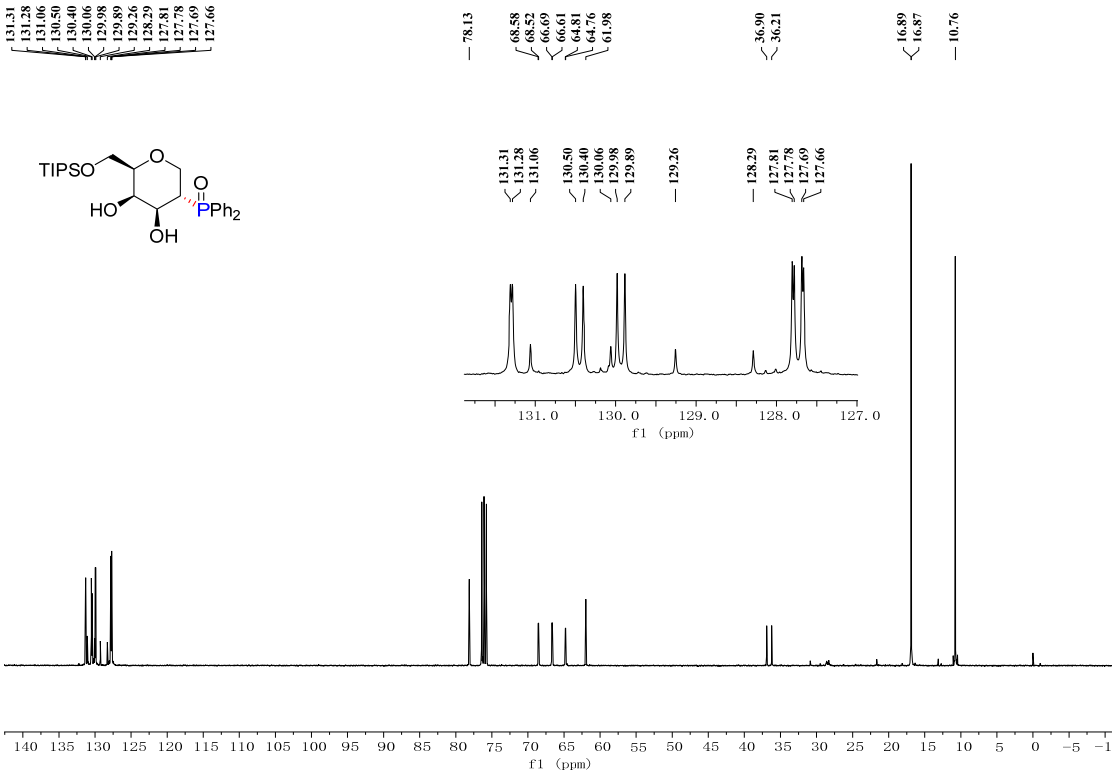

^{31}P NMR ($CDCl_3$, 162 MHz) of **3q**

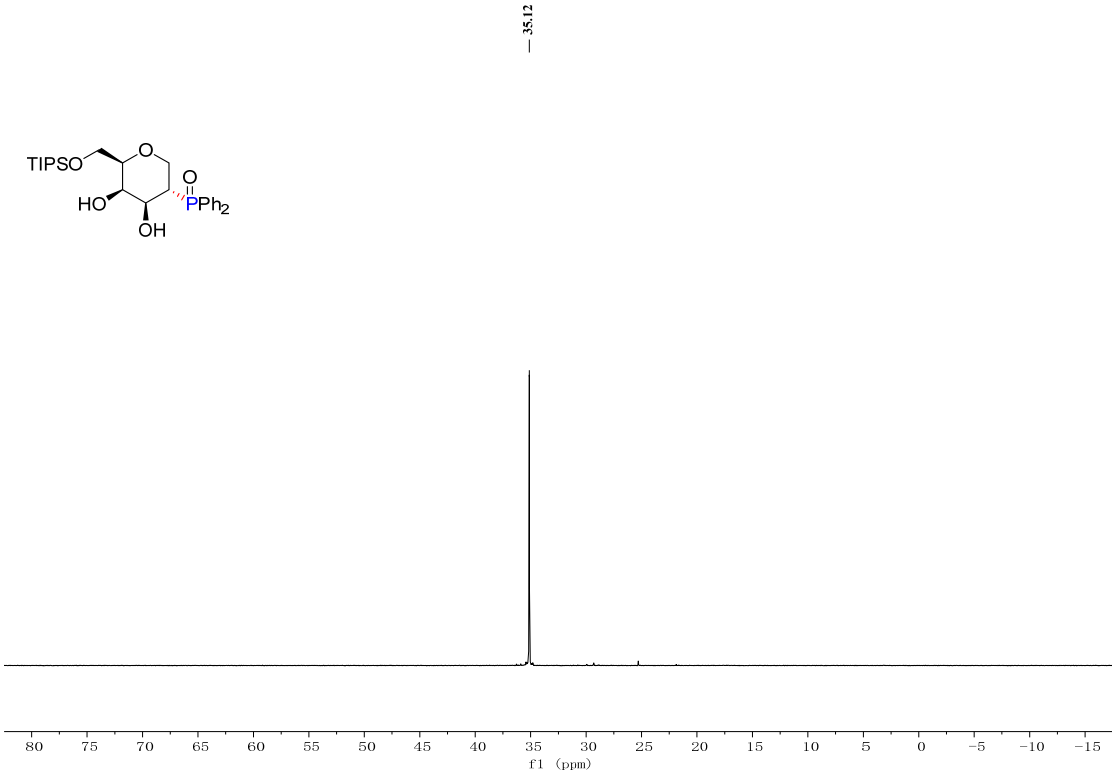

^{1}H NMR ($CDCl_3$, 400 MHz) of **3r**

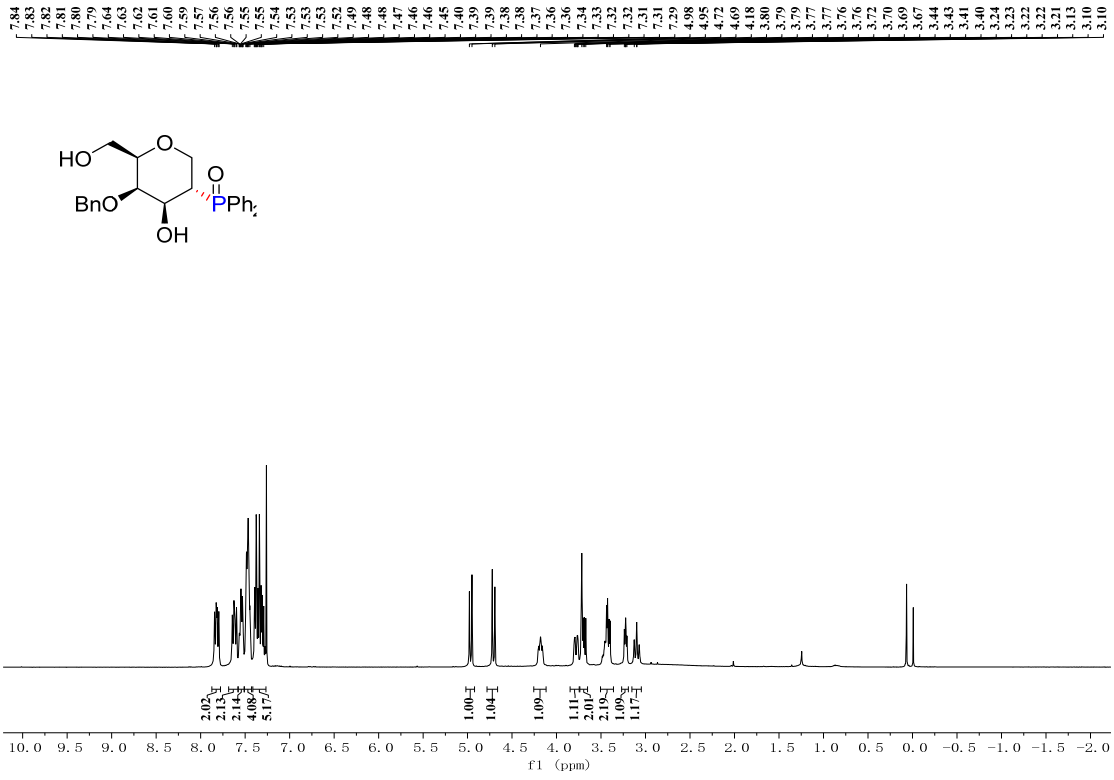

^{13}C NMR ($CDCl_3$, 100 MHz) of **3r**

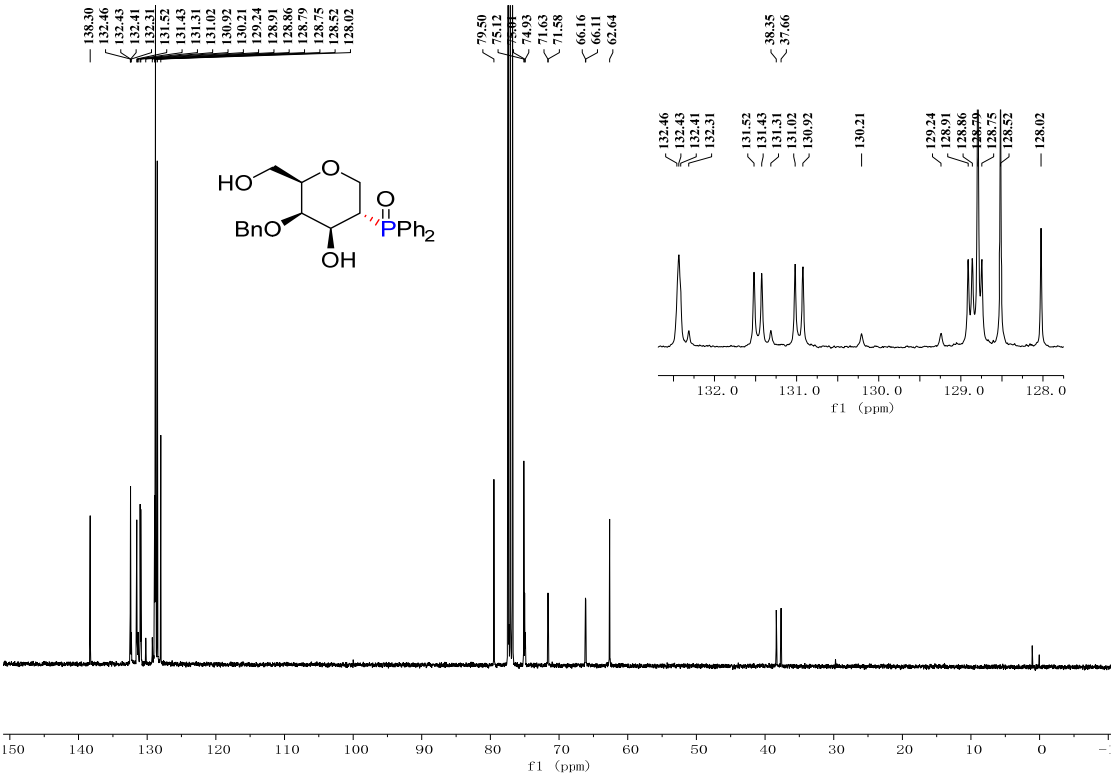

^{31}P NMR ($CDCl_3$, 162 MHz) of **3r**

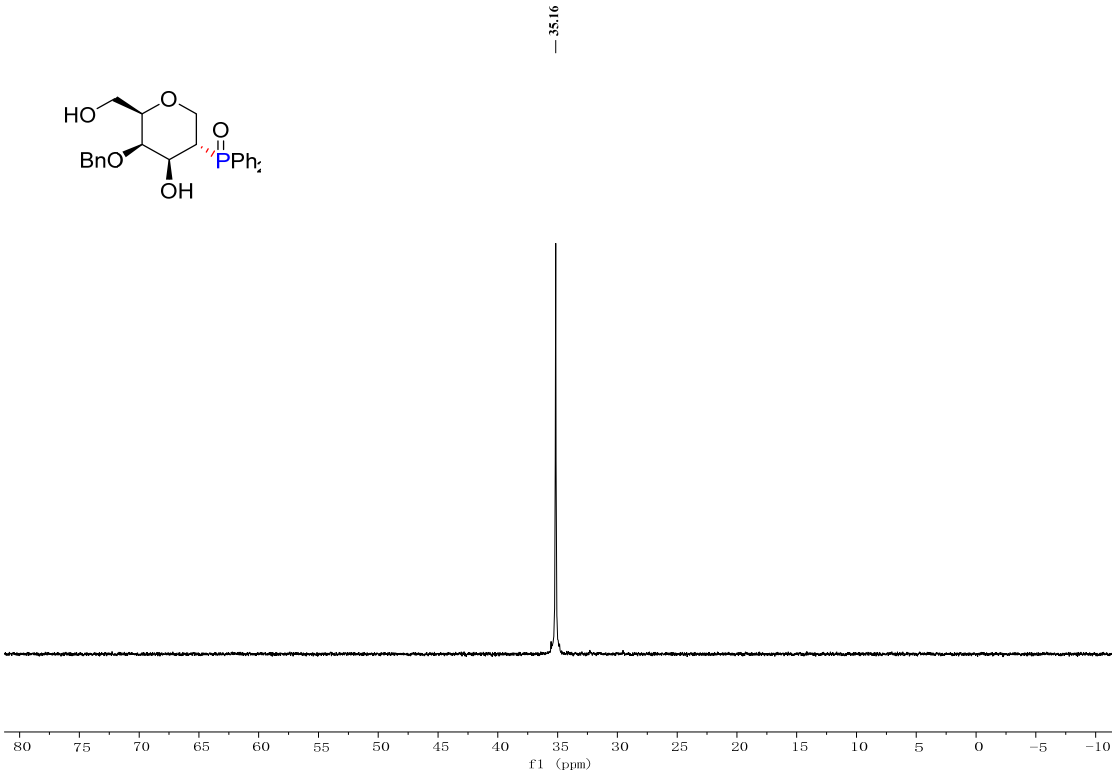

^{1}H NMR ($CDCl_3$, 400 MHz) of **3s**

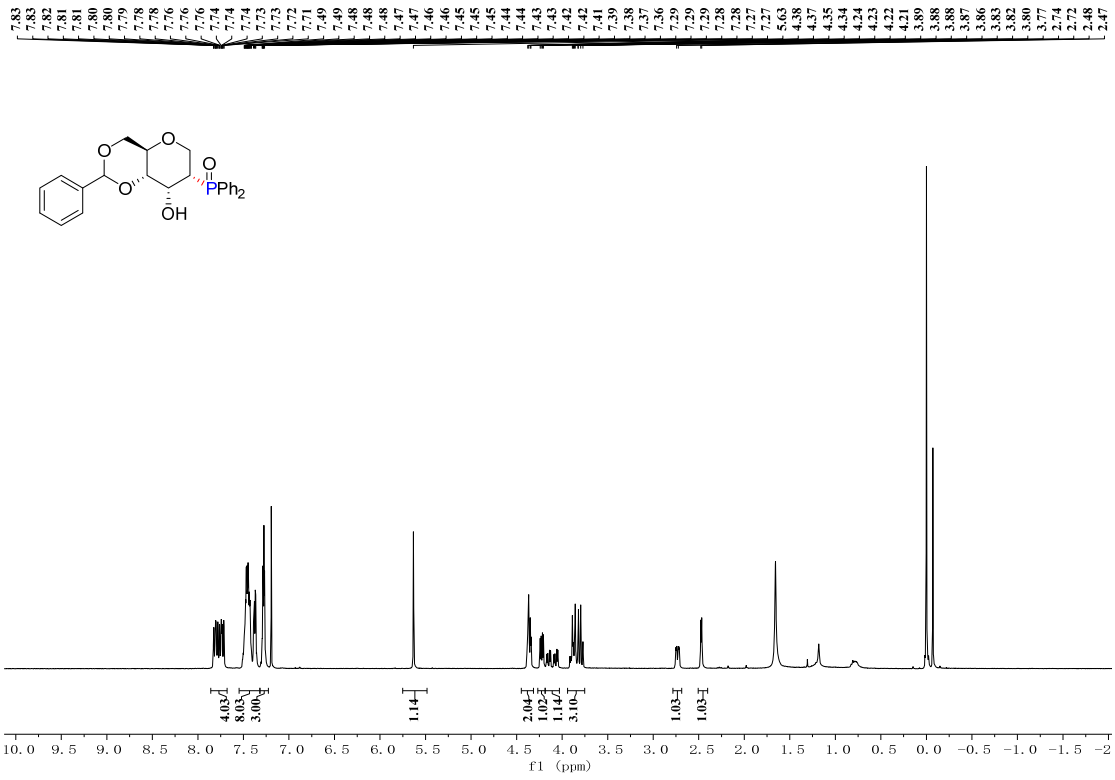

^{13}C NMR ($CDCl_3$, 100 MHz) of **3s**

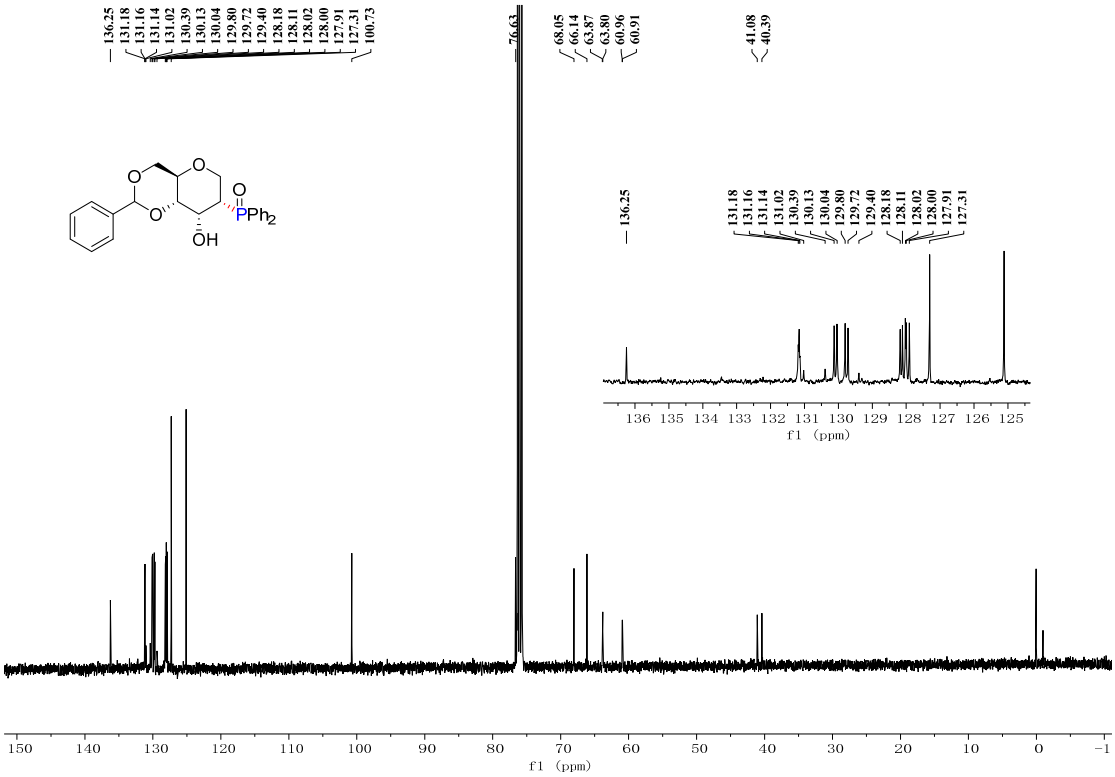

^{31}P NMR ($CDCl_3$, 162 MHz) of **3s**

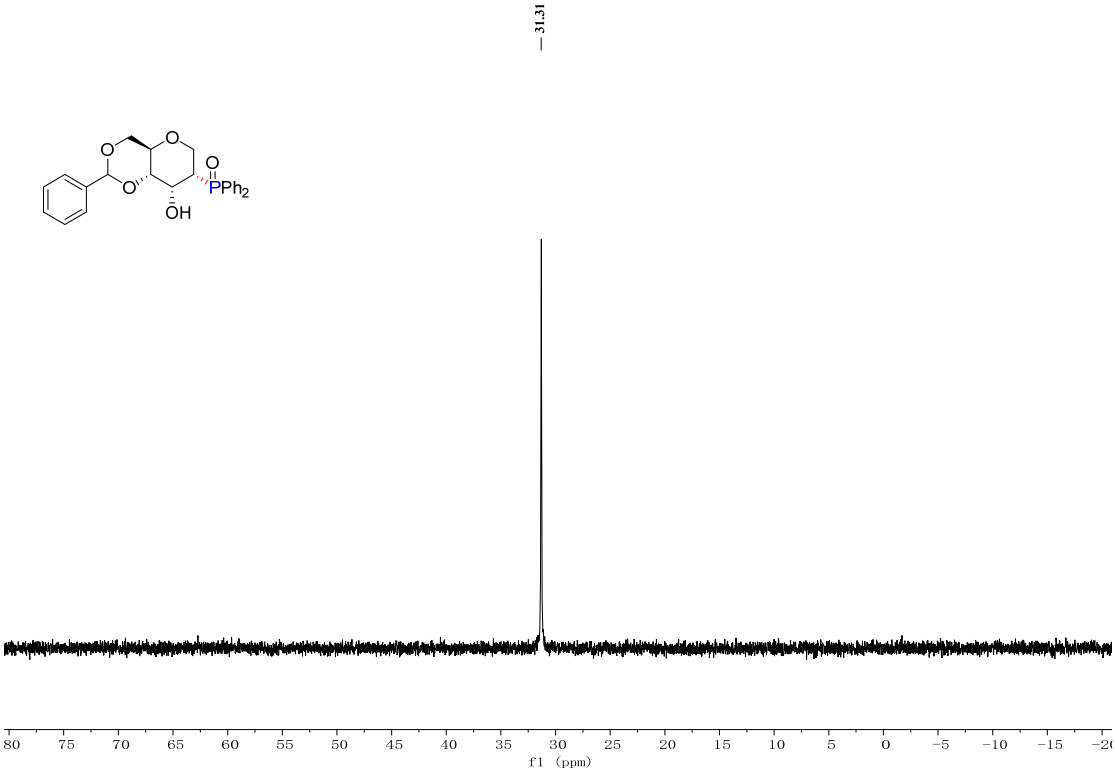

^{1}H NMR ($CDCl_3$, 400 MHz) of **3t**

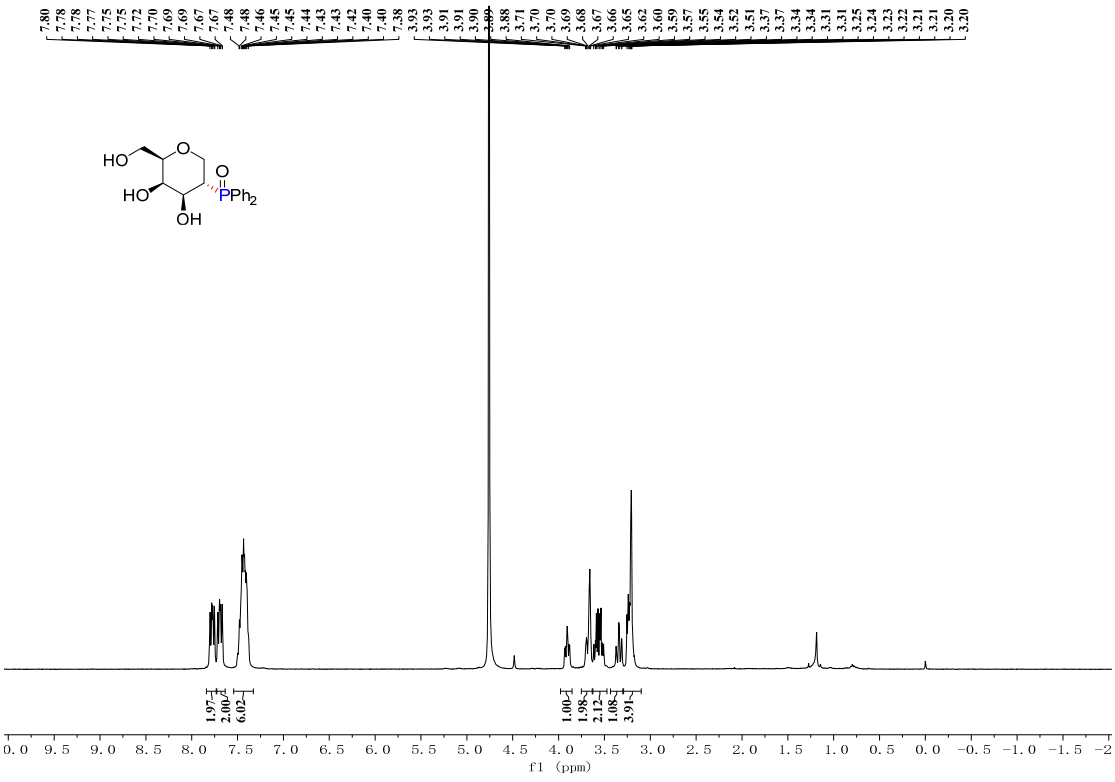

^{13}C NMR ($CDCl_3$, 100 MHz) of **3t**

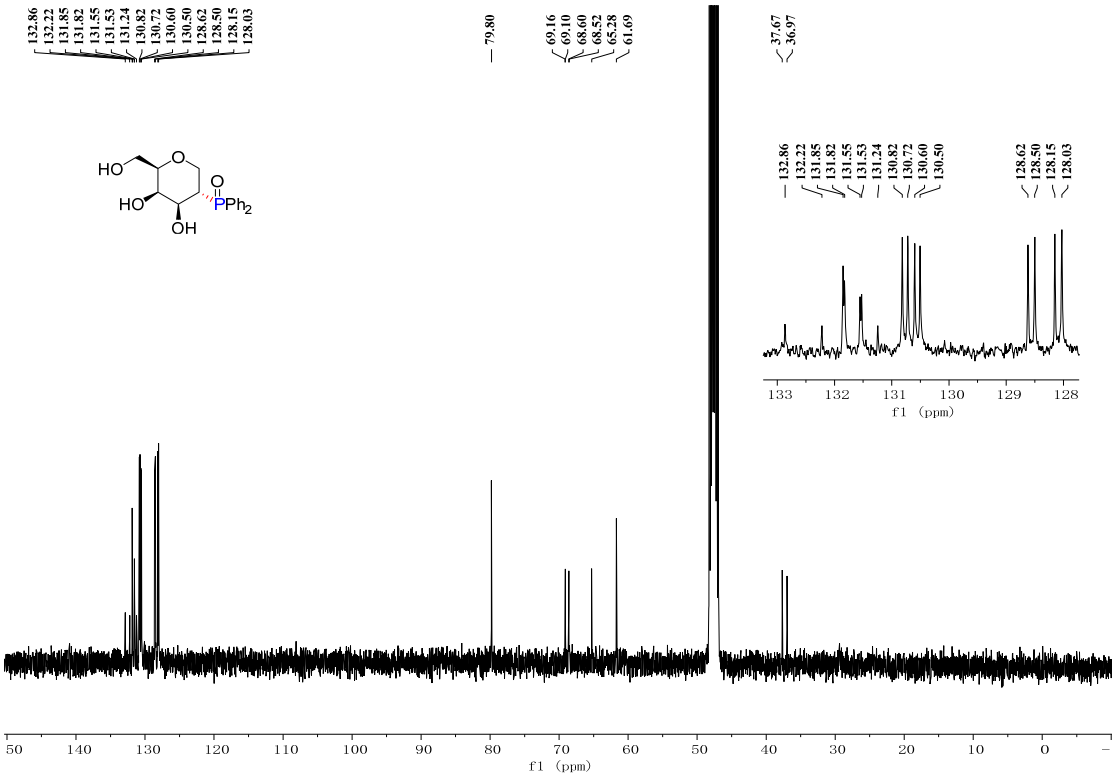

^{31}PNMR ($CDCl_3$, 162 MHz) of **3t**

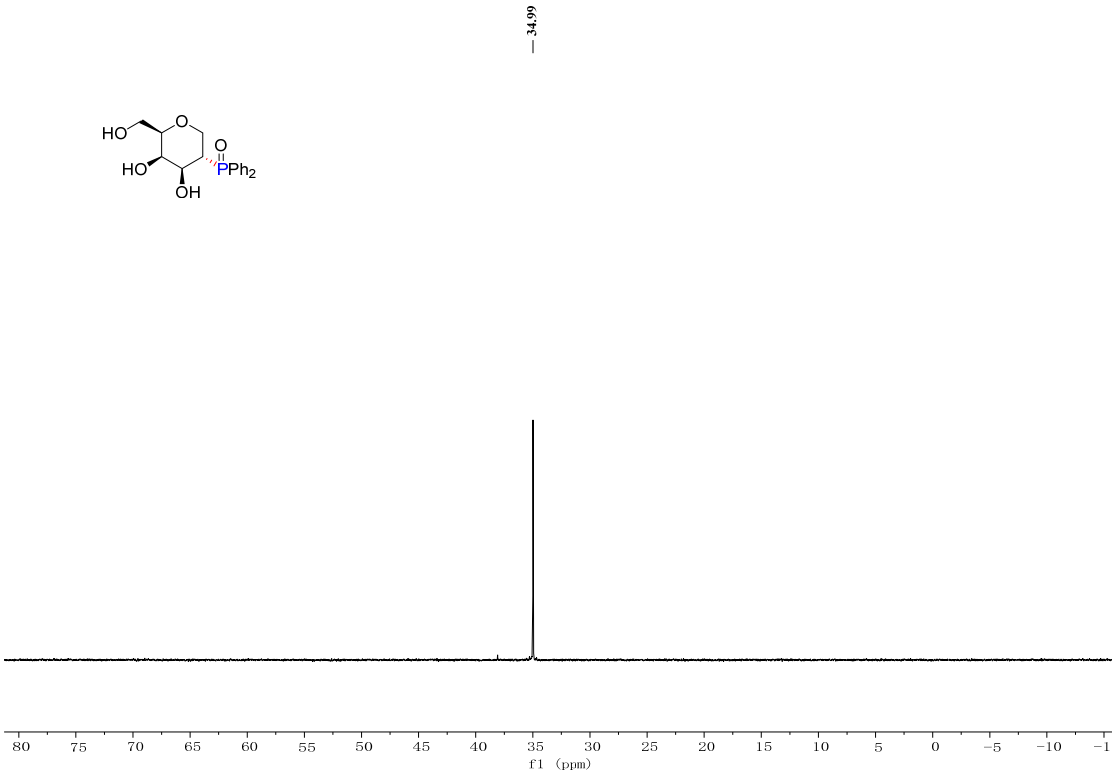

^{1}H NMR ($CDCl_3$, 400 MHz) of **3u**

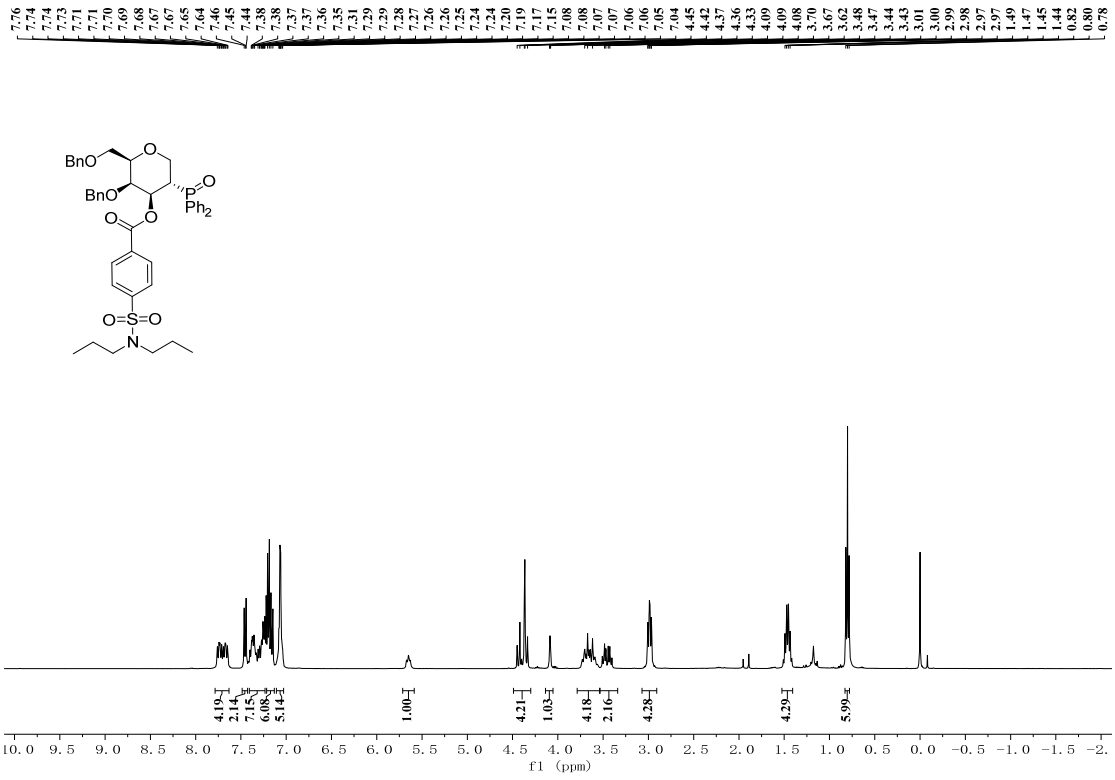

^{13}C NMR ($CDCl_3$, 100 MHz) of **3u**

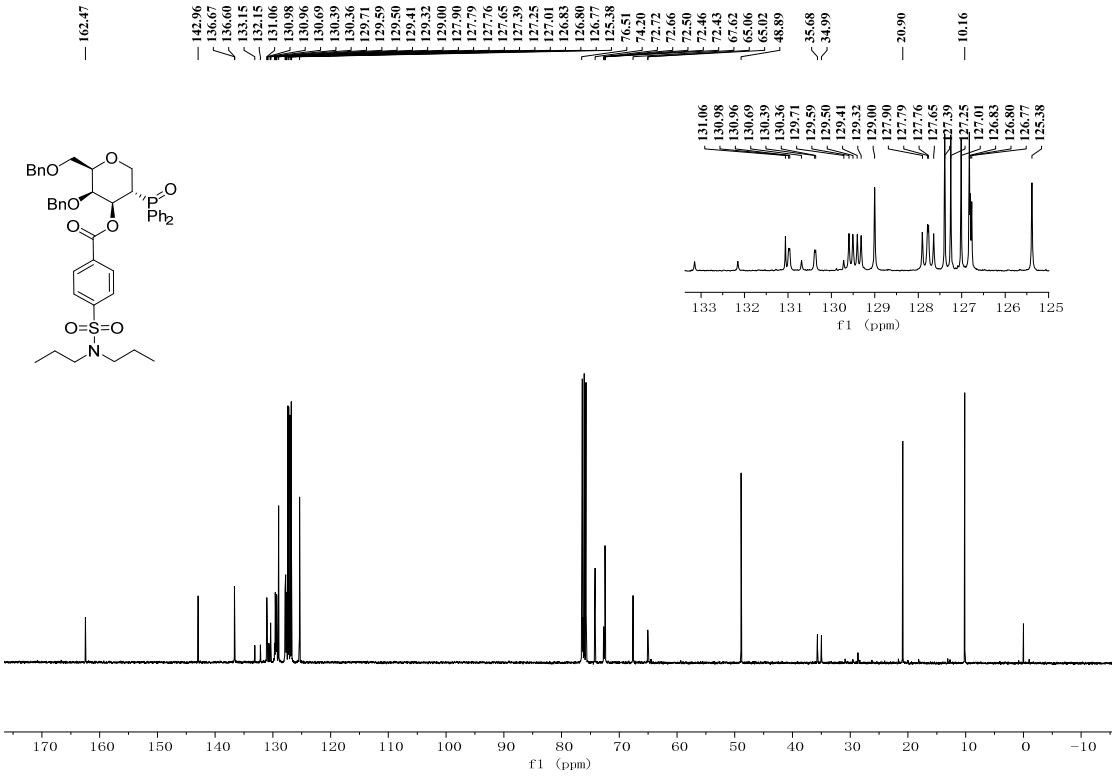

^{31}PNMR ($CDCl_3$, 162 MHz) of **3u**

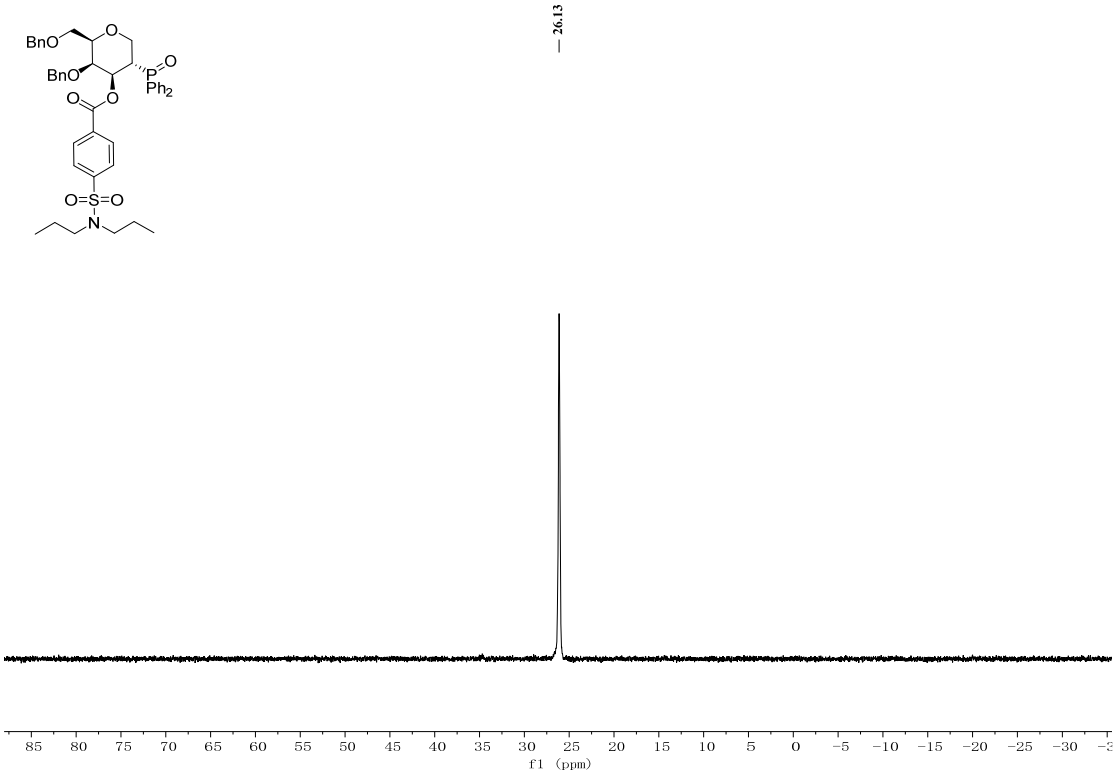

^{1}H NMR ($CDCl_3$, 400 MHz) of **3v**

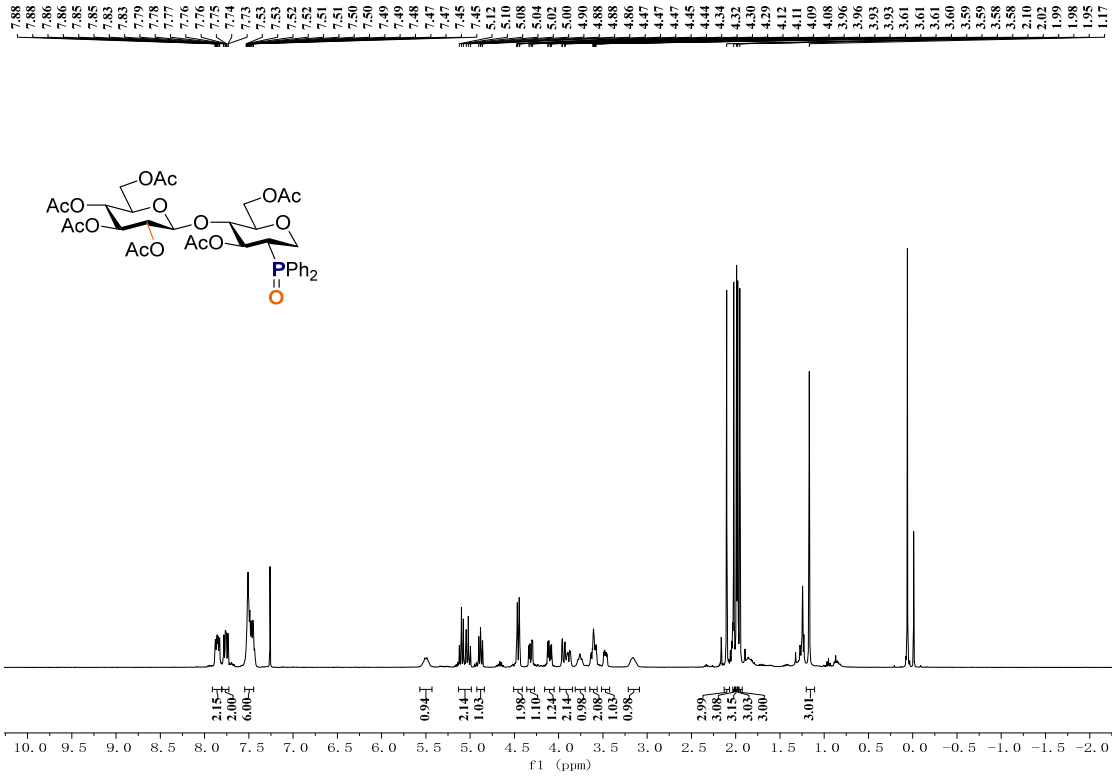

^{13}C NMR ($CDCl_3$, 100 MHz) of **3v**

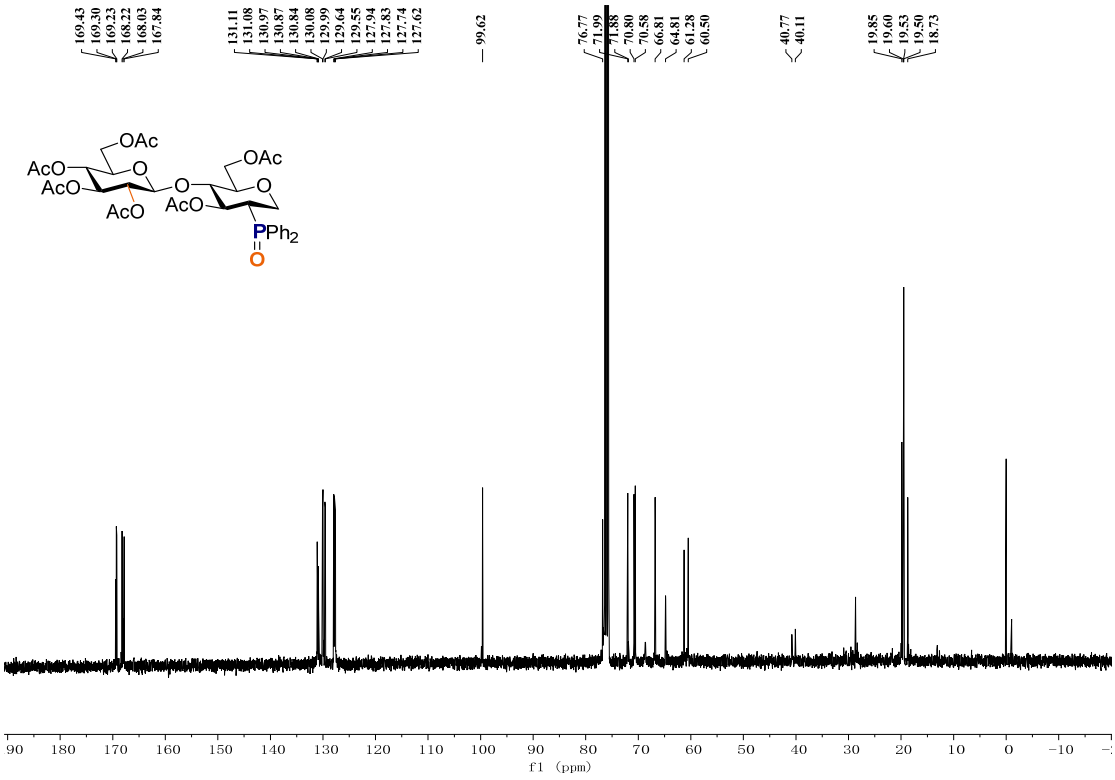

^{31}PNMR ($CDCl_3$, 162 MHz) of **3v**

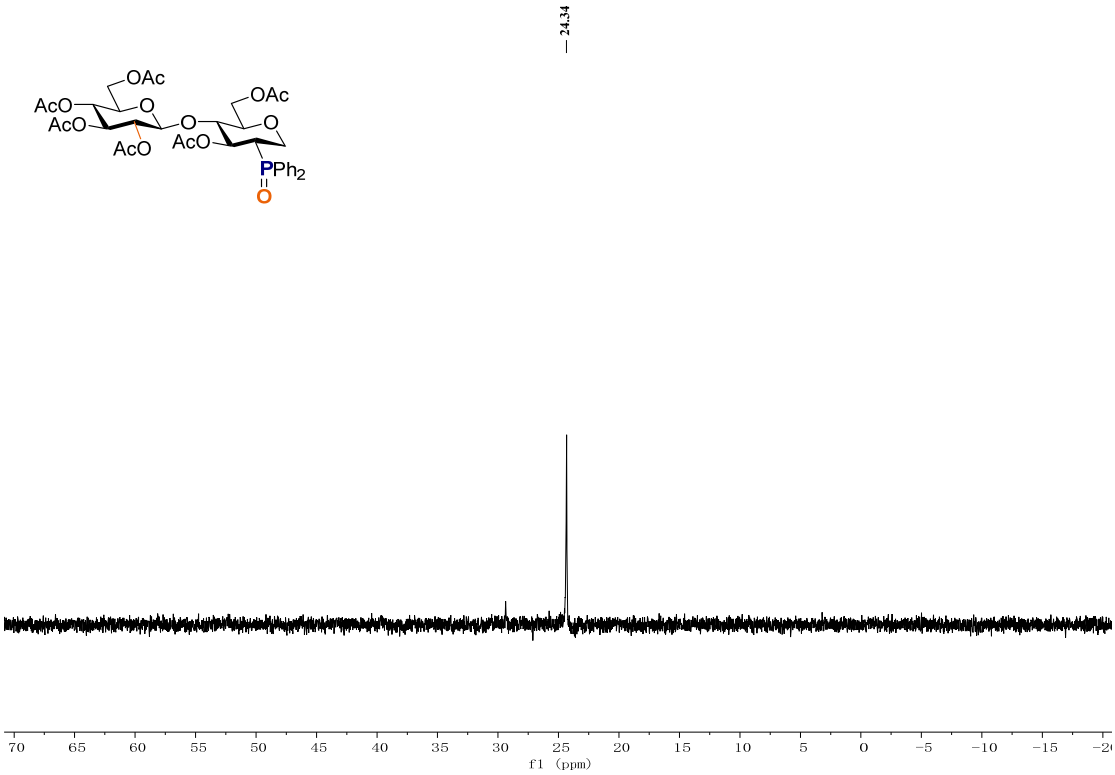

^{1}H NMR ($CDCl_3$, 400 MHz) of **3v'**

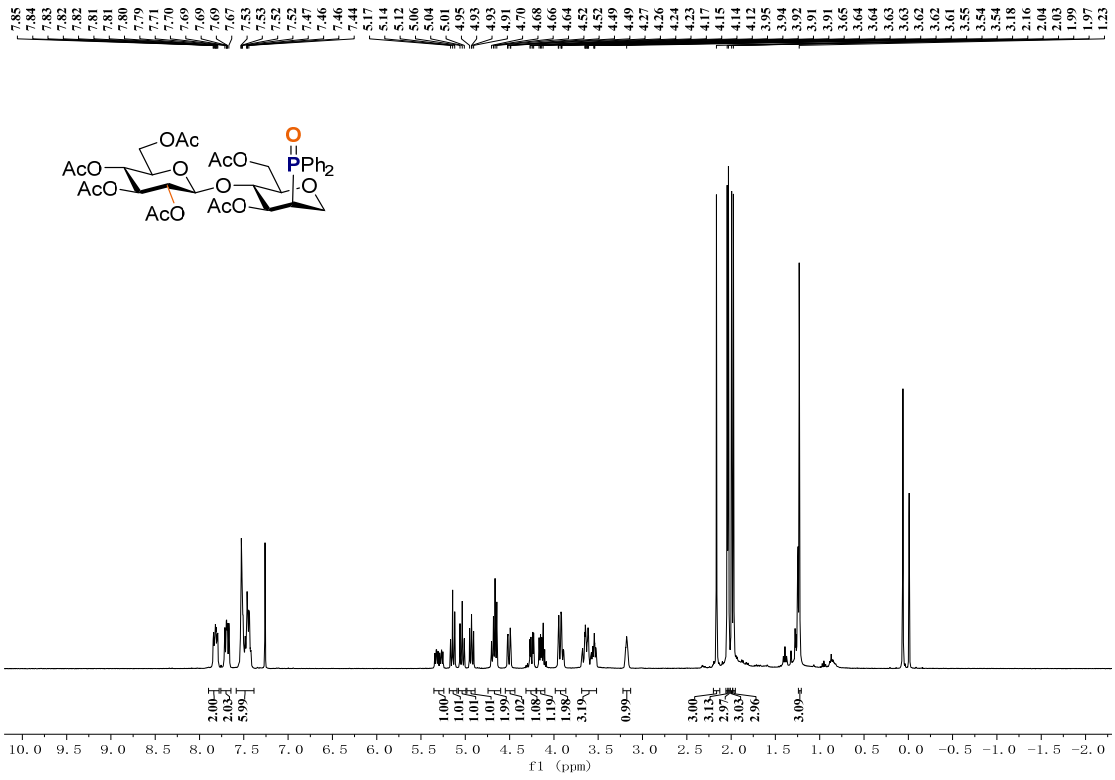

^{13}C NMR ($CDCl_3$, 100 MHz) of **3v'**

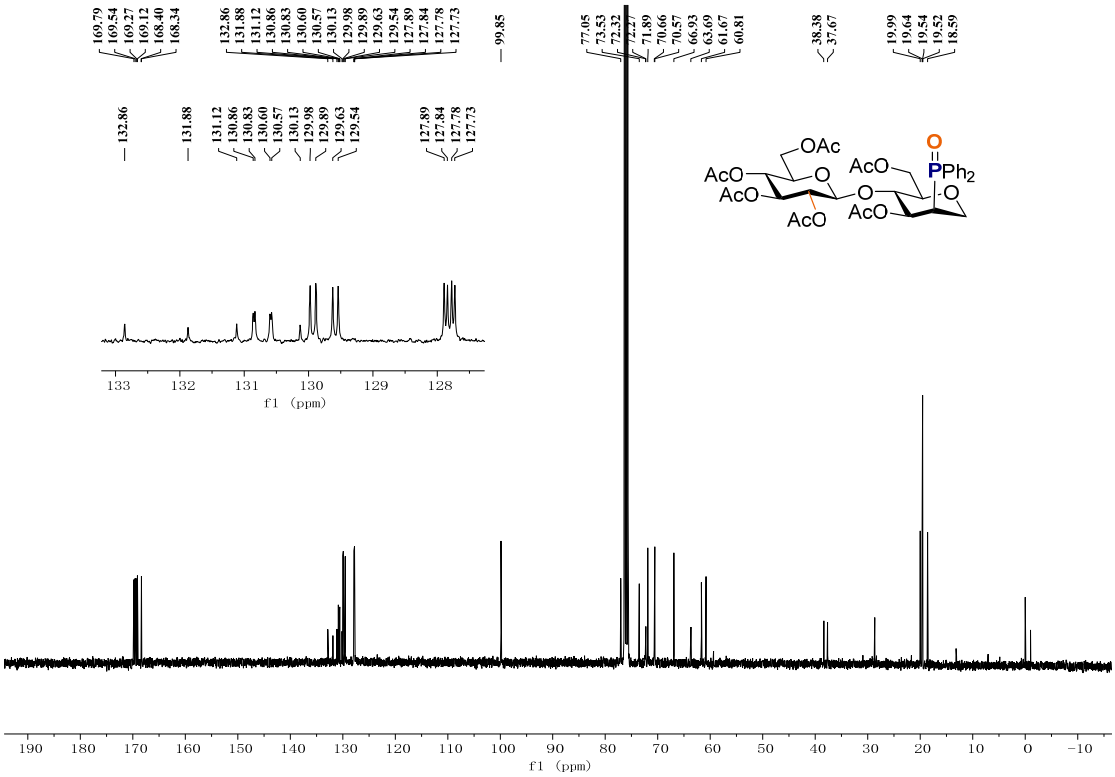

^{31}PNMR ($CDCl_3$, 162 MHz) of **3v'**

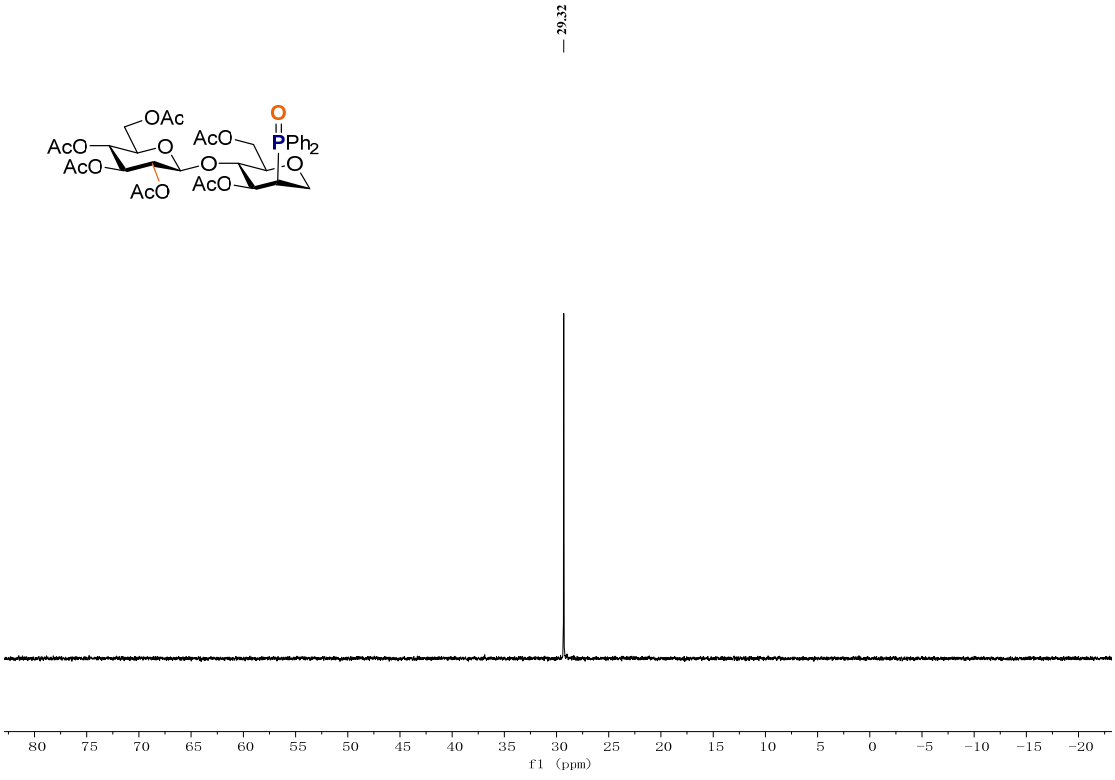

^{1}H NMR ($CDCl_3$, 400 MHz) of **3w**

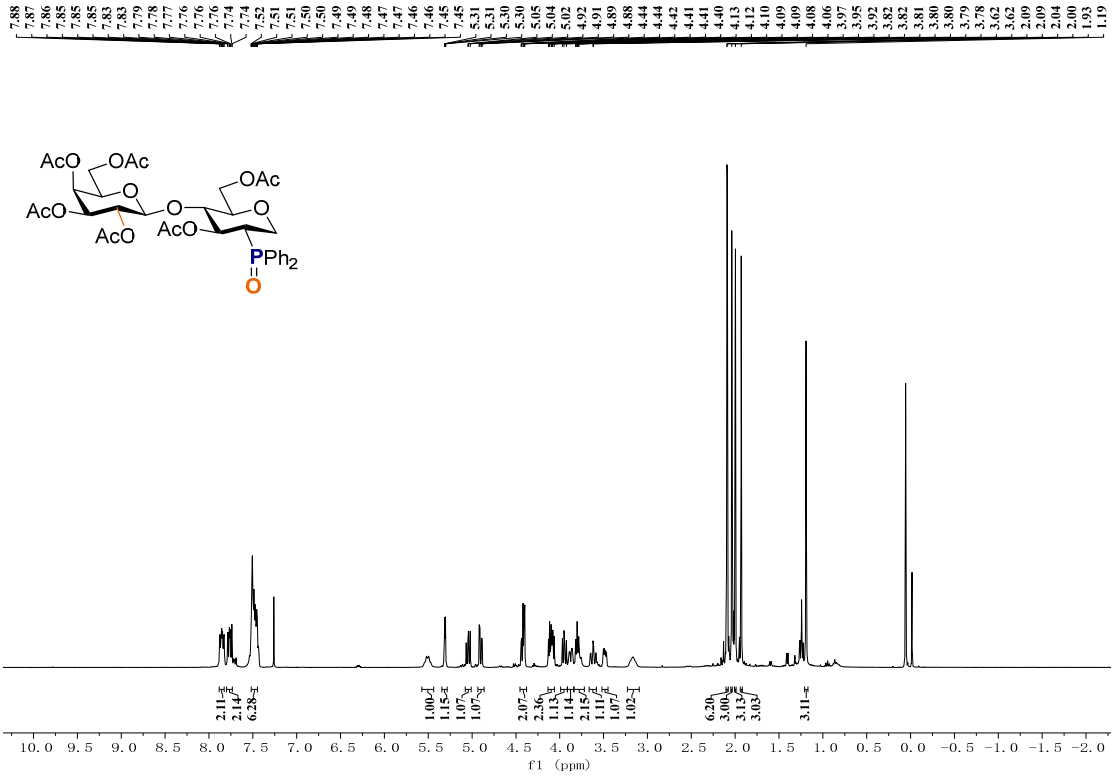

^{13}C NMR ($CDCl_3$, 100 MHz) of **3w**

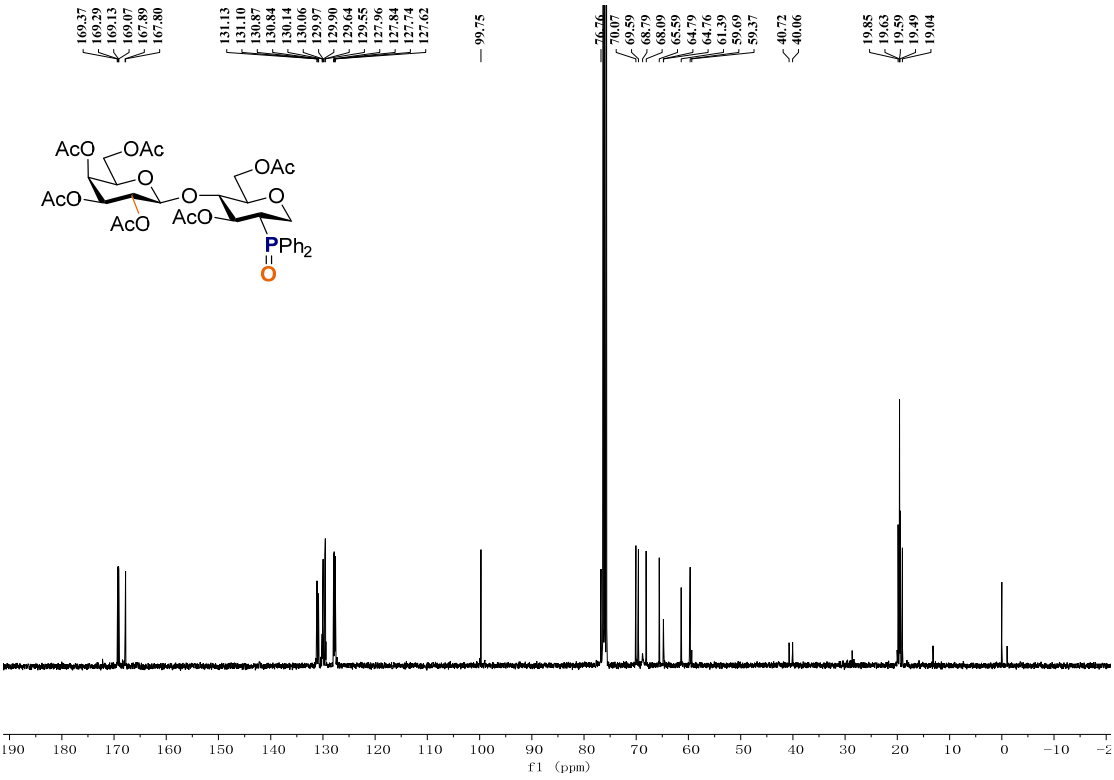

^{31}PNMR ($CDCl_3$, 162 MHz) of **3w**

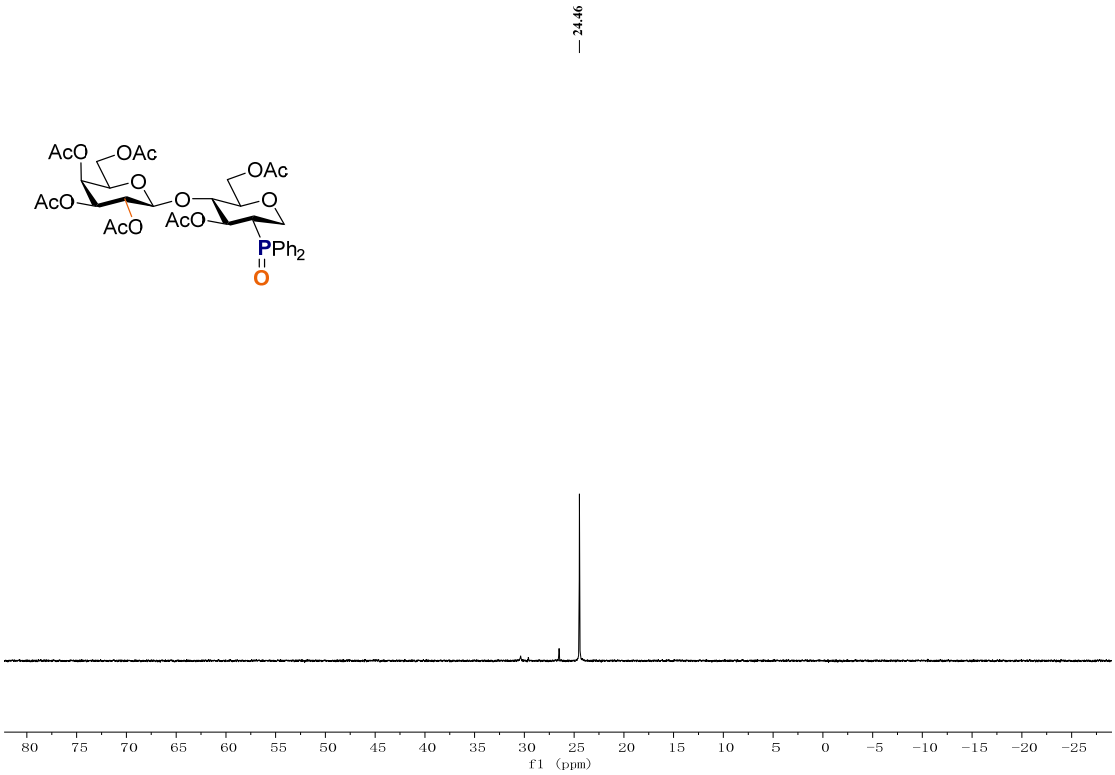

^{1}H NMR ($CDCl_3$, 400 MHz) of **3w'**

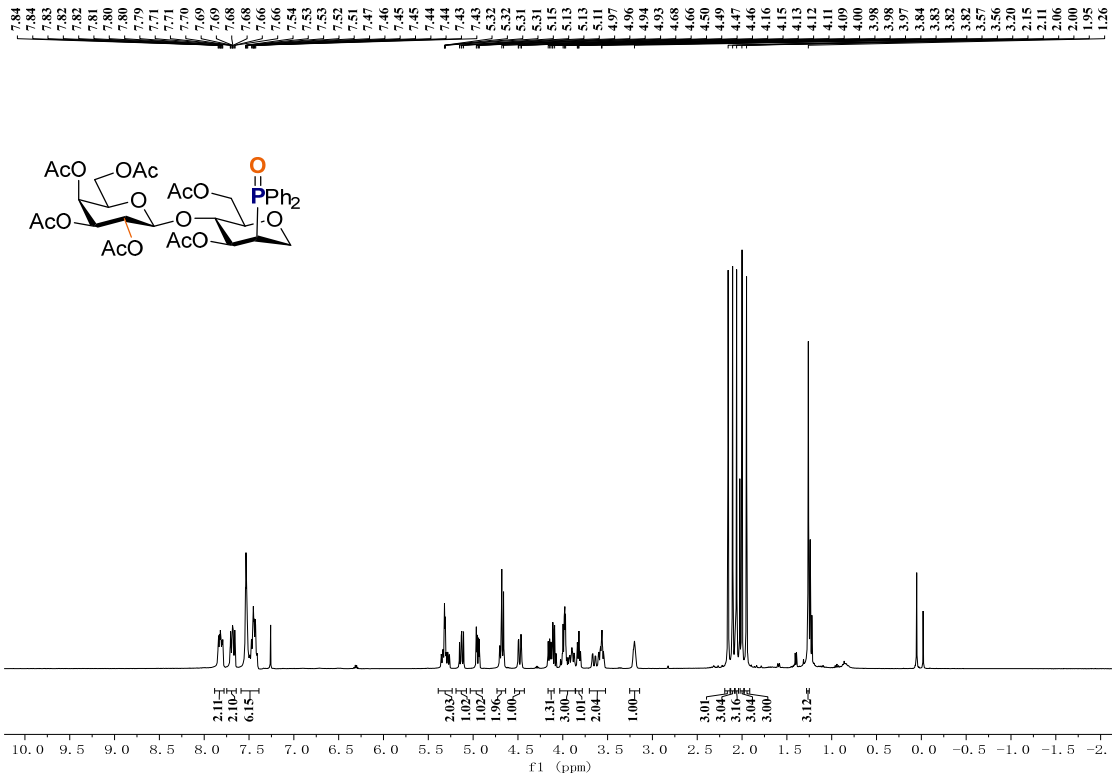

^{13}C NMR ($CDCl_3$, 100 MHz) of **3w'**

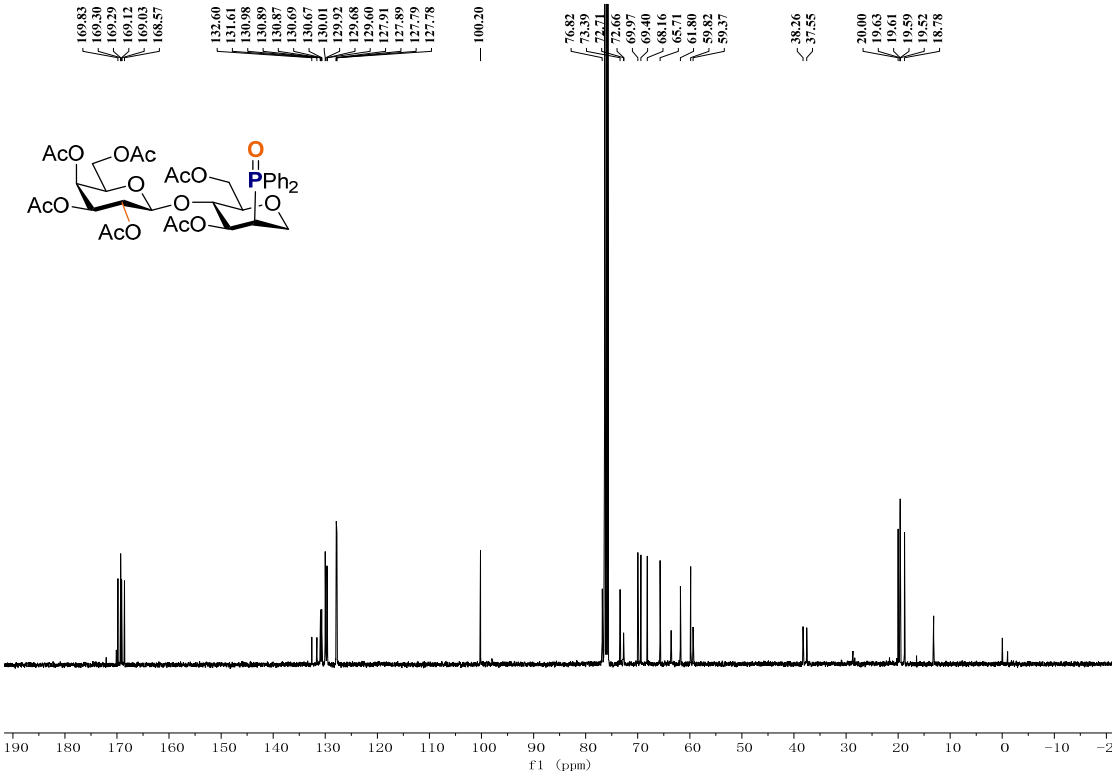

^{31}PNMR ($CDCl_3$, 162 MHz) of **3w'**

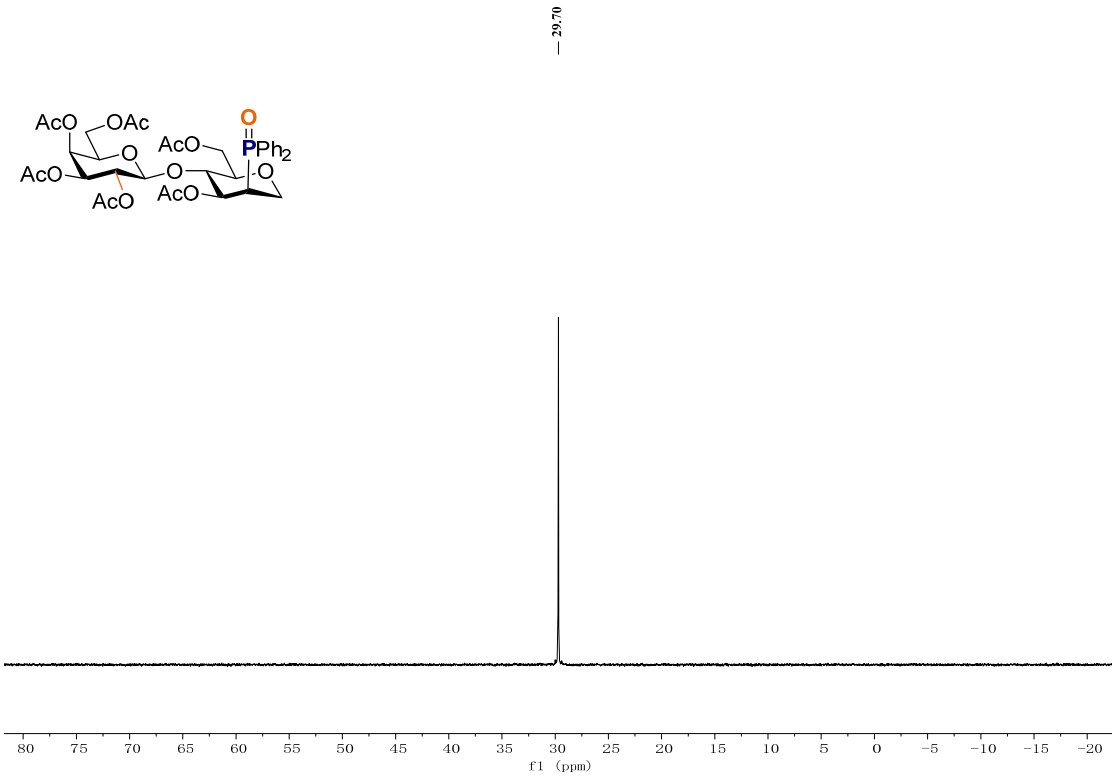

^{1}H NMR ($CDCl_3$, 400 MHz) of **4a**

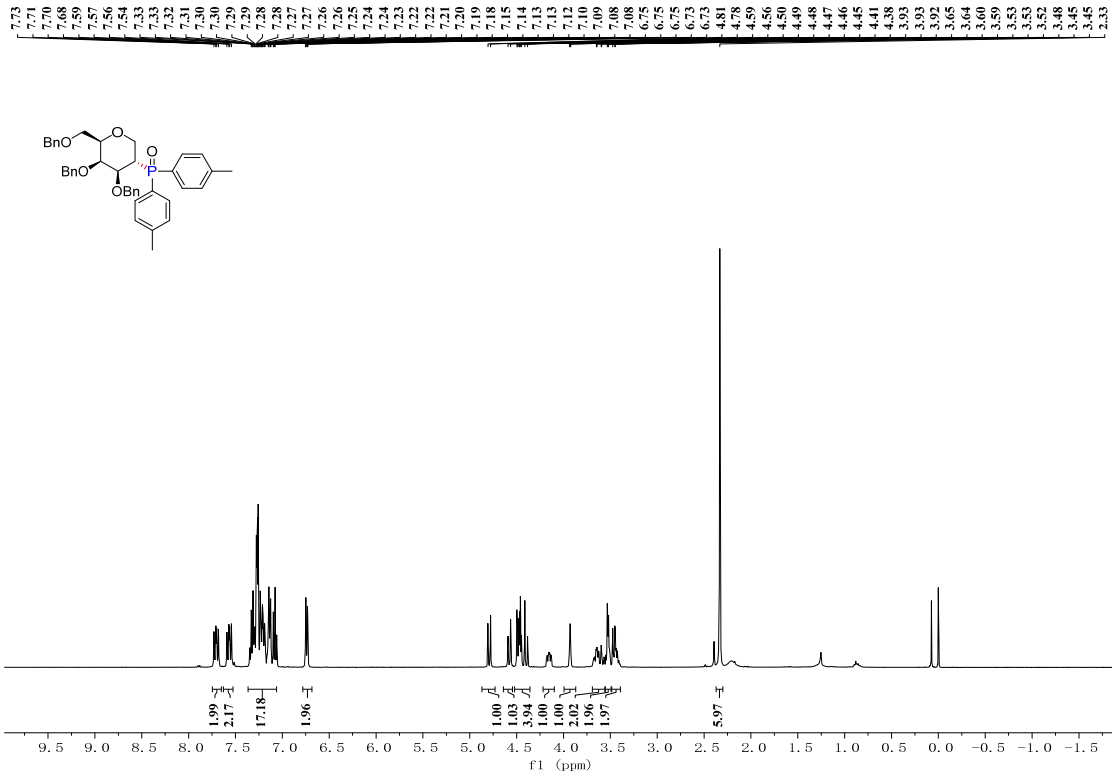

^{13}C NMR ($CDCl_3$, 100 MHz) of **4a**

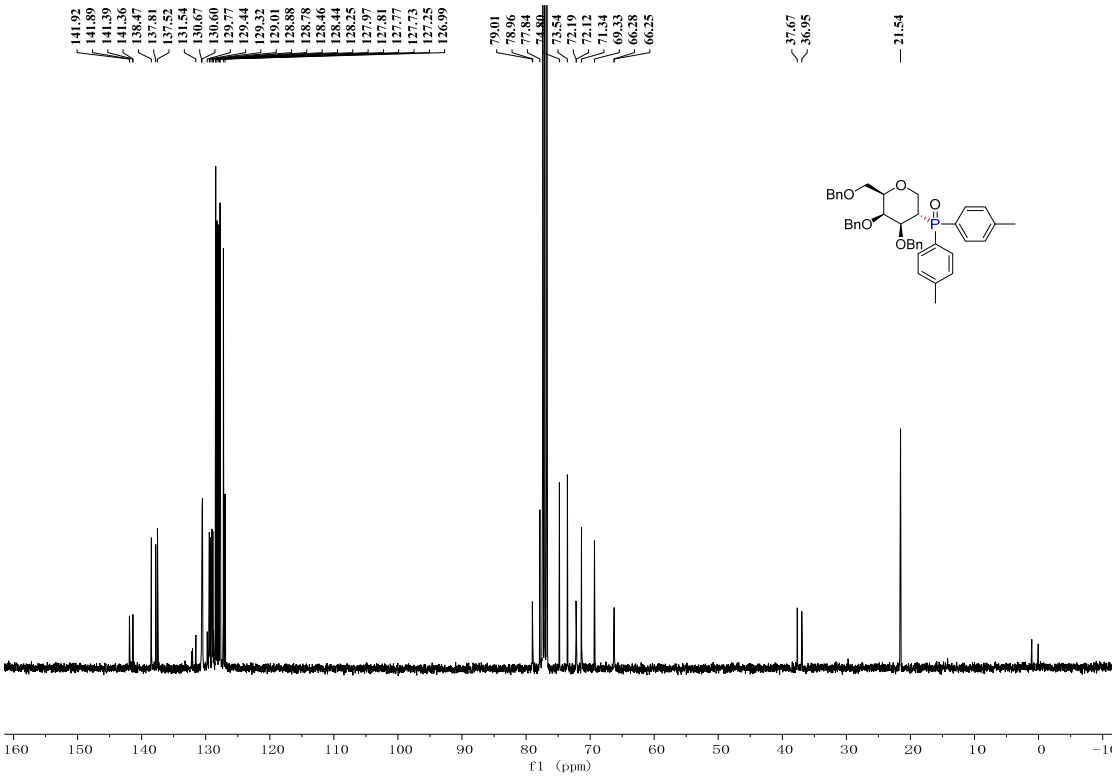

^{31}P NMR ($CDCl_3$, 162 MHz) of **4a**

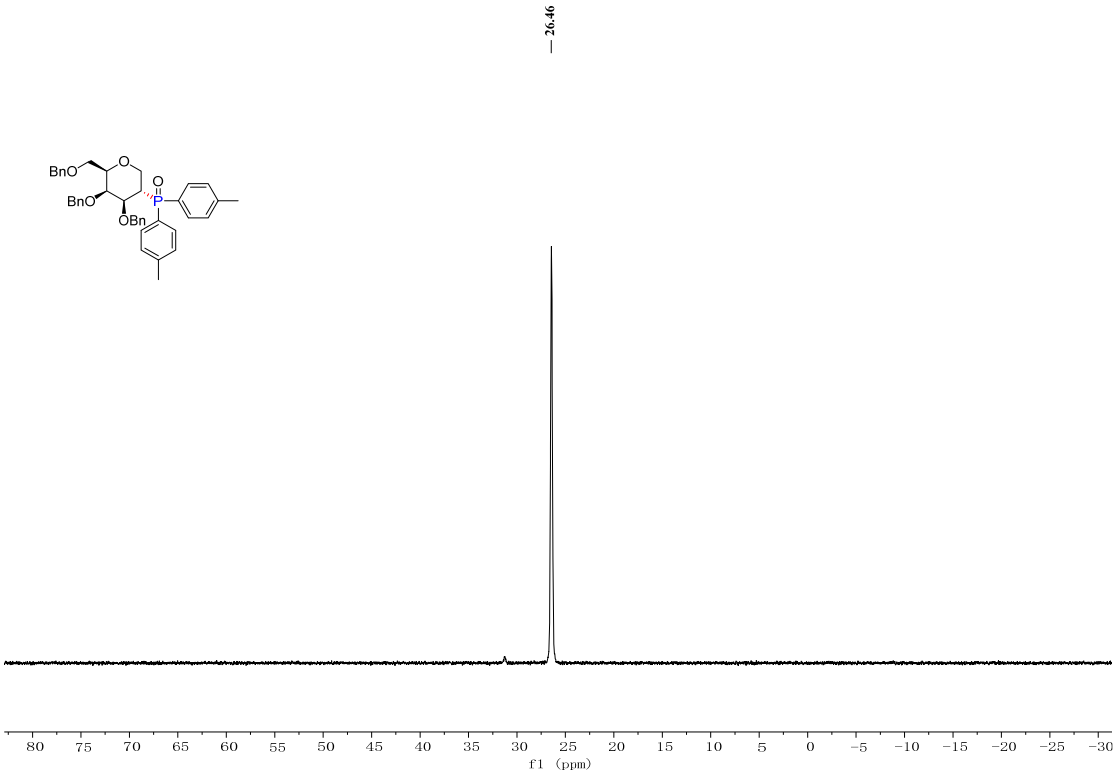

^{1}H NMR ($CDCl_3$, 400 MHz) of **4b**

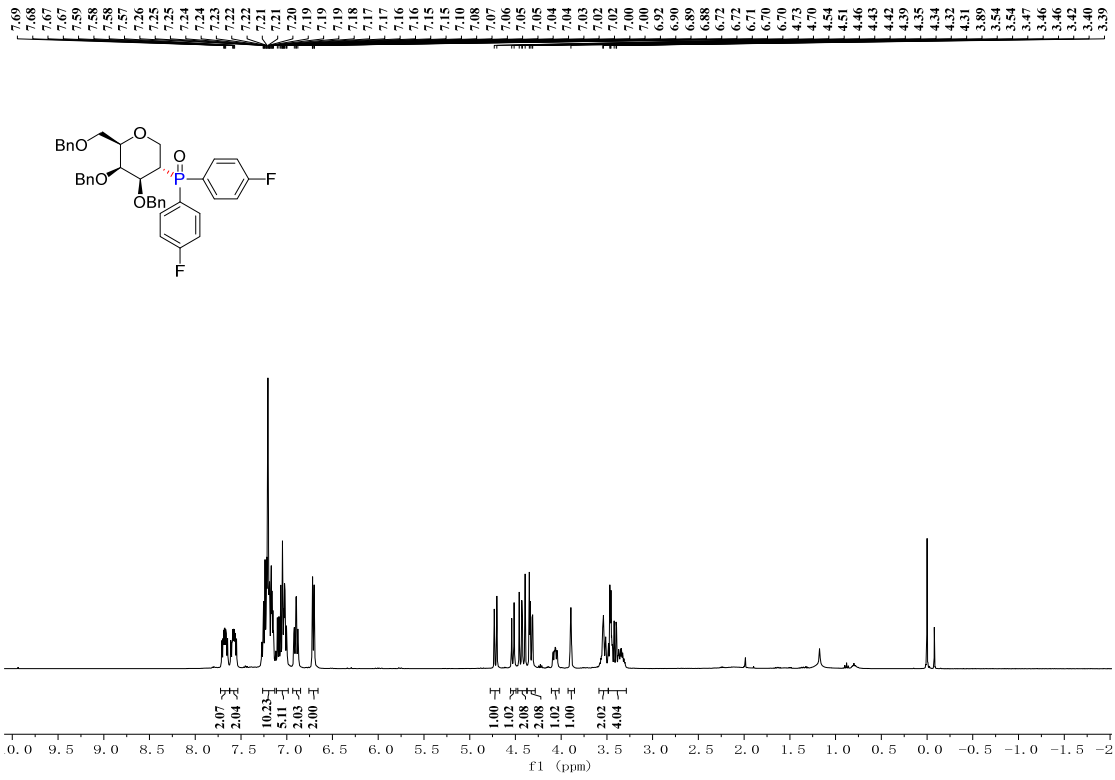

^{13}C NMR ($CDCl_3$, 100 MHz) of **4b**

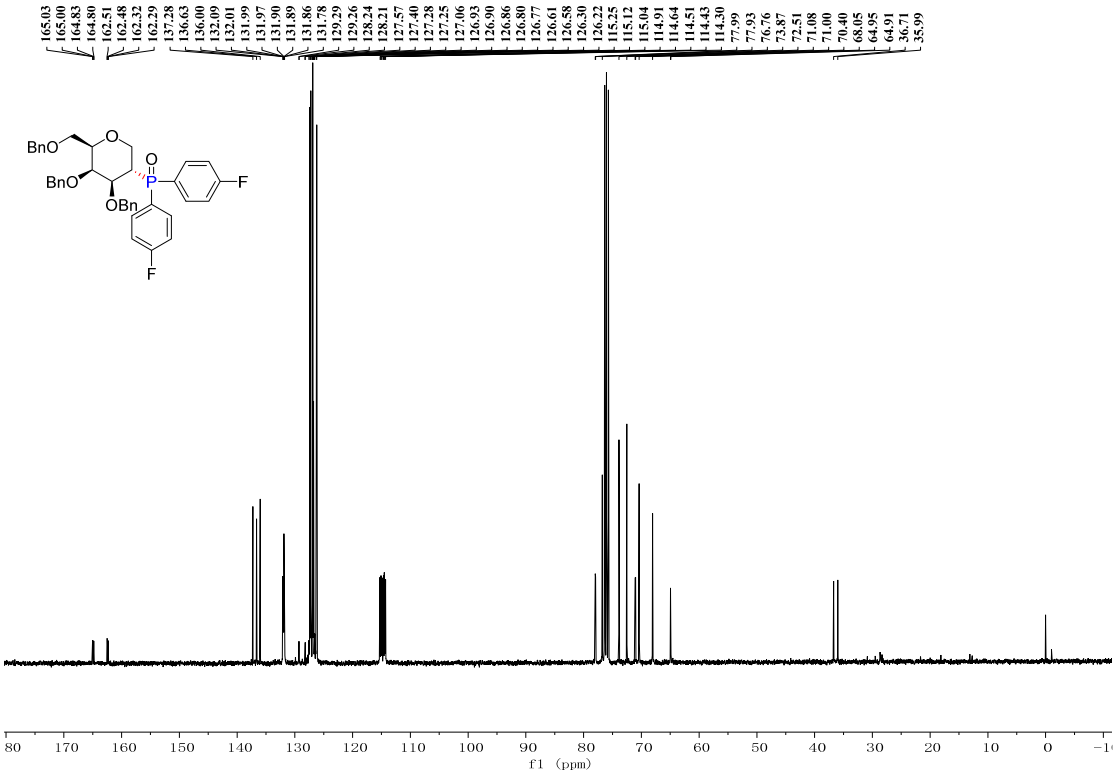

^{31}P NMR ($CDCl_3$, 162 MHz) of **4b**

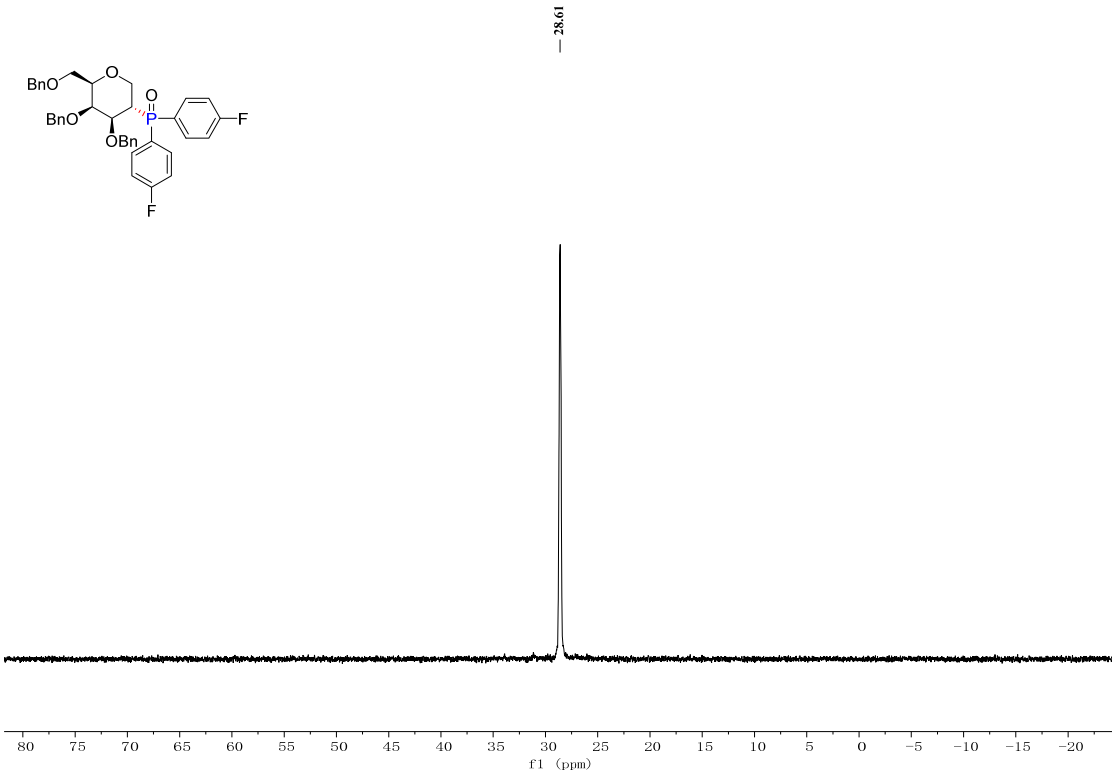

^{19}F NMR ($CDCl_3$, 101 MHz) of **4b**

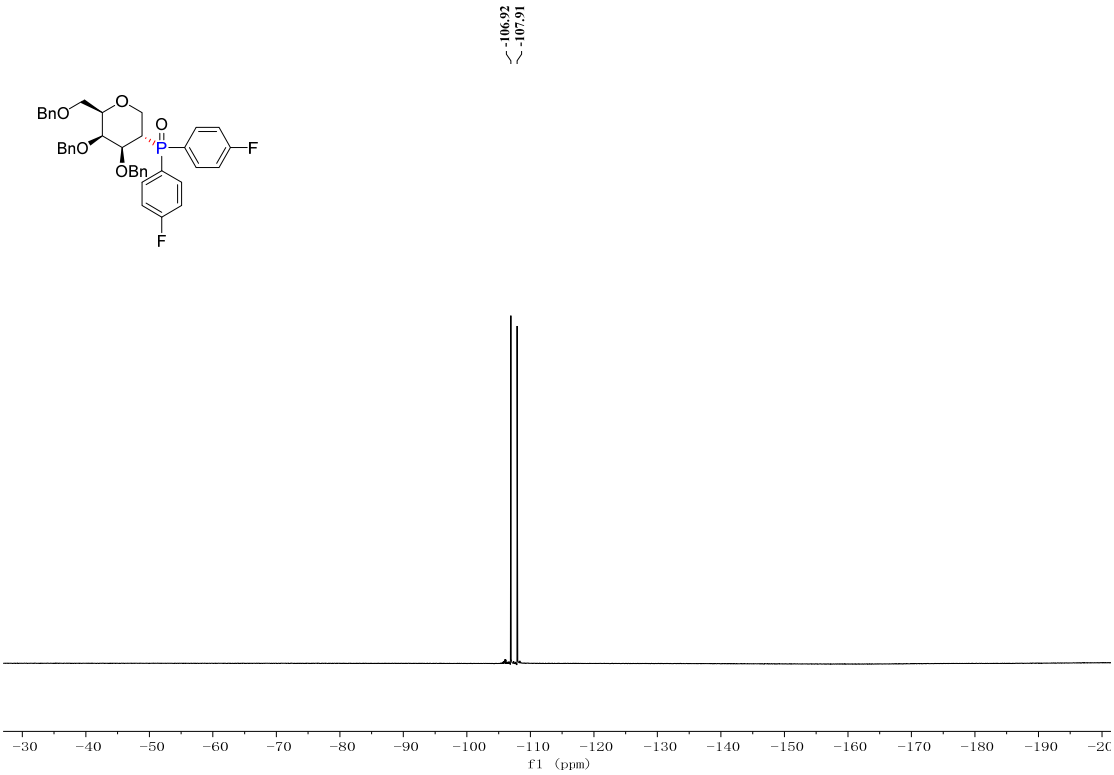

^{1}H NMR ($CDCl_3$, 400 MHz) of **4c**

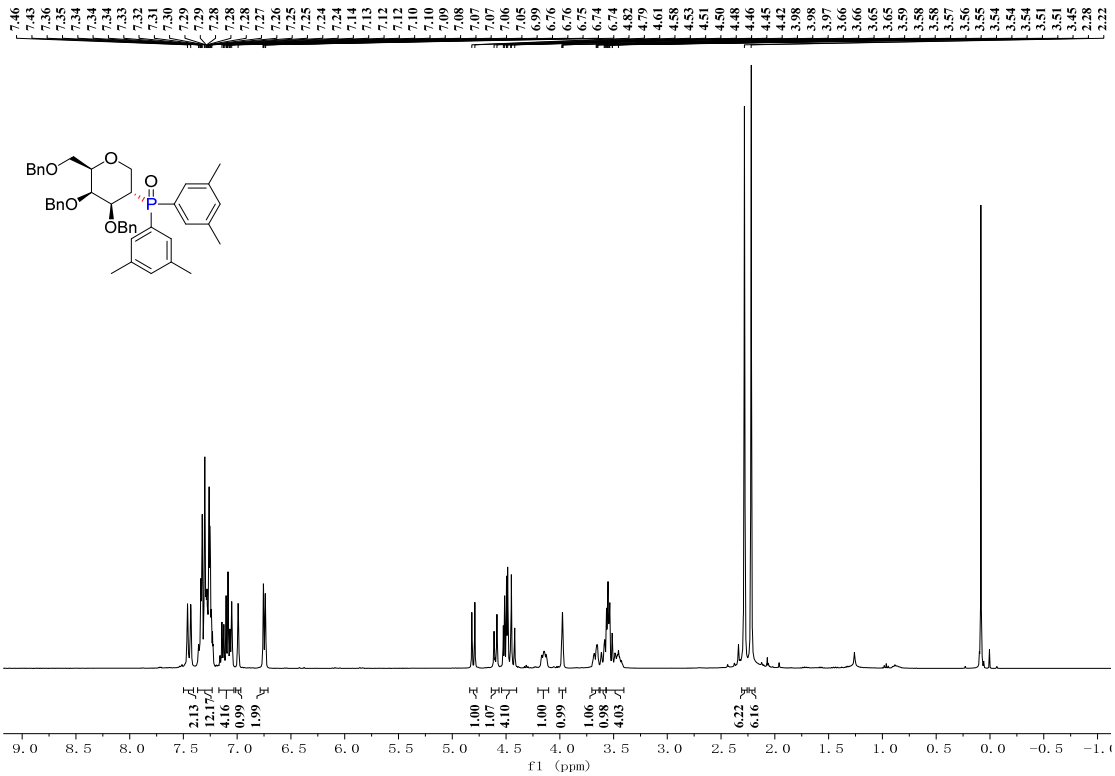

^{13}C NMR ($CDCl_3$, 100 MHz) of **4c**

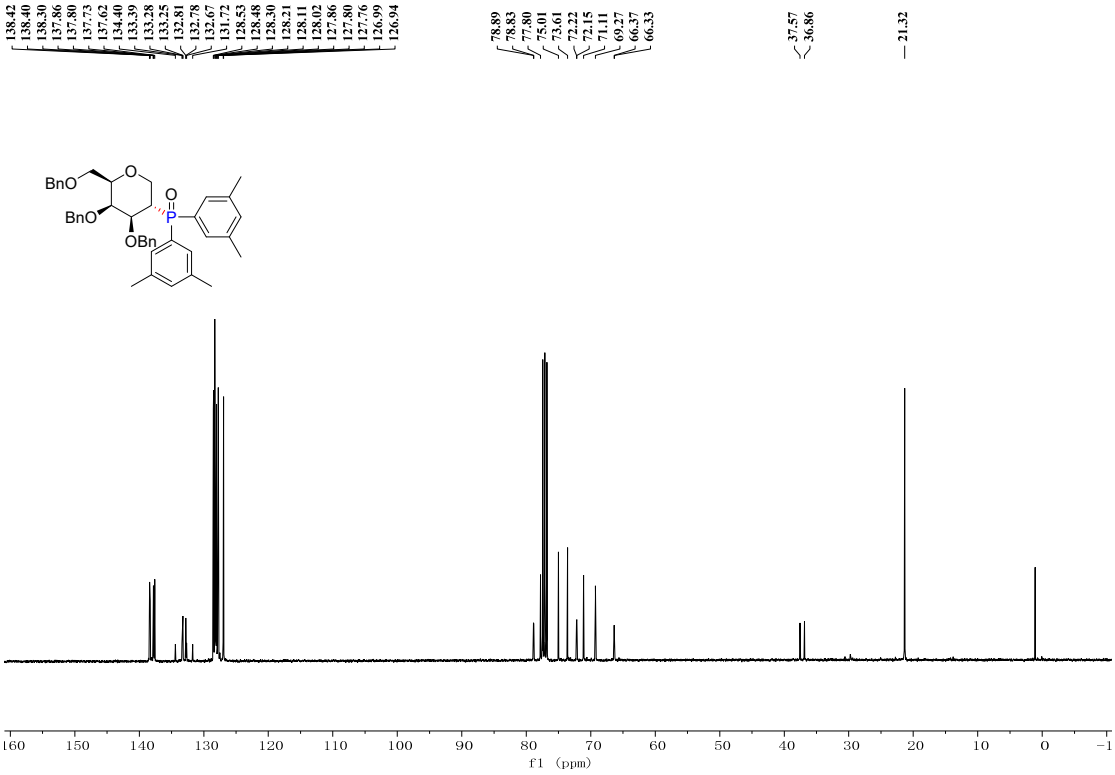

^{31}P NMR ($CDCl_3$, 162 MHz) of **4c**

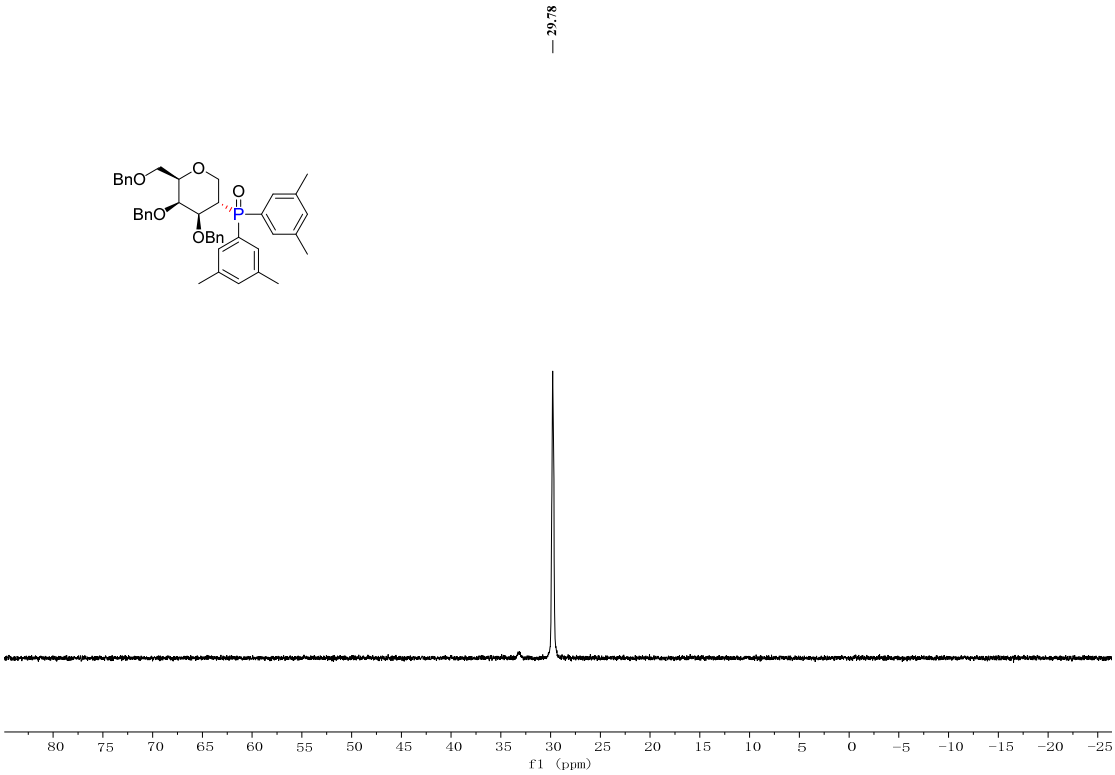

^{1}H NMR ($CDCl_3$, 400 MHz) of **4d**

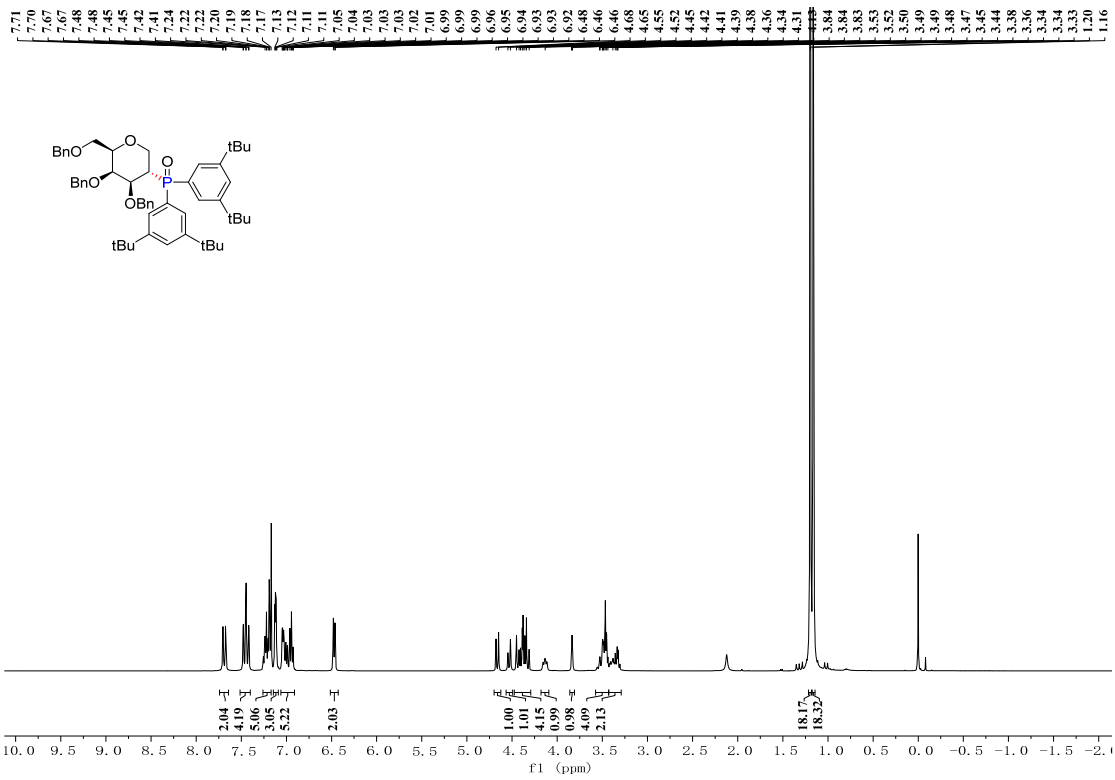

^{13}C NMR ($CDCl_3$, 100 MHz) of **4d**

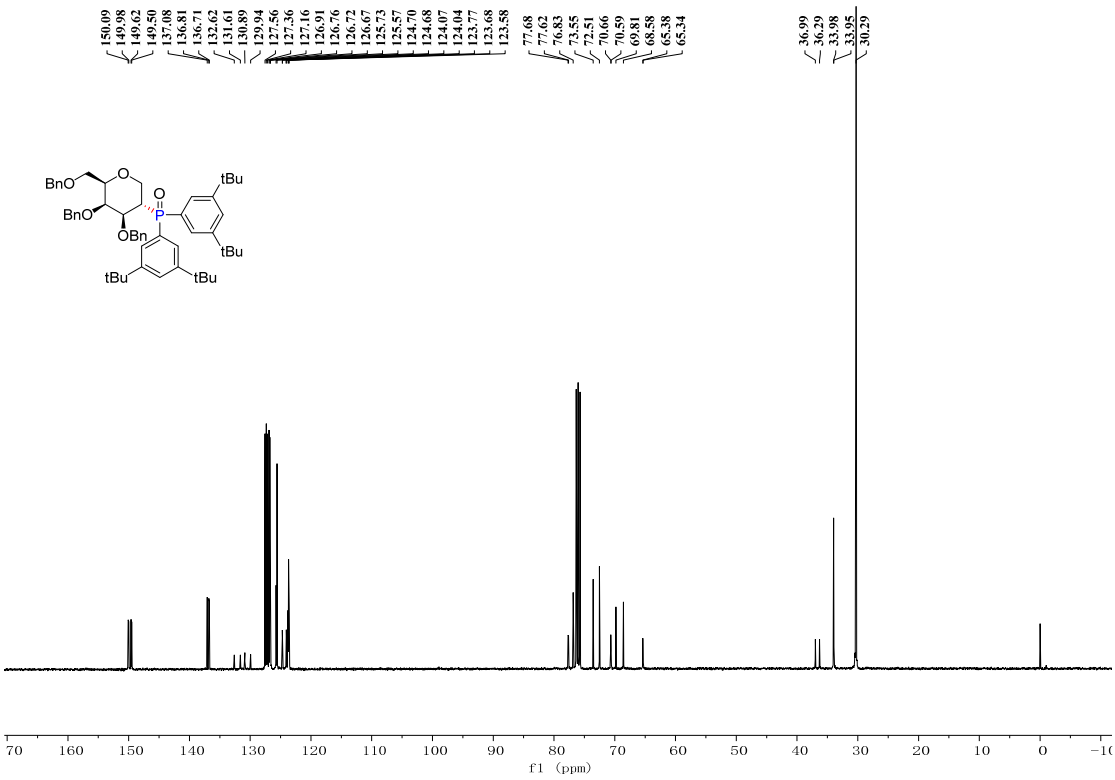

^{31}P NMR ($CDCl_3$, 162 MHz) of **4d**

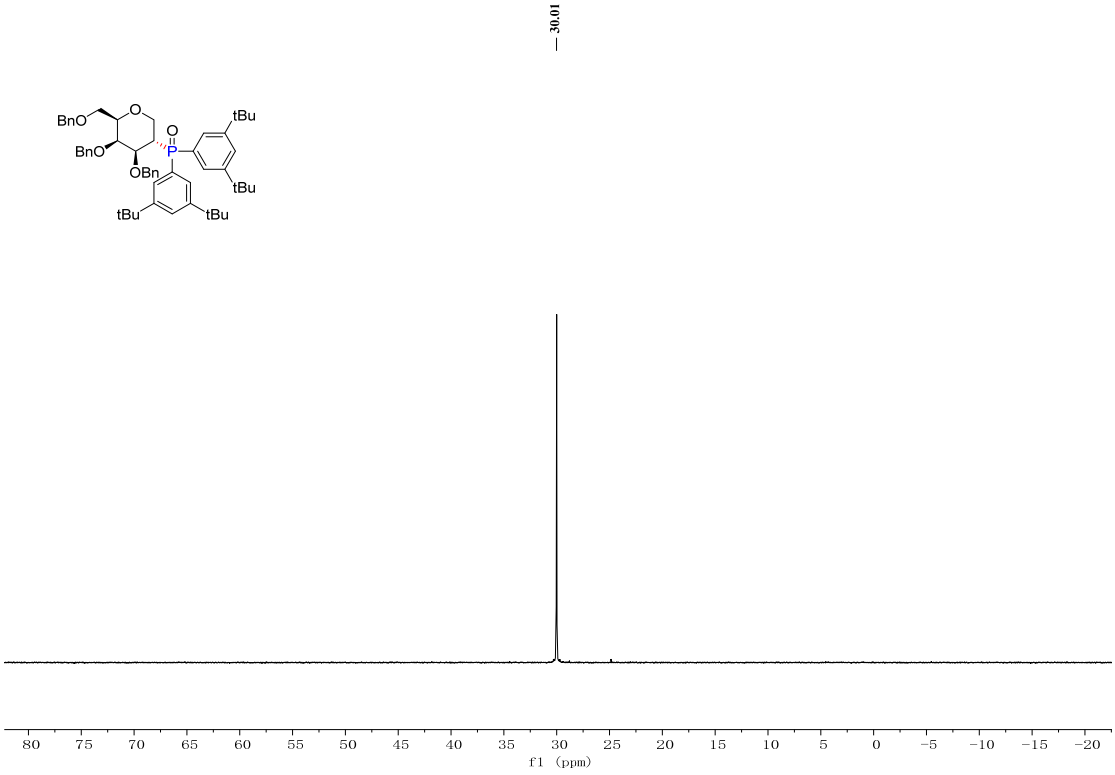

^{1}H NMR ($CDCl_3$, 400 MHz) of **4e**

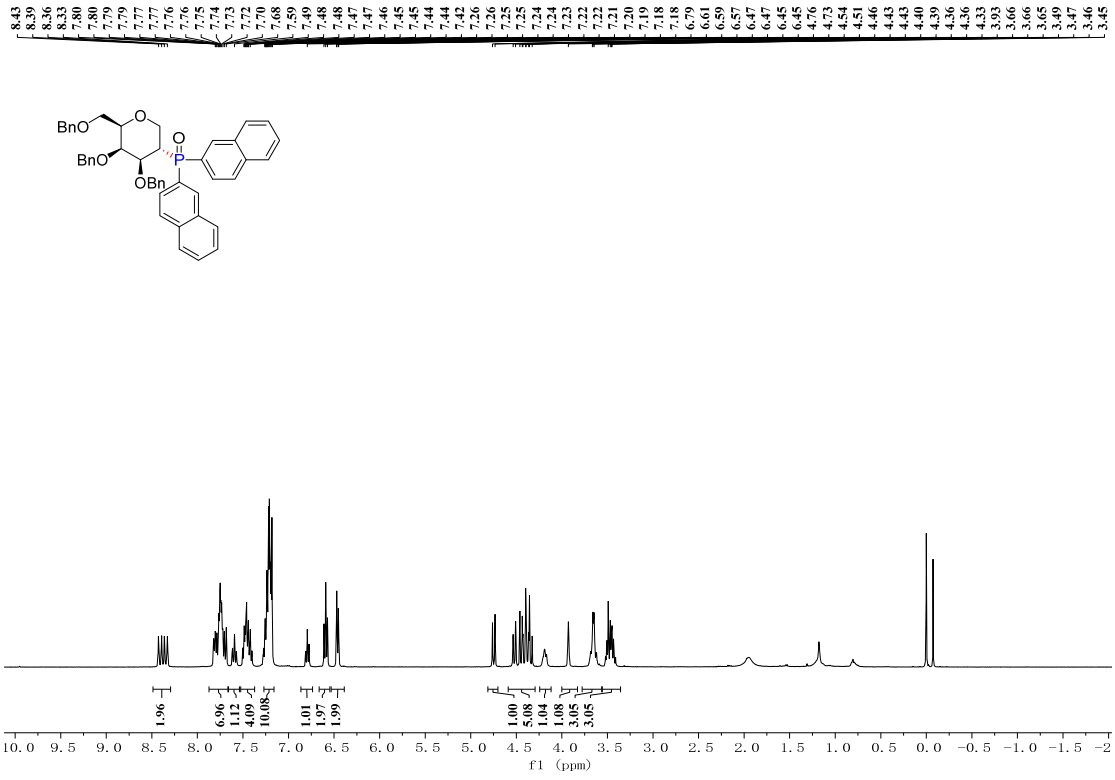

^{13}C NMR ($CDCl_3$, 100 MHz) of **4e**

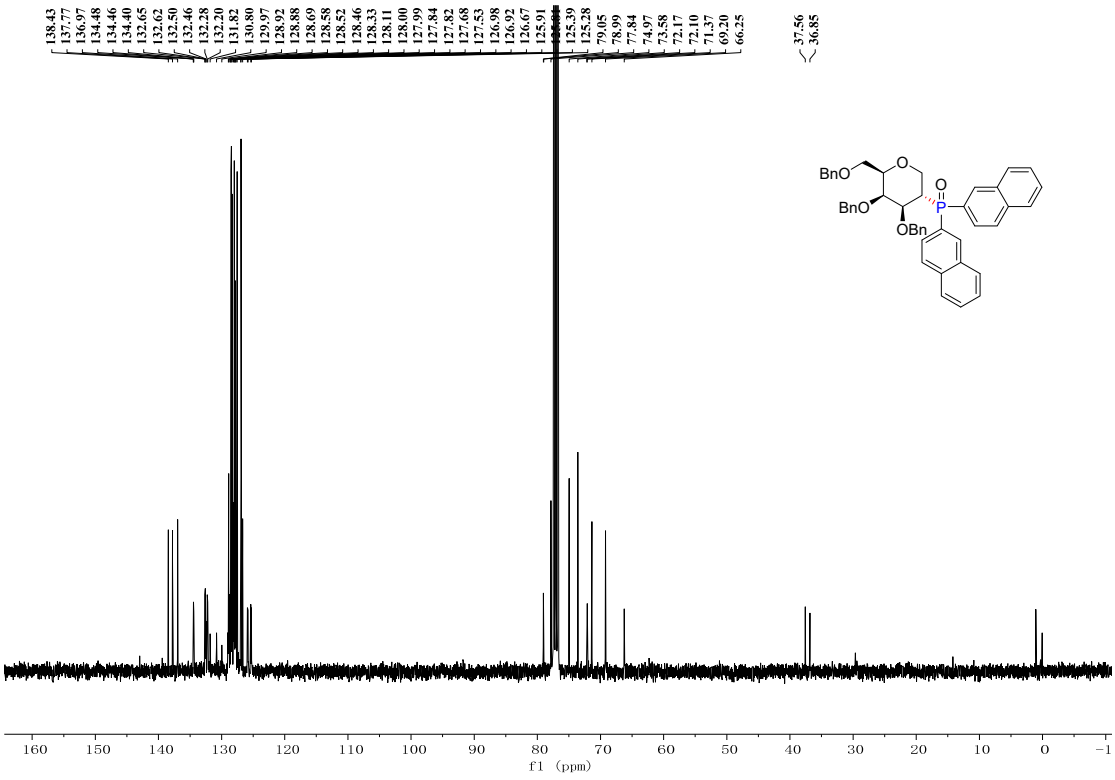

^{31}P NMR ($CDCl_3$, 162 MHz) of **4e**

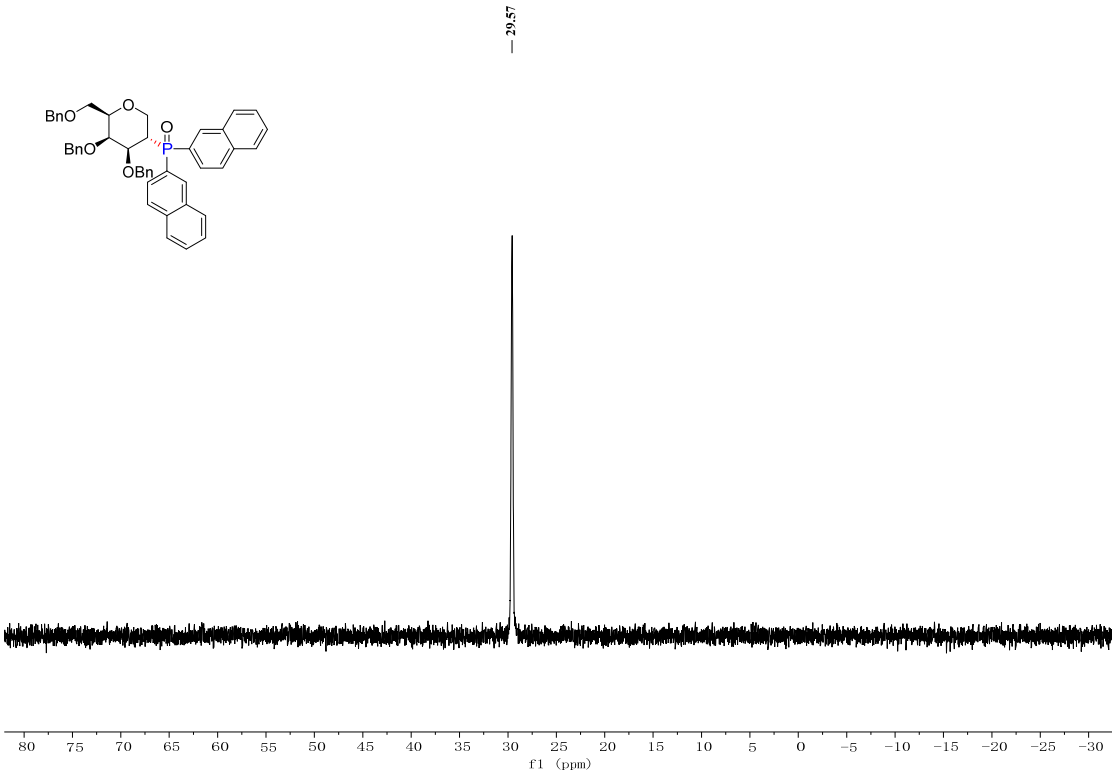

^{1}H NMR ($CDCl_3$, 400 MHz) of **4f**

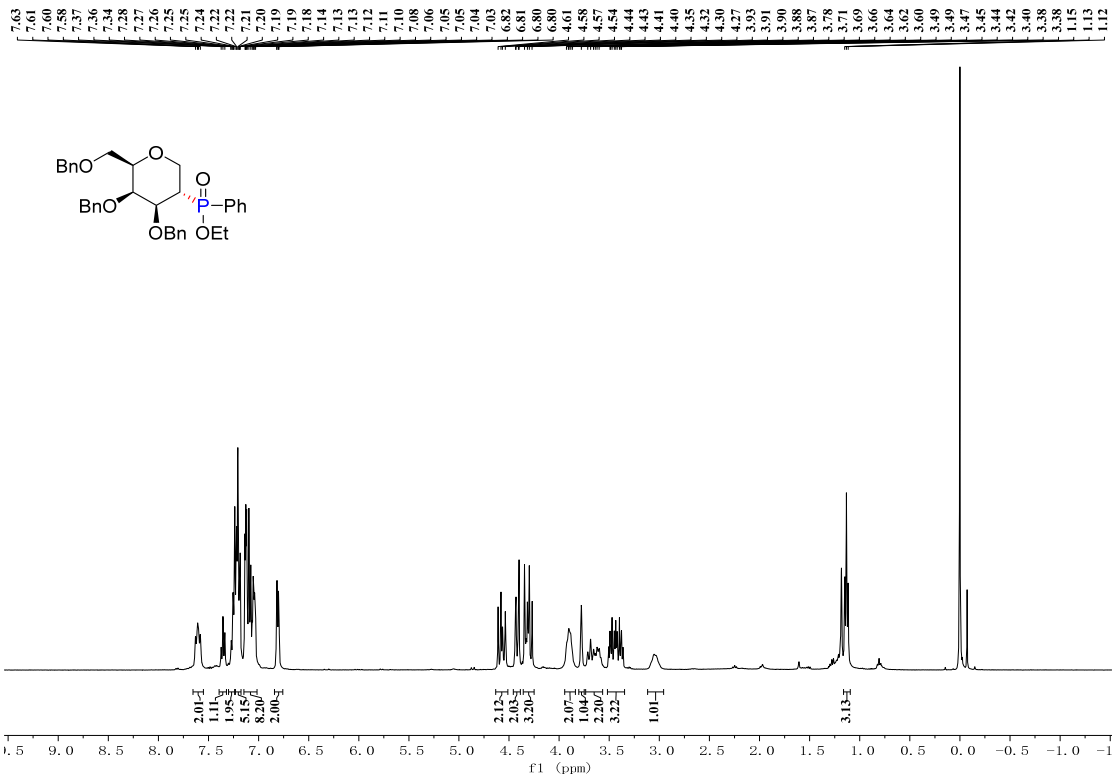

^{13}C NMR ($CDCl_3$, 100 MHz) of **4f**

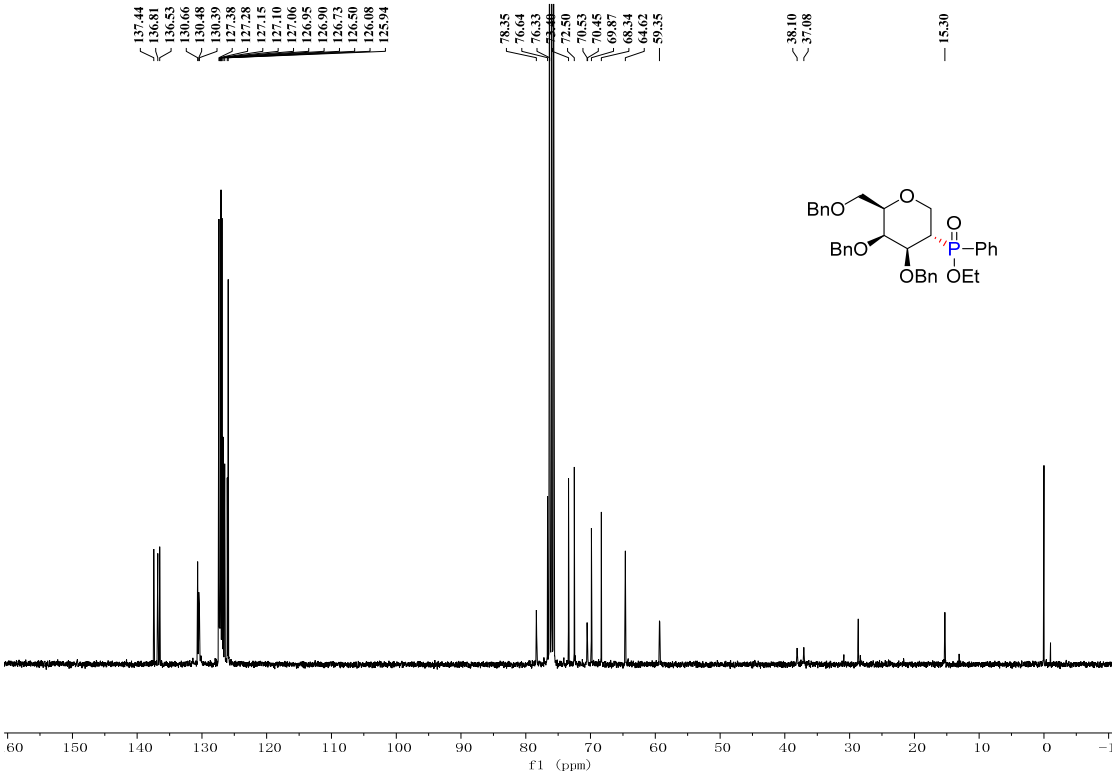

^{31}P NMR ($CDCl_3$, 162 MHz) of **4f**

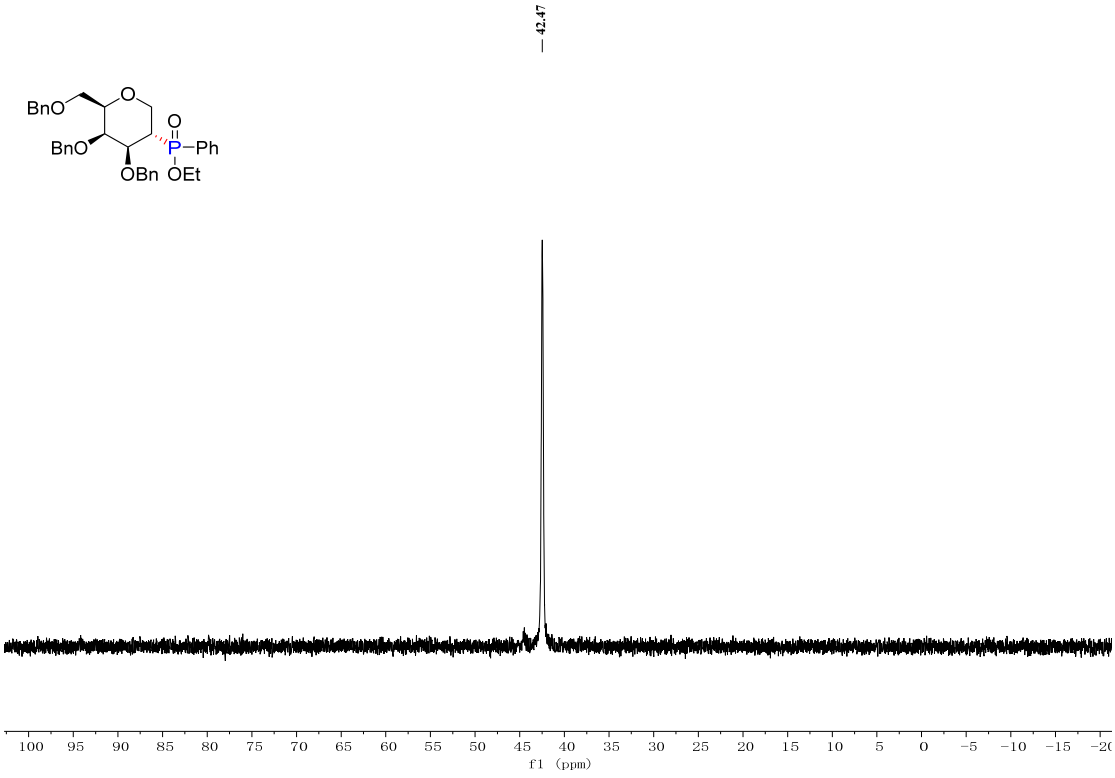

^{1}H NMR ($CDCl_3$, 400 MHz) of **6**

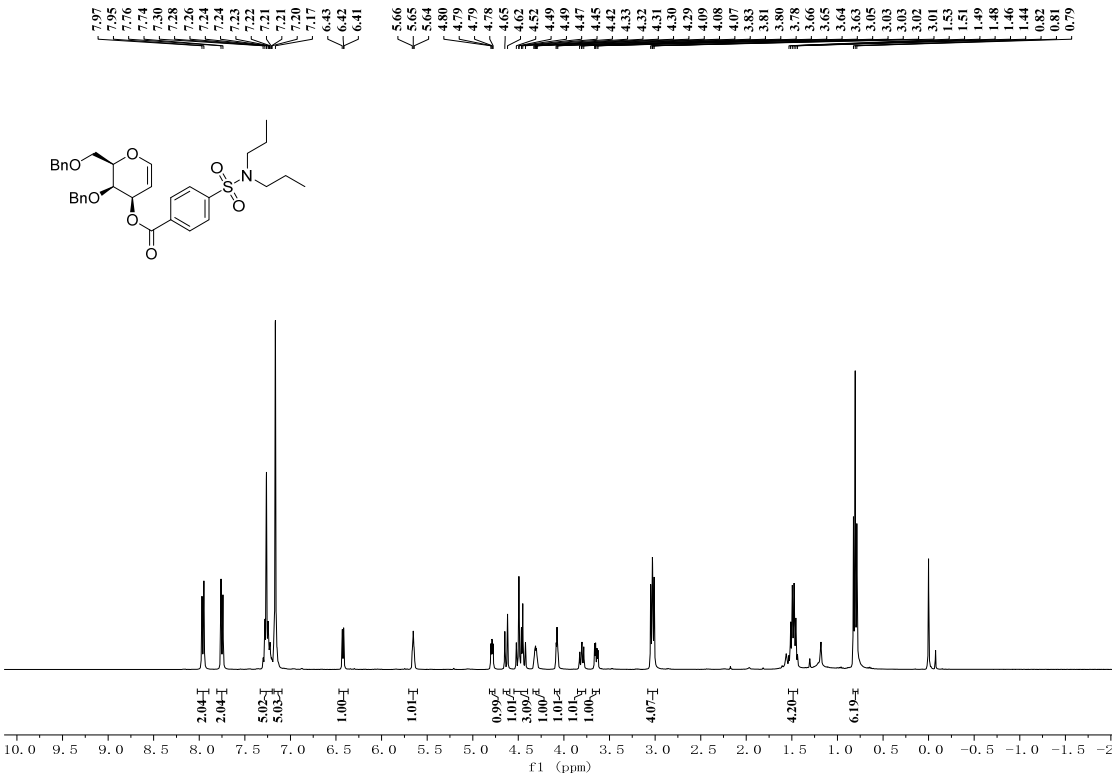

^{13}C NMR ($CDCl_3$, 100 MHz) of **6**

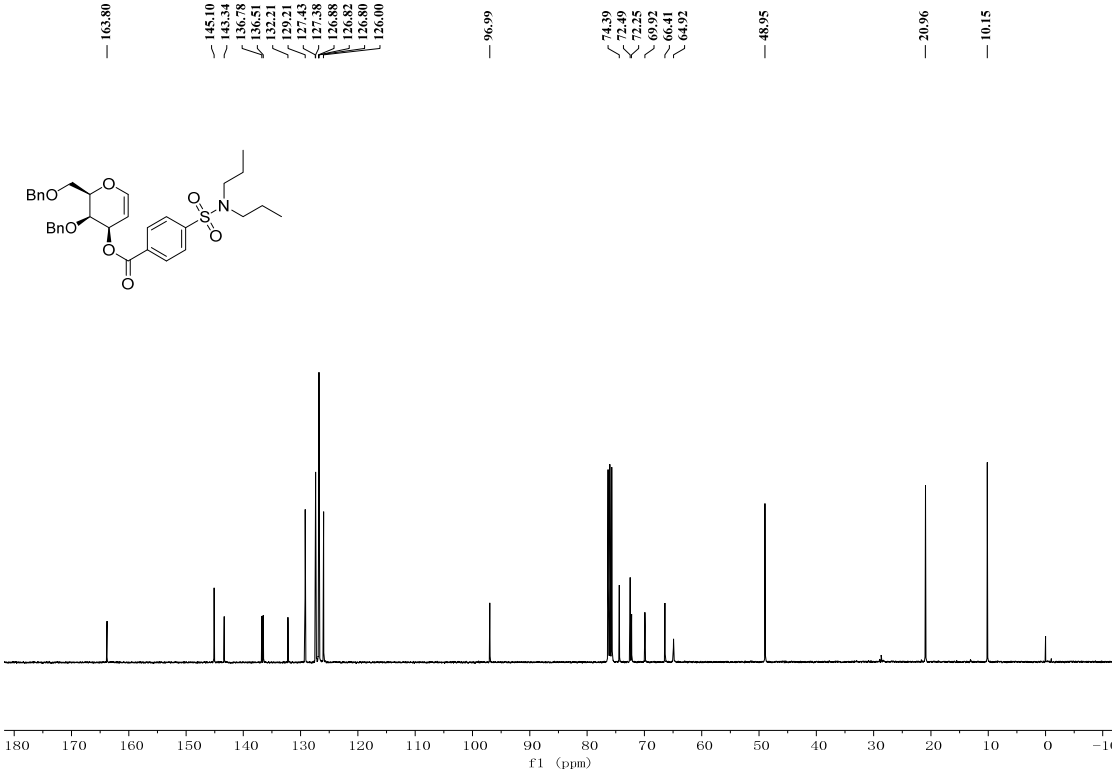

6. Structure Determination and Representative 2D NMR Spectra

To determine the stereochemistry of the anomeric carbon, one compound from each sugar class was selected for detailed NMR analyses. Firstly, most meaningful protons were assigned with the aid of COSY and HSQC. Then, characteristic NOE signals between H-2 adjacent to the hydrogens on the sugar ring were identified as shown in the following spectra. The structures of 3m-3t were confirmed unambiguously by relating to their corresponding fully protected products presented in Table 2 as well as NOE experiments.

Protective group conversion experiments

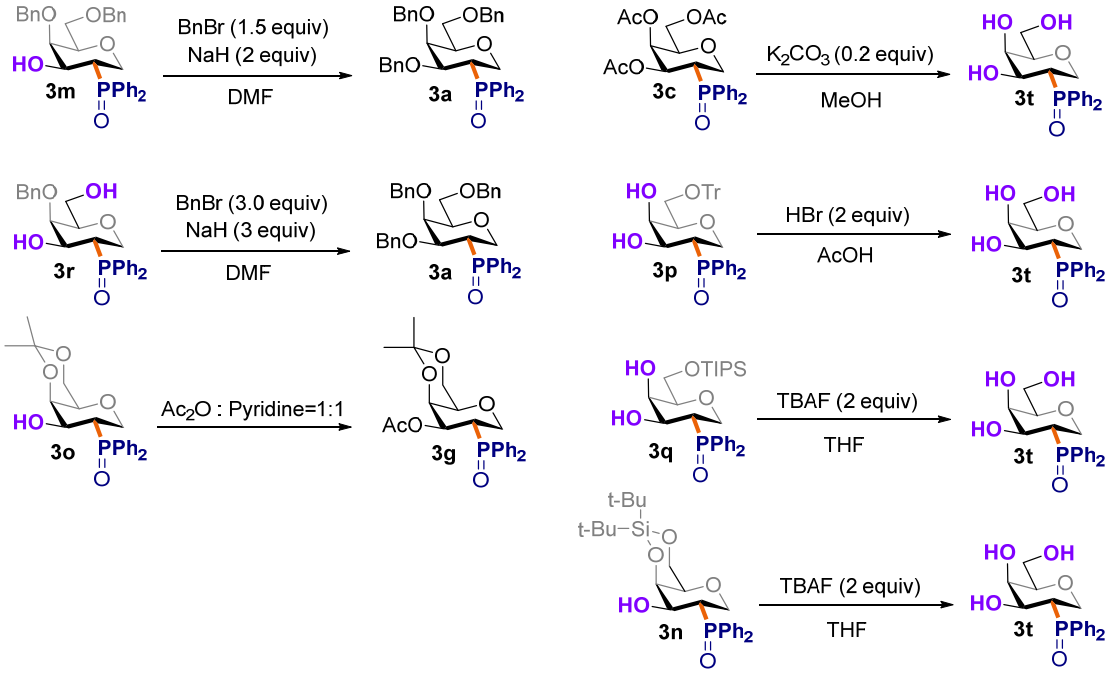

^{1}H-^{1}H HSQC ($CDCl_3$, 400MHz) of **3d**

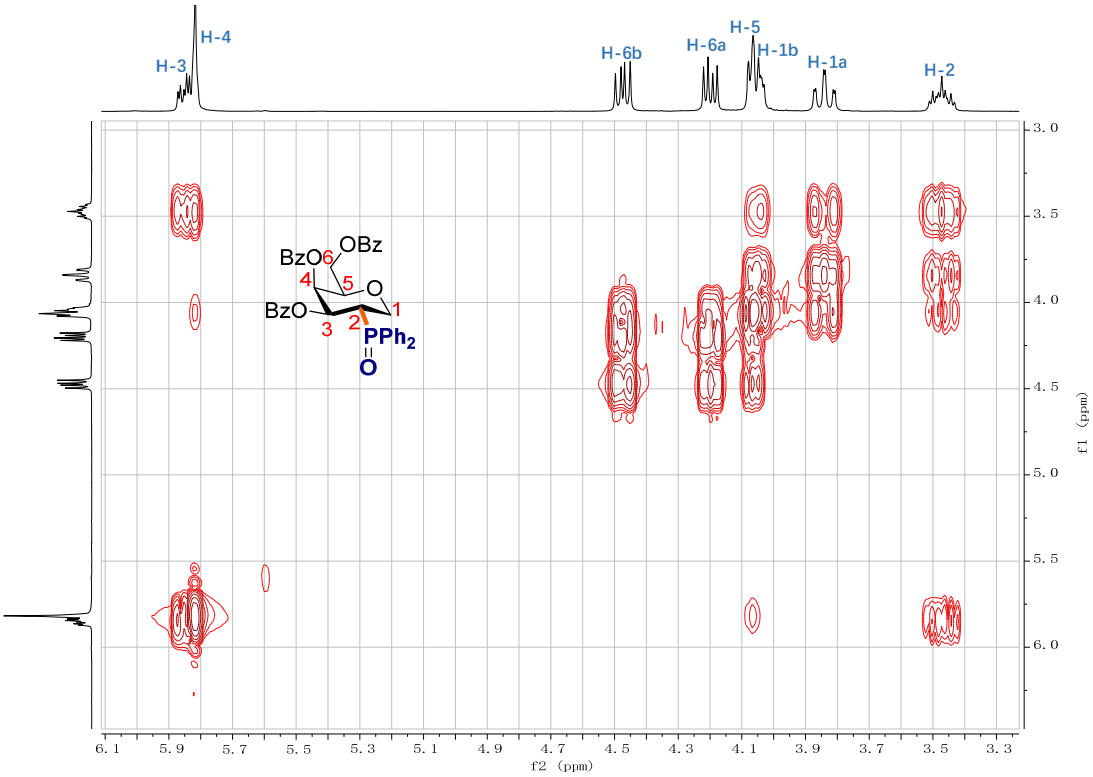

^{1}H-^{13}C HSQC ($CDCl_3$, 400MHz) of **3d**

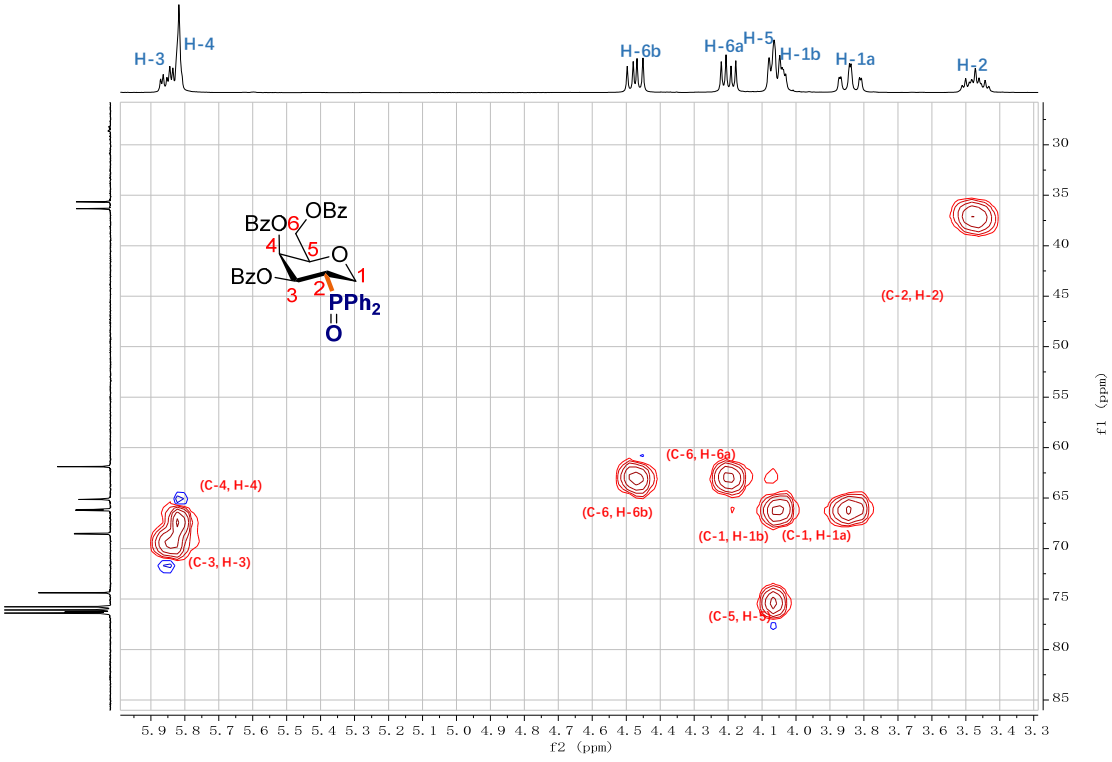

^{1}H-^{1}H NOESY ($CDCl_3$, 400MHz) of **3d**

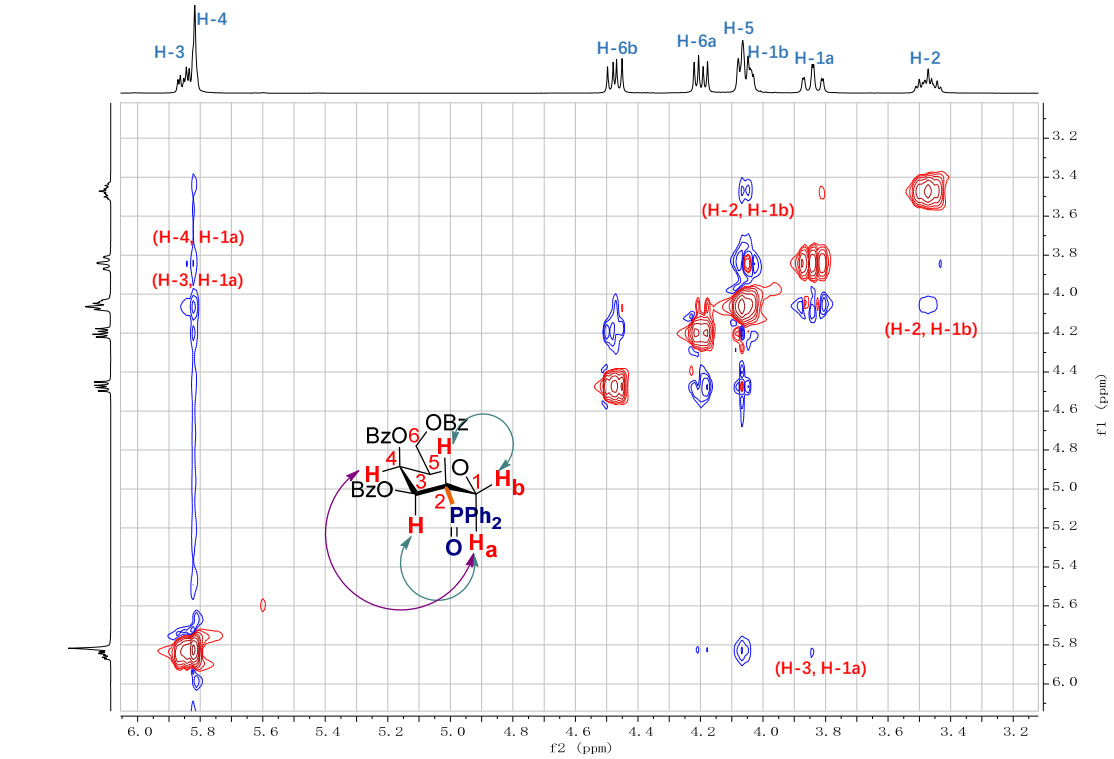

^{1}H-^{1}H HSQC ($CDCl_3$, 400MHz) of **3f**

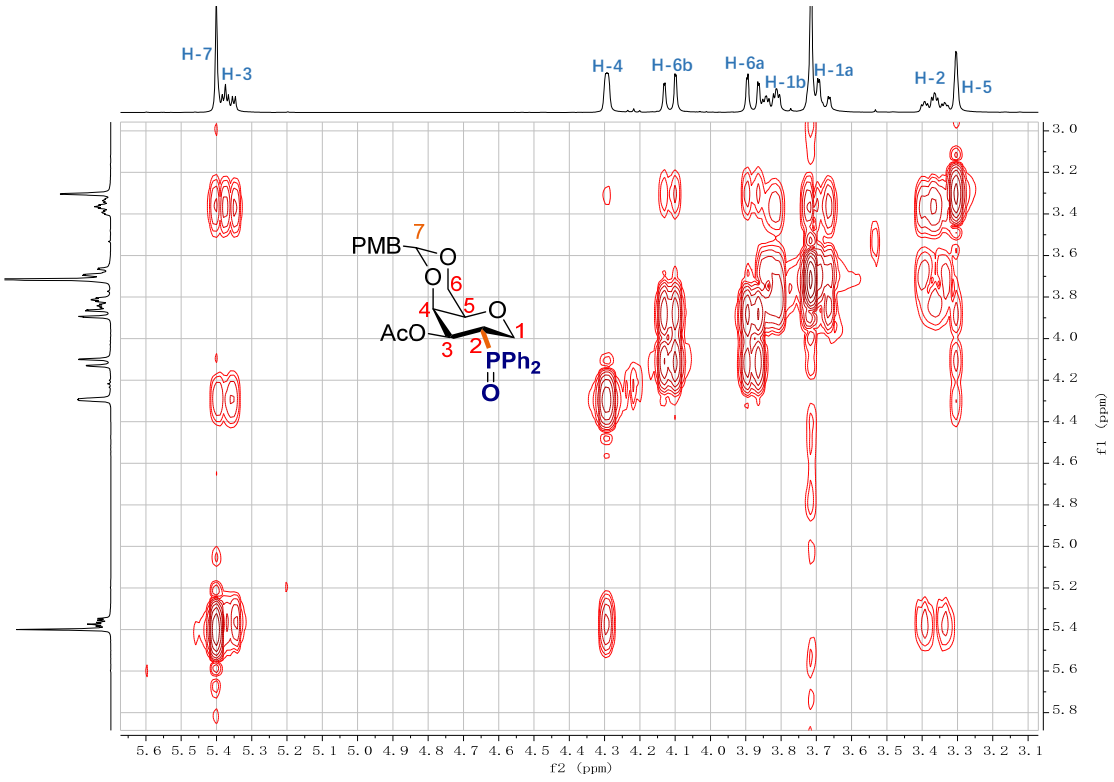

^{1}H-^{13}C HSQC ($CDCl_3$, 400MHz) of **3f**

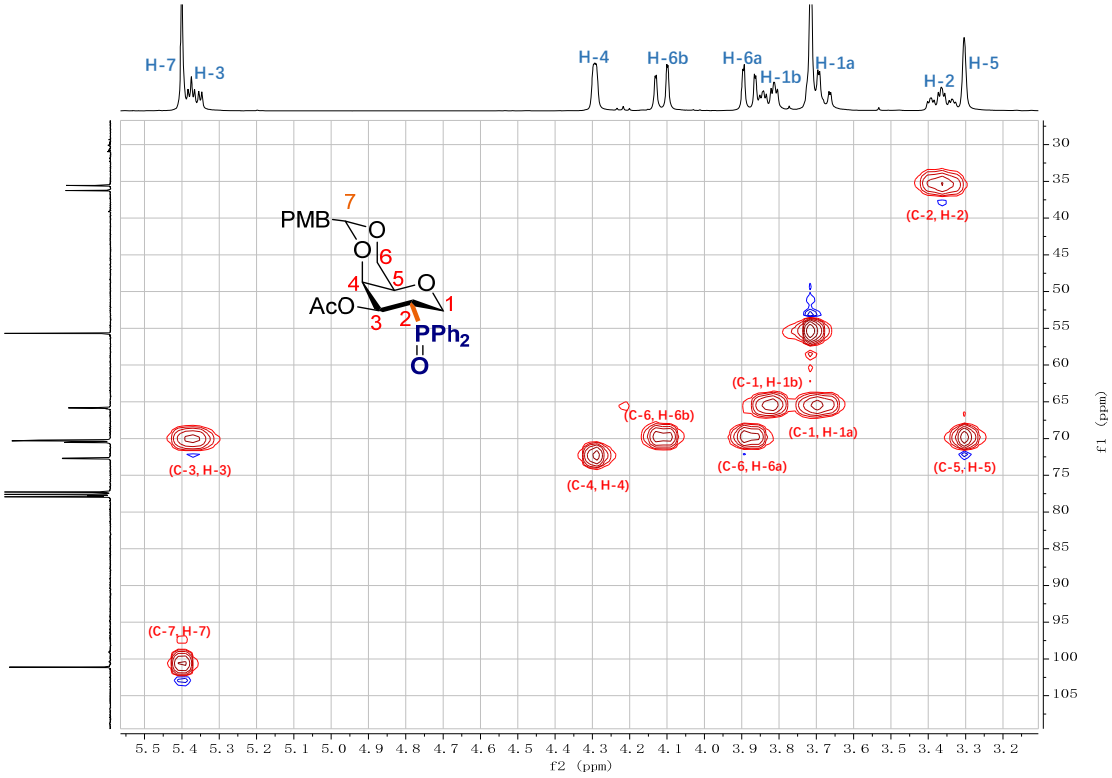

^{1}H-^{1}H NOESY ($CDCl_3$, 400MHz) of **3f**

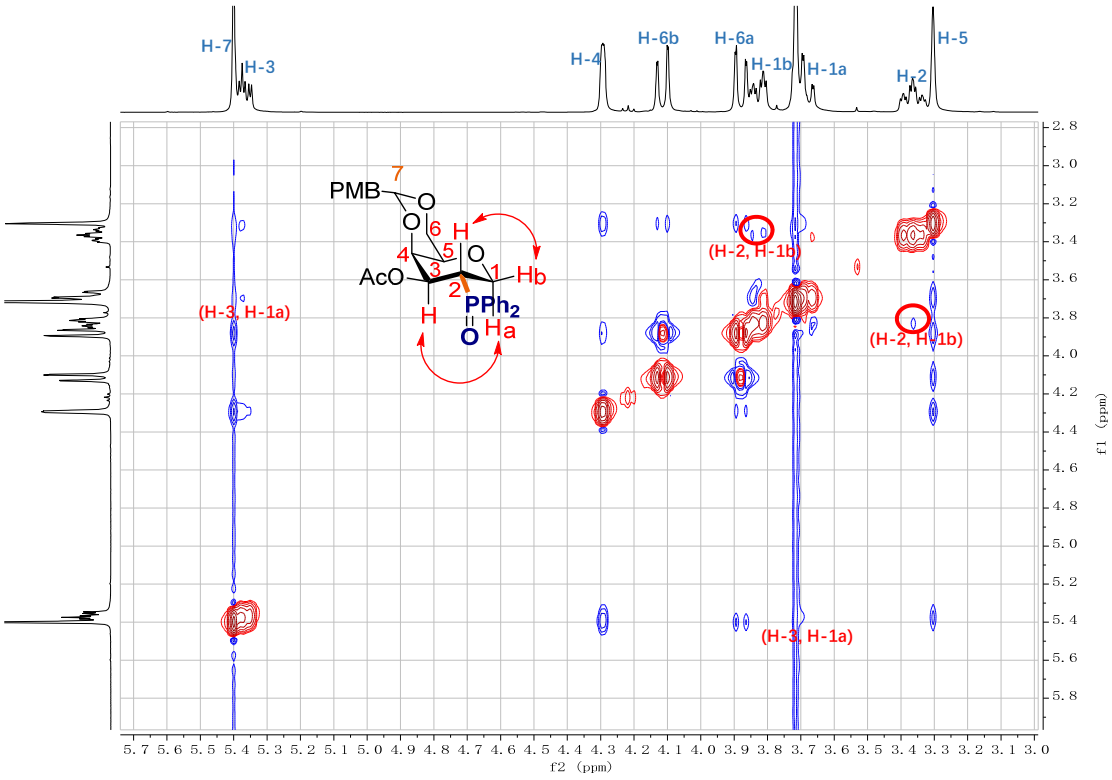

^{1}H-^{1}H COSY ($CDCl_3$, 400MHz) of **3i**

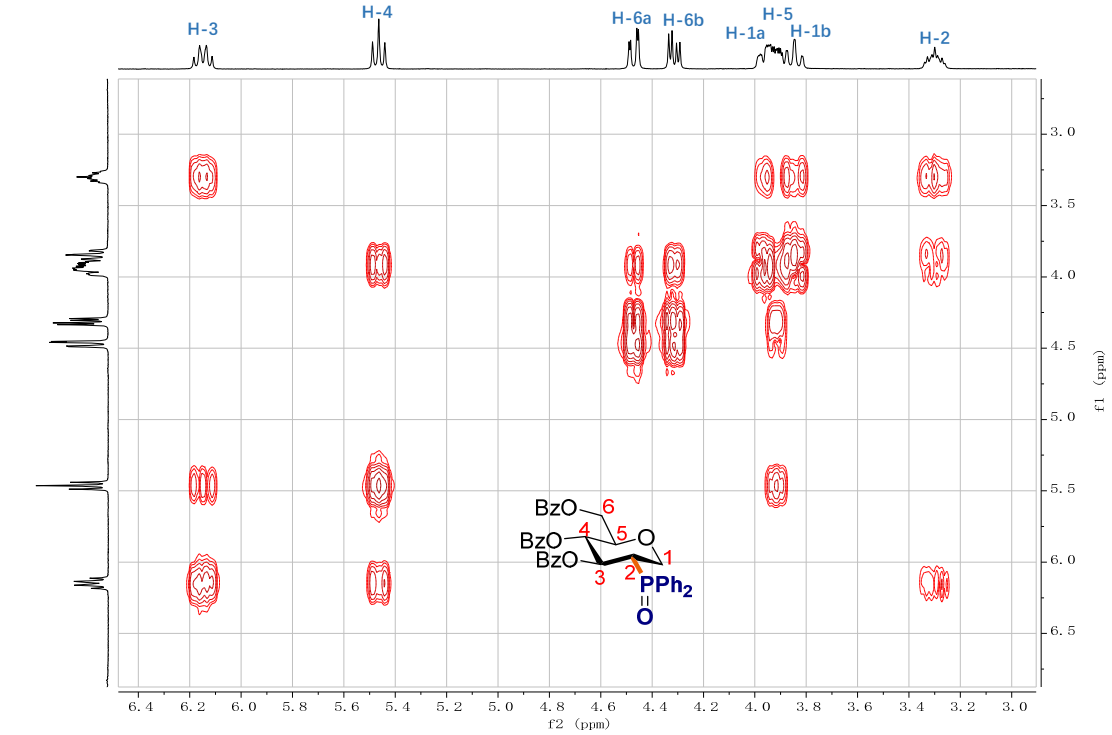

^{1}H-^{13}C HSQC ($CDCl_3$, 400MHz) of **3i**

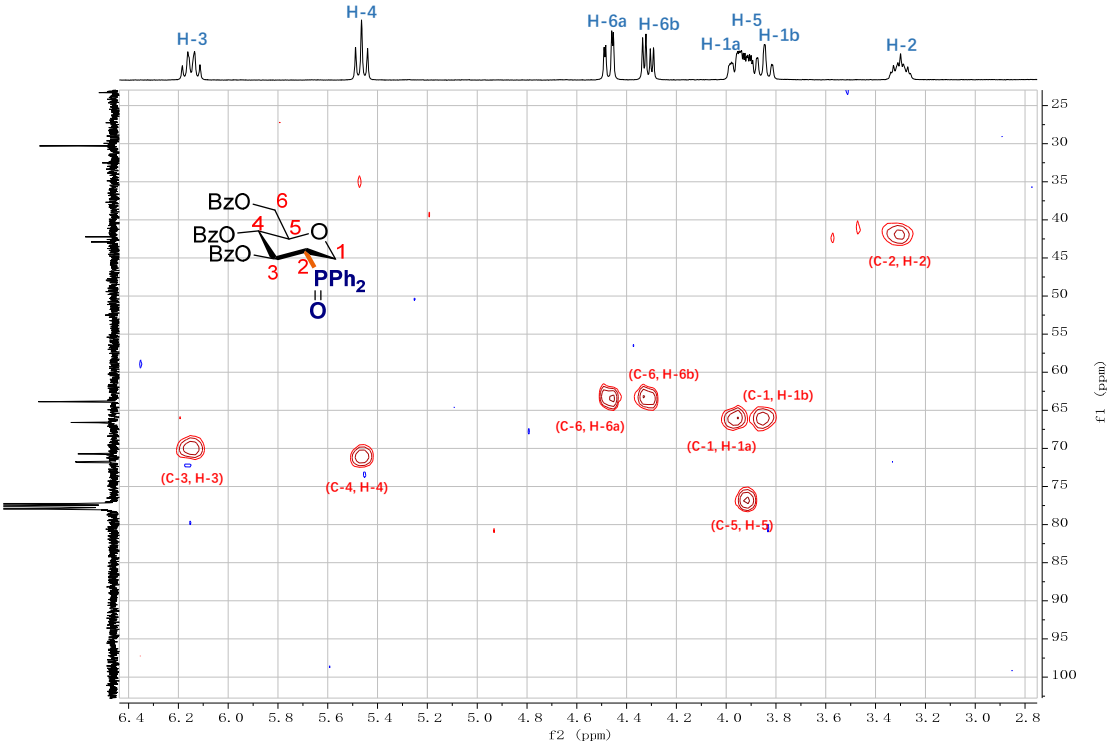

^{1}H-^{1}H NOESY ($CDCl_3$, 400MHz) of **3i**

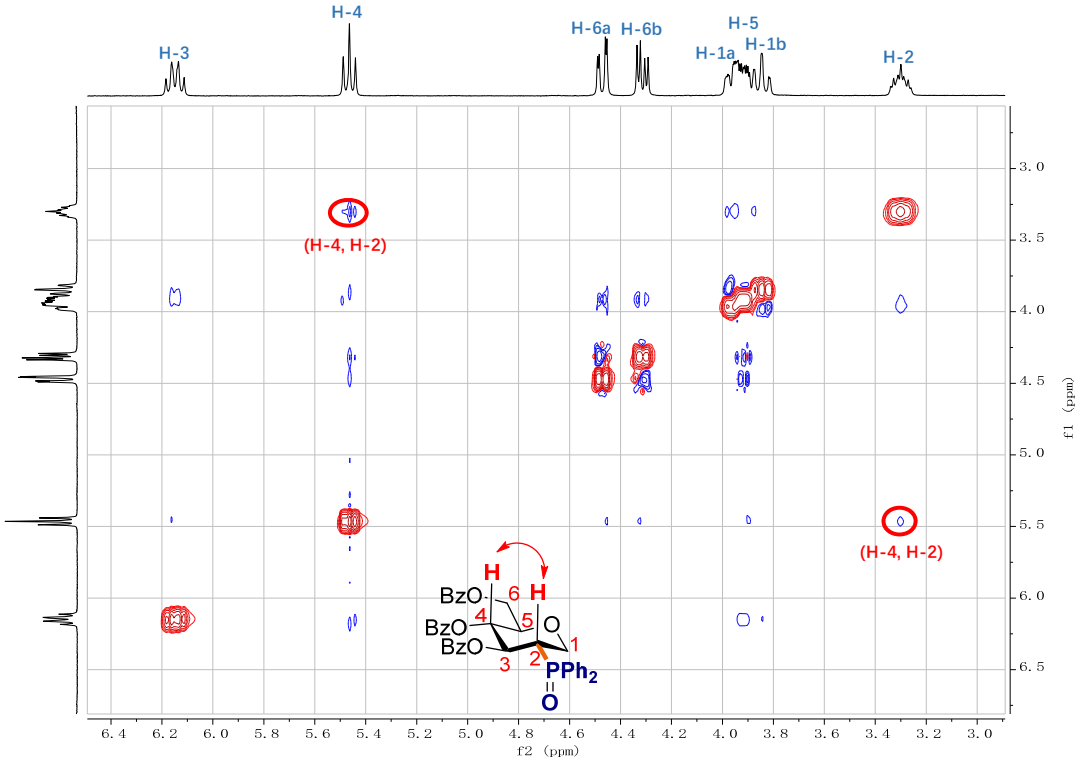

^{1}H-^{1}H COSY ($CDCl_3$, 400MHz) of **3i'**

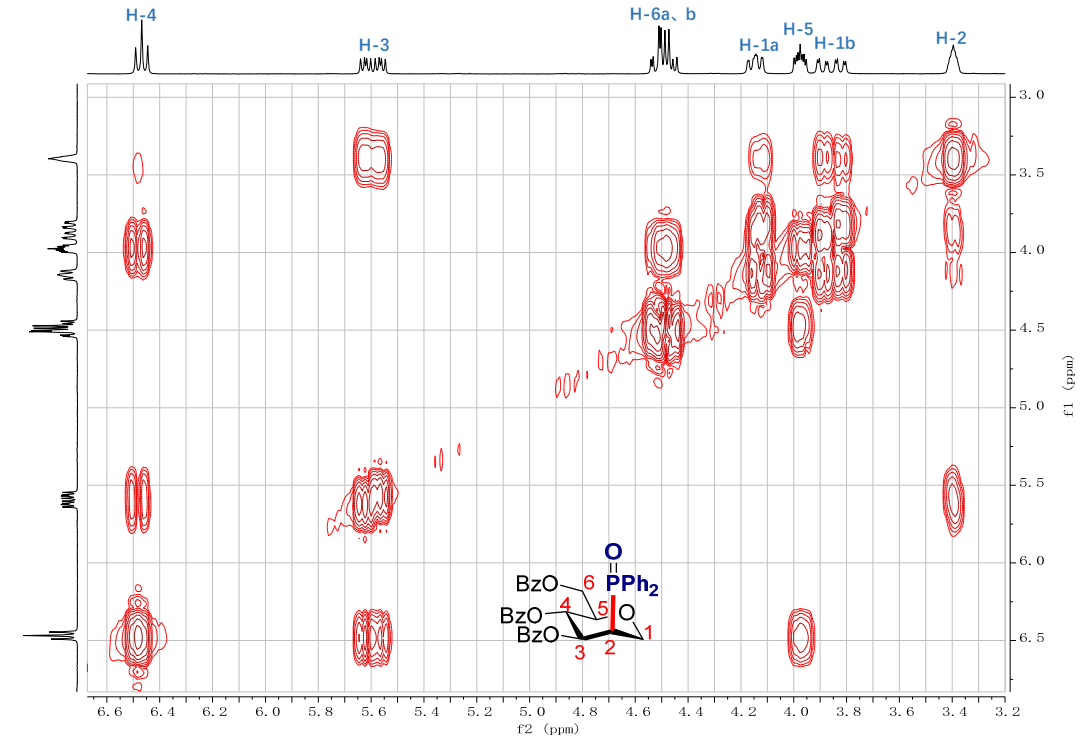

^{1}H-^{13}C HSQC (CDl_3, 400MHz) of **3i'**

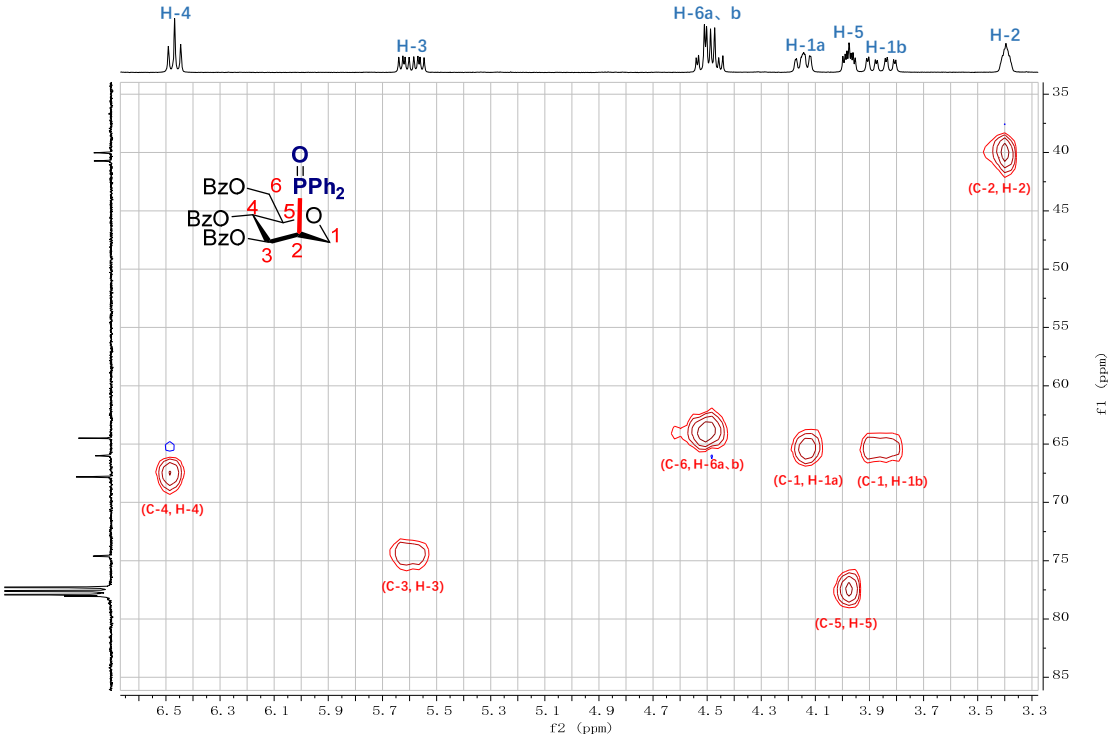

^{1}H-^{1}H NOESY ($CDCl_3$, 400MHz) of **3i'**

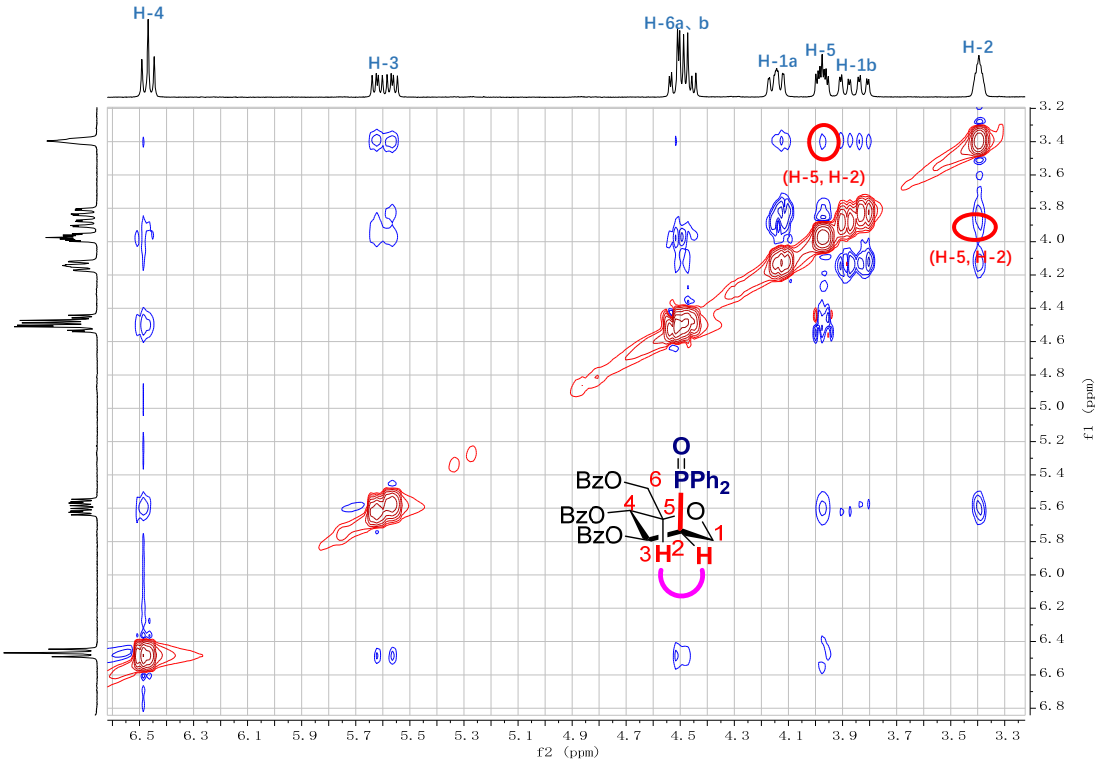

^{1}H-^{1}H COSY ($CDCl_3$, 400MHz) of **3h**

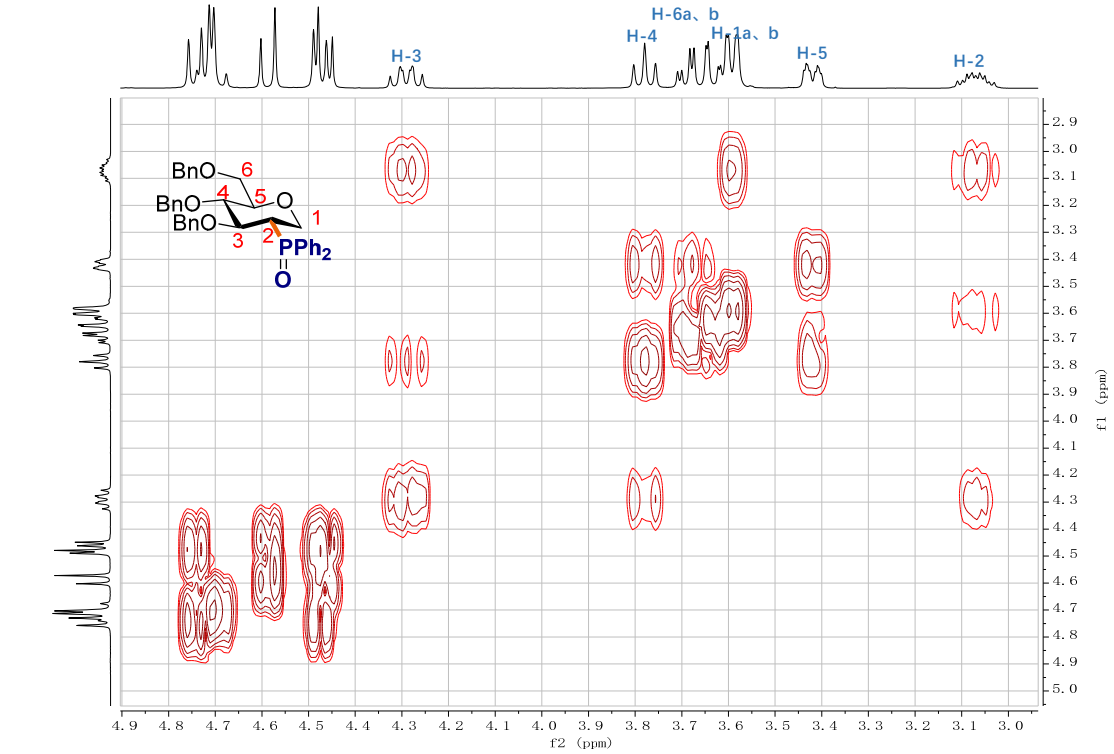

^{1}H-^{13}C HSQC (CDl_3, 400MHz) of **3h**

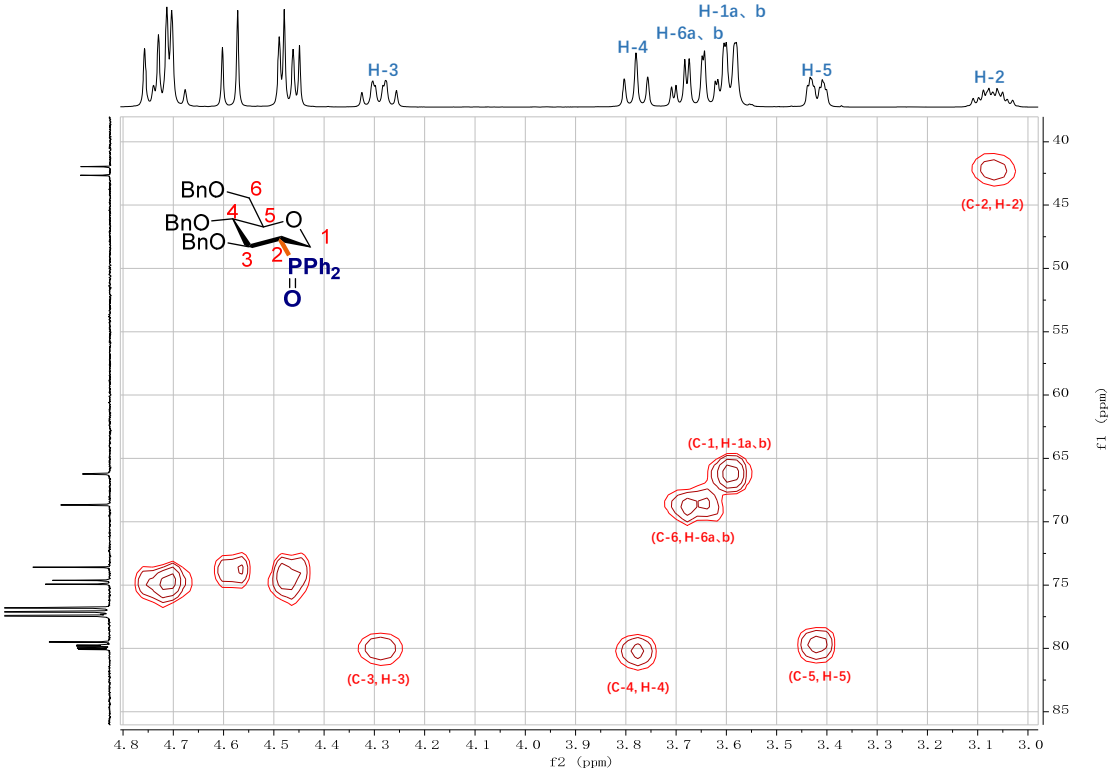

^{1}H-^{1}H NOESY ($CDCl_3$, 400MHz) of **3h**

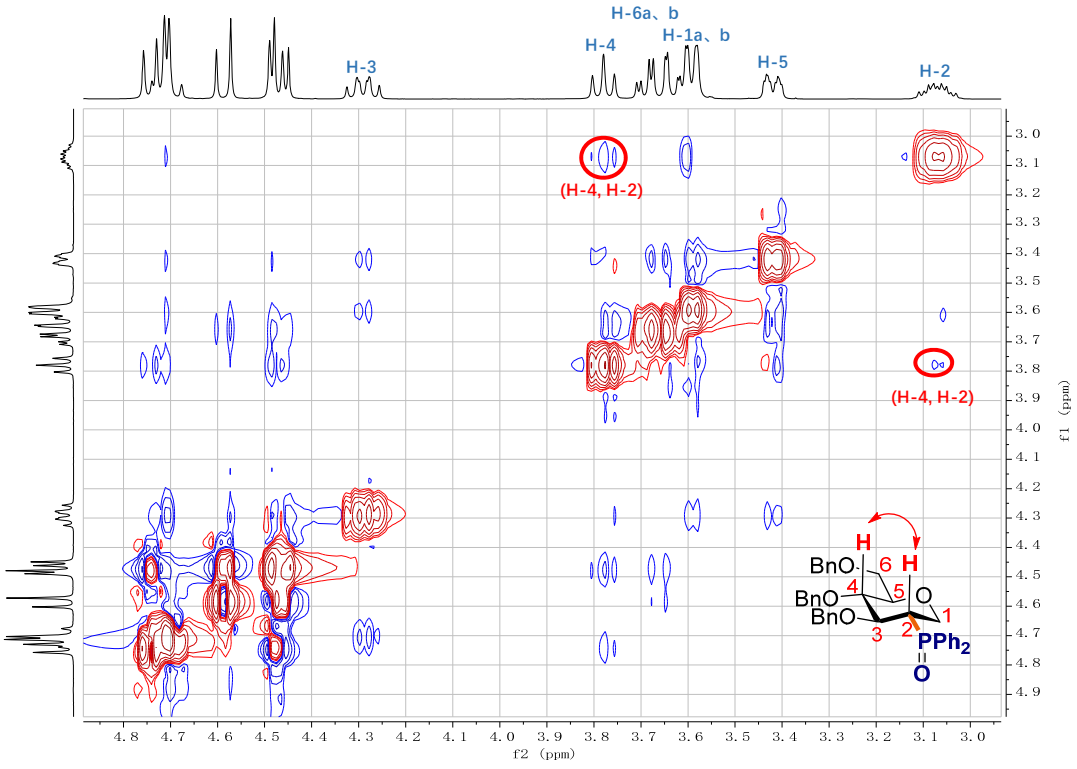

^{1}H-^{1}H COSY ($CDCl_3$, 400MHz) of **3h'**

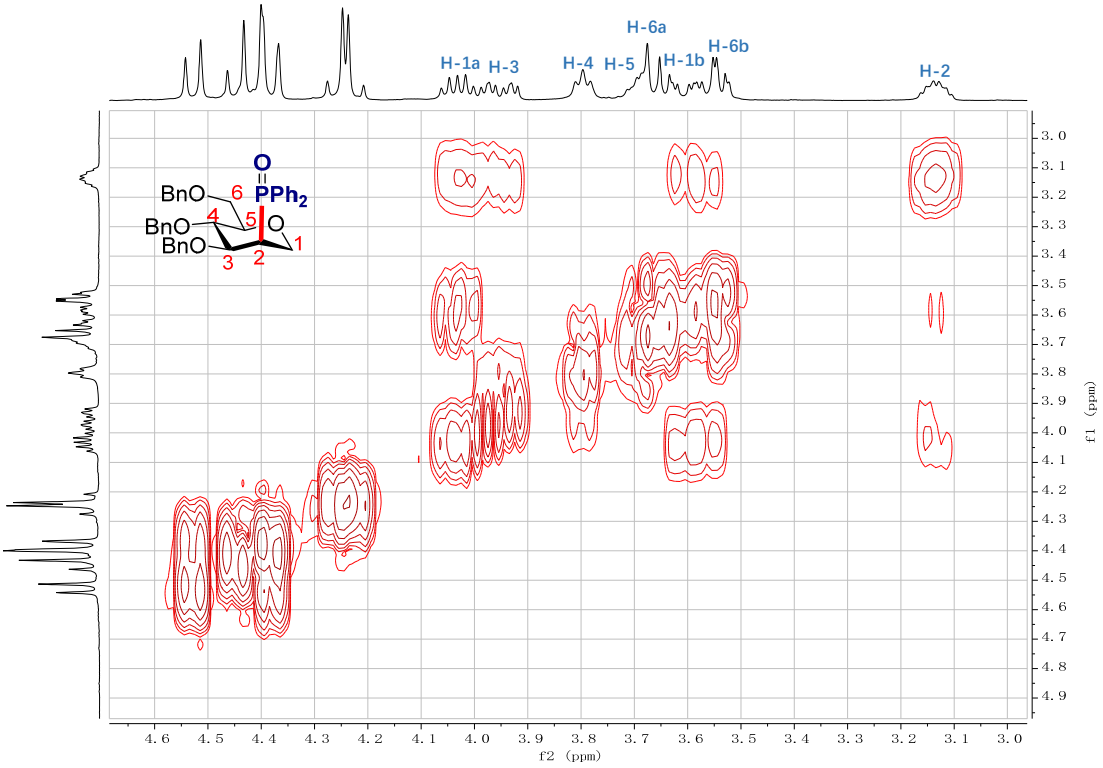

^{1}H-^{13}C HSQC ($CDCl_3$, 400MHz) of **3h'**

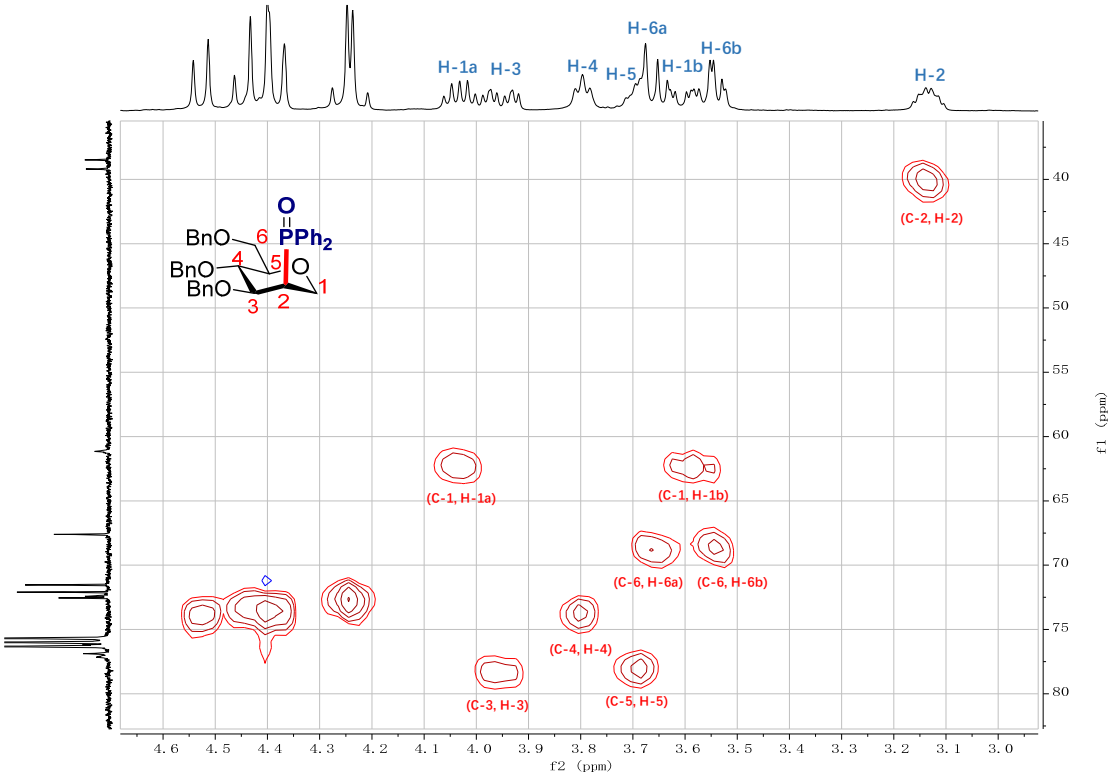

^{1}H-^{1}H NOESY ($CDCl_3$, 400MHz) of **3h'**

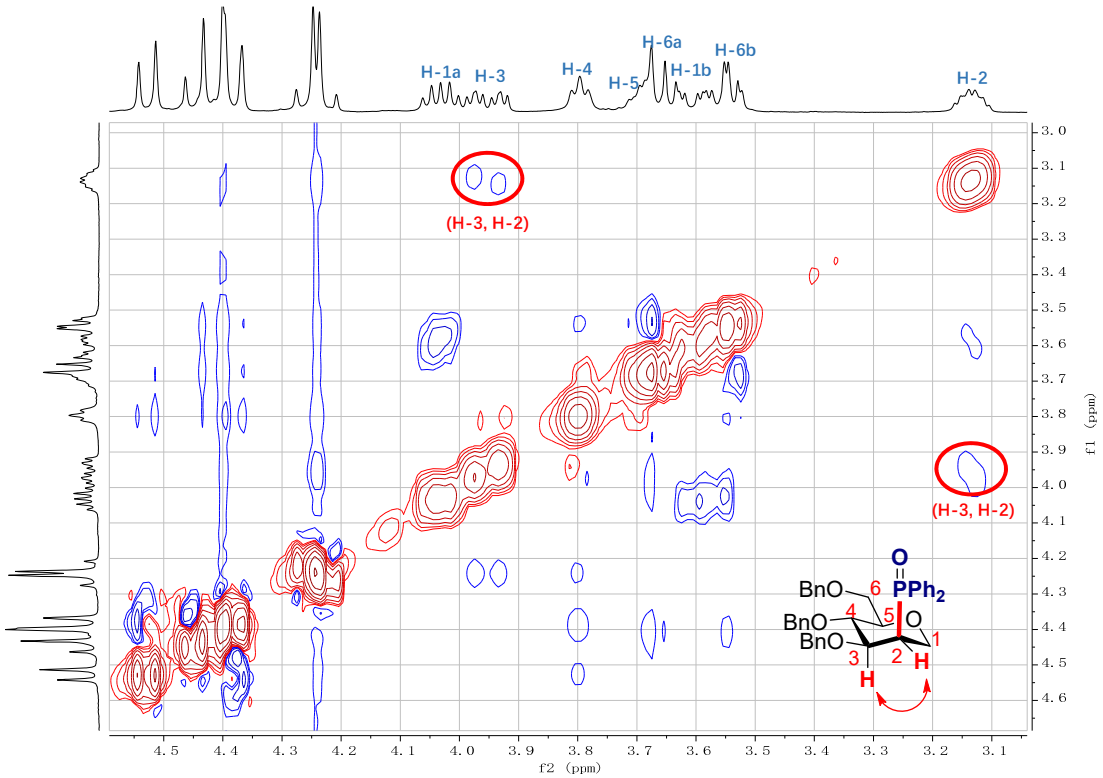

^{1}H-^{1}H COSY ($CDCl_3$, 400MHz) of **3k**

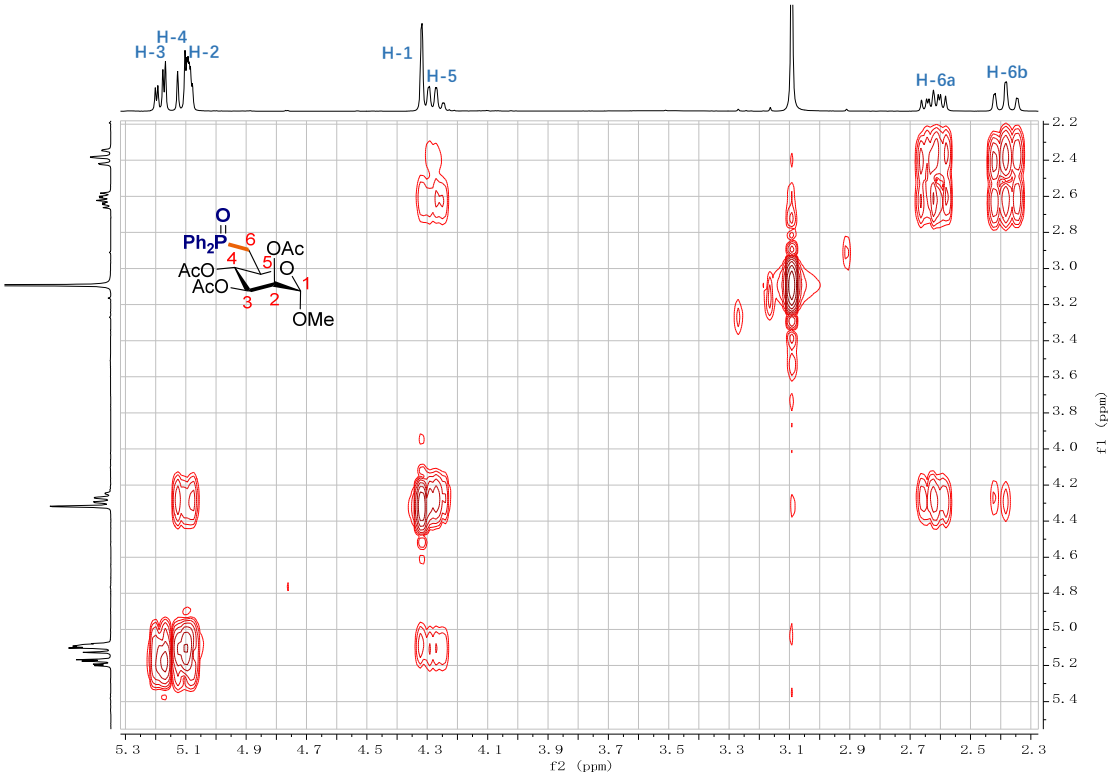

^{1}H-^{13}C HSQC ($CDCl_3$, 400MHz) of **3k**

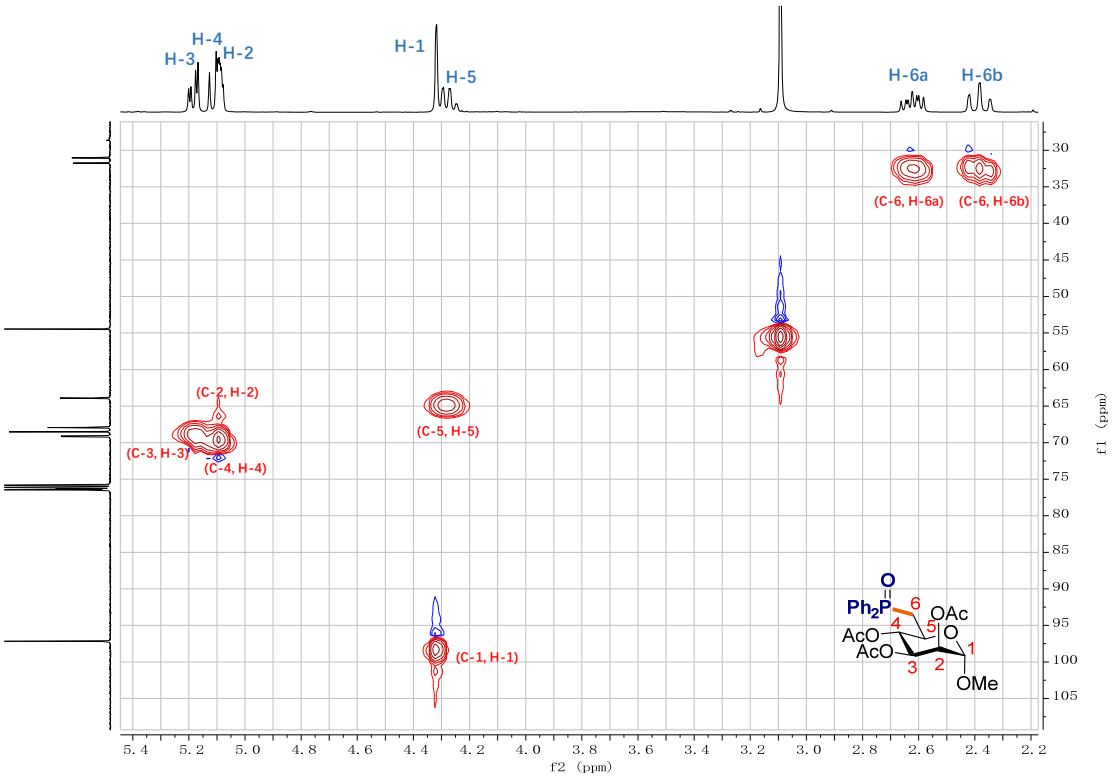

^{1}H-^{1}H NOESY ($CDCl_3$, 400MHz) of **3k**

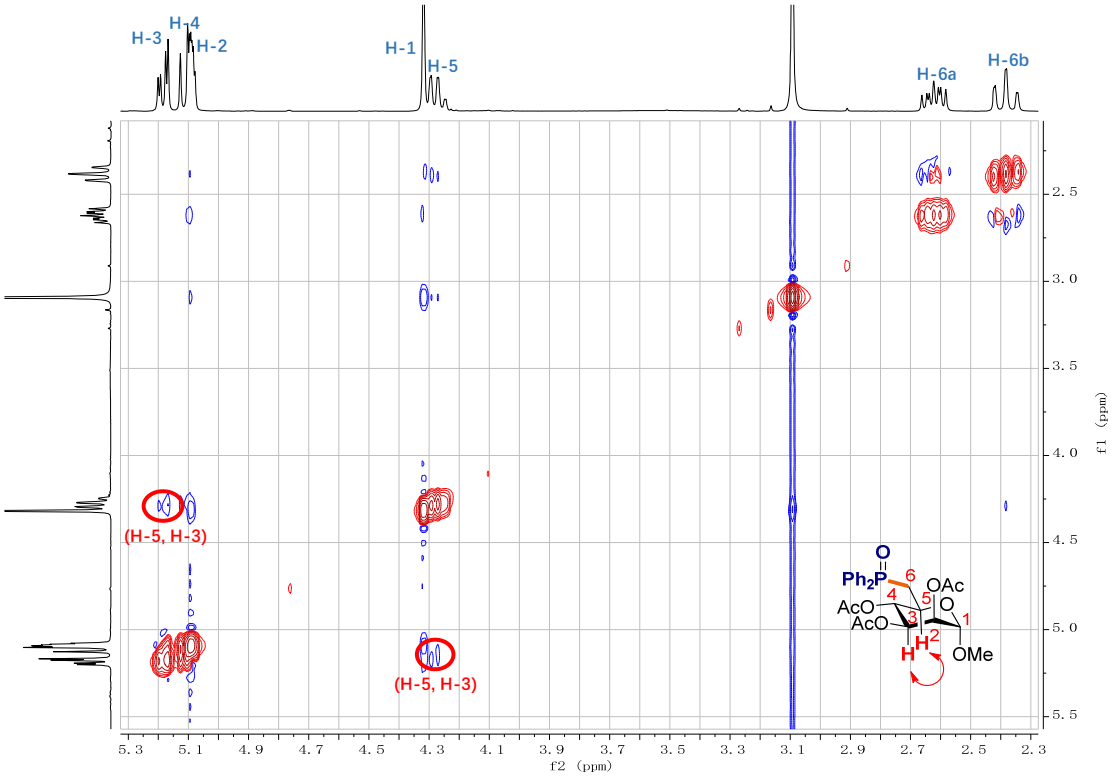

^{1}H-^{1}H COSY ($CDCl_3$, 400MHz) of **3s**

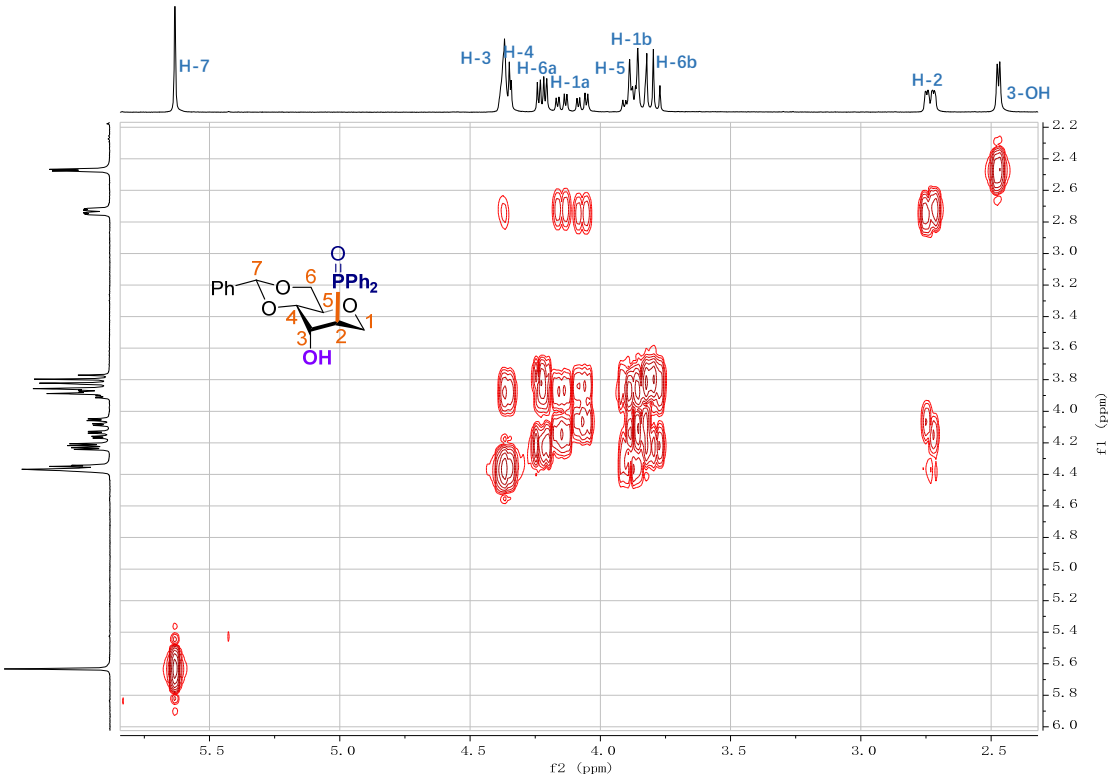

^{1}H-^{13}C HSQC ($CDCl_3$, 400MHz) of **3s**

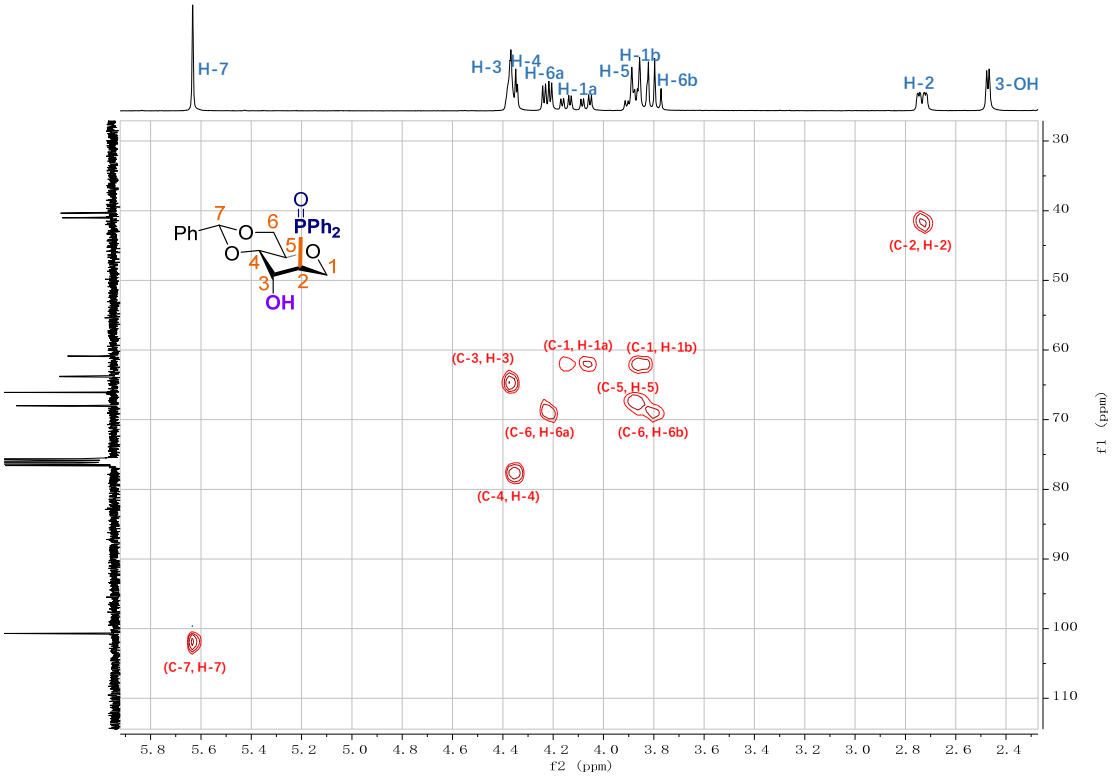

^{1}H-^{1}H NOESY ($CDCl_3$, 400MHz) of **3s**

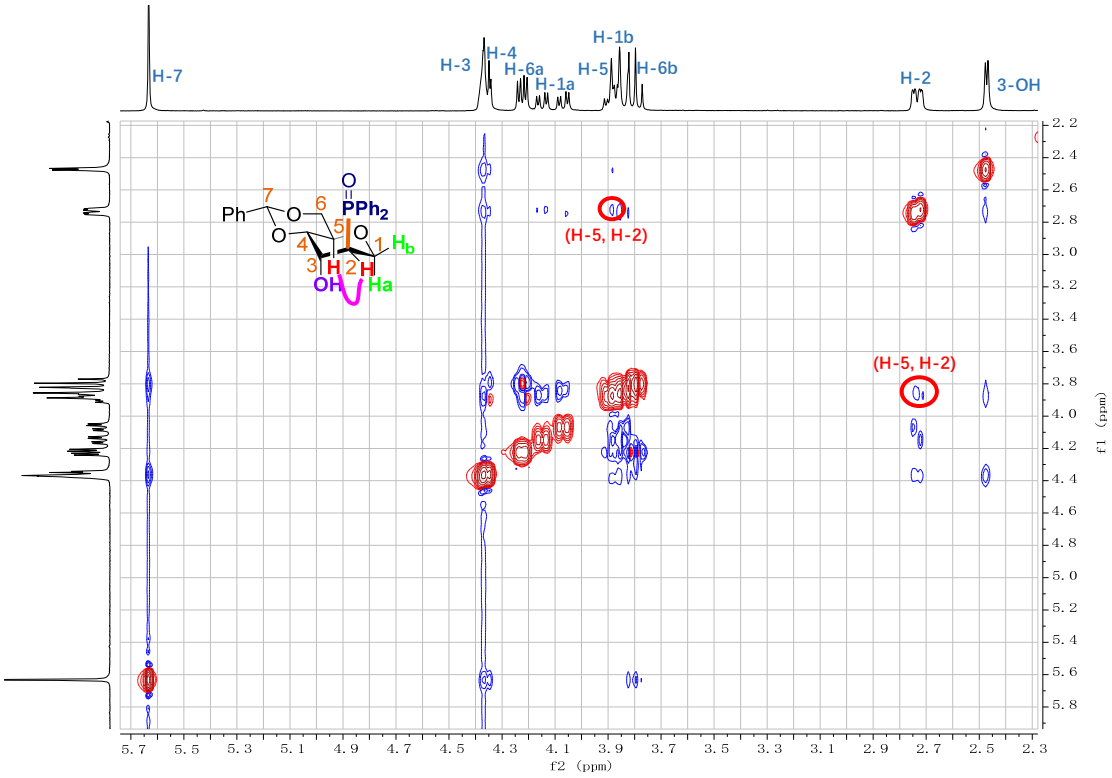

7. X-ray Structure of 3c, 3j

Single crystal was grown by slow evaporation method at room temperature using the petroleum ether: methanol solvent mixture (2:1, v/v) for 3c, 3j; The X-ray intensity data were collected at room temperature (296 K) on a Bruker SMART APEX II CCD diffractometer using Mo Kα radiation (λ = 0.71073Å). Structure was solved by the direct method using the SHELXS97. All nonhydrogen atoms were refined by full-matrix least squares on F2 using SHELXL-2014/7. All H atoms were placed at calculated ideal positions using a riding model approach. The ORTEP diagram was generated using the Mercury. CCDC 2123292, 2123293 contains the supplementary crystallographic data for this paper. These data can be obtained free of charge via www.ccdc.cam.ac.uk/data_request/cif, or by emailing data_request @ccdc.cam.ac.uk, or by contacting The Cambridge Crystallographic Data Centre, Union Road, Cambridge CB2 1EZ, UK; fax: +44 1223 336033.

Table S_1. Crystal data and structure refinement for 3c and 3j.

Identification code	3c	3j
Empirical formula	C24 H27 O8 P	C23 H27 O6 P
Formula weight	474.42	430.41
Temperature	293(2) K	296(2) K
Wavelength	0.71073 Å	0.71073 Å
Crystal system	Orthorhombic	Tetragonal
Space group	$P2_12_12_1$	$P4_12_12$
Unit cell dimensions	a = 11.9882(7) Å α= 90°. b = 12.7368(8) Å β= 90°. c = 16.1339(9) Å γ = 90°.	a = 9.4927(5) Å α= 90°. b = 9.4927(5) Å β= 90°. c = 47.965(5) Å γ = 90°.
Volume	2463.5(3) $Å^3$	4322.2(6) $Å^3$
Z	4	8
Density (calculated)	1.279 Mg/m^3	1.323 Mg/m^3
Absorption coefficient	0.156 mm^{-1}	0.164 mm^{-1}
F(000)	1000	1824
Crystal size	0.180 x 0.160 x 0.150 mm^3	0.190 x 0.180 x 0.150 mm^3
Theta range for data collection	3.399 to 25.496°.	2.187 to 25.496°.
Index ranges	-14<=h<=14, -15<=k<=15, -19<=l<=19	-11<=h<=11, -11<=k<=11, -58<=l<=58
Reflections collected	20045	33464
Independent reflections	4583 [R(int) = 0.0295]	4035 [R(int) = 0.0434]
Completeness to theta = 25.242°	99.7 %	99.9 %
Absorption correction	None	None

Refinement method	Full-matrix least-squares on F^2	Full-matrix least-squares on F^2
Data / restraints / parameters	4583 / 0 / 301	4035 / 0 / 275
Goodness-of-fit on F^2	1.047	1.145
Final R indices [I>2sigma(I)]	R1 = 0.0420, wR2 = 0.1002	R1 = 0.0454, wR2 = 0.0966
R indices (all data)	R1 = 0.0476, wR2 = 0.1033	R1 = 0.0505, wR2 = 0.0988
Absolute structure parameter	0.02(4)	-0.01(17)
Extinction coefficient	n/a	n/a
Largest diff. peak and hole	0.198 and -0.178 e.Å^{-3}	0.196 and -0.265 e.Å^{-3}

compound 3c

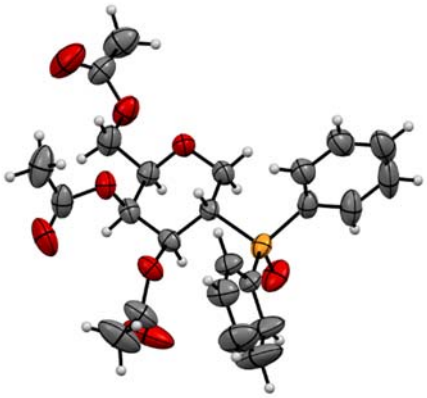

Figure S1. ORTEP diagram of the compound **3c**, Thermal ellipsoids are drawn at the 50% probability level.

compound 3j

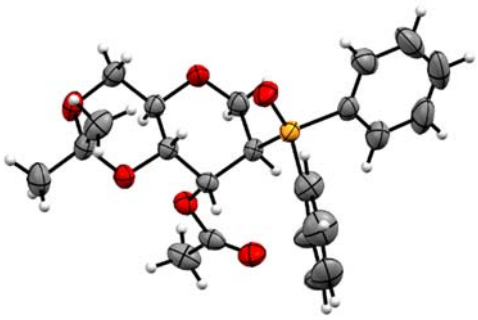

Figure S2. ORTEP diagram of the compound **3j**, Thermal ellipsoids are drawn at the 50% probability level.